Polarimetric RADARSAT-2 and ALOS PALSAR multi-frequency analysis over the archaeological site of Gebel Barkal (Sudan)

Jolanda Patruno

ANNÉE 2014

THÈSE / UNIVERSITÉ DE RENNES 1
sous le sceau de l'Université Européenne de Bretagne

En Cotutelle Internationale avec
Université de Rome « La Sapienza », Italie

pour le grade de

DOCTEUR DE L'UNIVERSITÉ DE RENNES 1

Mention : Traitement du signal et télécommunications

Ecole doctorale MATISSE

présentée par

Jolanda PATRUNO

préparée à l'unité de recherche IETR UMR 6164
Institut d'Electronique et de Télécommunications de Rennes
IFSIC - UFR Informatique Electronique

Polarimetric RADARSAT-2 and ALOS PALSAR multi-frequency analysis over the archaeological site of Gebel Barkal (Sudan)

Thèse soutenue à Rome

le 10 Avril 2014

devant le jury composé de :

Rudi GOOSSENS
Professeur, Université de Gand / Président

Jean BOURGEOIS
Professeur, Université de Gand / *Rapporteur*

Shane CLOUDE
Professeur, AELC / *Rapporteur*

Yves Louis DESNOS
Docteur, ESA-ESRIN / *invité*

Mario HERNANDEZ
Docteur, UNESCO / *invité*

Rosa LASAPONARA
Docteur, CNR-IMAA / *invitée*

Alessandro Maria JAIA
Professeur, Université of Rome La Sapienza / *invité*

Mattia Giovanni CRESPI
Professeur, Université de Rome «La Sapienza» / *co-directeur*

Eric POTTIER
Professeur, Université de Rennes 1 / *co-directeur*

"What we are capable of, he thought. To grow, to love, have children, get older - and all this while we are also elsewhere, in the long waiting time of a response not arrived, or a gesture not completed. How many paths, how many different paces in what looks like a unique trip."

Alessandro Baricco, Mr Gwyn

In that particular world, horizon was always changing its direction.

Anonimous

To my parents and to myself, for all these years.

Acknowledgments

The present PhD thesis has been resulting from a five years' experience in the field of remote sensing applications for archaeology, carried out at the Italian Establishment of the European Space Agency (ESA/ESRIN) of Frascati (Italy), where I was hosted since 2008 for my Master Degree in Archaeology. In this occasion, a strict collaboration between ESA and the University of Rome "La Sapienza" (Italy) started, and then continued in the following years, involving the Institut d'Electronique et de Télécommunications de Rennes (IETR) of the University of Rennes 1 (France) for a joint PhD program between the two universities. Therefore, it has to be said that this manuscript is the result of the scientific interaction I had in years with several scientists coming from ESRIN, Rome and Rennes.

I first would like to thank my Professor Mattia Crespi who gave me the chance to start my PhD adventure in 2010 at the University of Rome "La Sapienza", believing in a so pioneering scientific approach and supporting the activities and the ideas that were carried out during the PhD research. Also, I would like to thank him for the constant kindness, availability and appreciation of the work he always demonstrated in these last three years and half.

I would like to express my gratitude to Professor Eric Pottier, who since the first time we met during PolInSAR 2011 in Frascati, demonstrated great interest and complete availability for working together at the SAR polarimetric part of the PhD research. I would like to thank him for the productive and wonderful period spent in his team in Rennes, for his scientific and human support, his encouragement and infinite kindness that I will never forget.

I would like to thank all the members of the jury who accepted to participate at my PhD defence, contributing with many helpful comments to my research activity and its future development.

In particular, I am grateful to Professor Rudi Goossens, who accepted to be the President of the jury and to the reviewers, Professor Jean Bourgeois and Professor Shane Cloude, who evaluated the manuscript. With all of them I had constructive

and multidisciplinary exchanges from an archaeological and a "polarimetric" point of view.

I would like to thank Yves Louis Desnos for his presence in a so important day, for his appreciation of the research activities carried out in a so specific and new topic, and for his support that opened the doors to a TV interview about the research.

Special thanks go to Mario Hernandez and Rosa Lasaponara, invited members of the jury, as well as to Nicola Masini who could not participate to the PhD defence. They followed with interest my growing experience in the field of SAR polarimetric applications to archaeology, always providing precious suggestions and helping me with their knowledge. I am glad to consider them the major representatives of the "scientific family" I know since several years.

I would like to thank Professor Alessandro M. Jaia, who first introduced me in the topic of Aerial Photography in Archaeology in the first years of University.

I am grateful for the possibility given by the GIS BRETEL (VigiSAT) program for providing and acquiring RADARSAT-2 data for the PhD research. My gratitude goes also to the European Space Agency and all the people that contributed to my scientific and social growth. Among them, I would like to mention Francesco Sarti, with whom I had the opportunity to participate actively to conferences and organize courses about Polarimetric application for archaeology; Andrea Minchella, with his unceasing support and friendship during all these years and Chris Stewart, who, like me, deepened the interest in the topic of SAR Remote Sensing for Archaeology.

In addition, I would like to thank Professor Luigi Perotti, from the University of Turin (Geositlab - Dipartimento di Scienze della Terra). I appreciated his enthusiastic availability to work together to the GIS project developed in the frame of the present PhD thesis, his availability and I thank him for my very first and fantastic walk on the Miage glacier.

I would like to thank Professor Emanuele Ciampini for his availability and his support in the ground truth validation at Gebel Barkal.

My gratitude goes also to the whole IETR of Rennes, and especially to Joelle, Martine, Noelle, for their incredible support, Laurent and Stefano Tebaldini, with whom I shared the very first printed version of the manuscript, Bassam, Hongquan, Francesco, who all filled the time outside the office.

I would like to mention also my far but so close friends, Manuel, Fabio, Eric and Mariangela, each of them for their special and unforgettable presence. I will never forget the time spent together, their scientific support, late-night talks and philosophic silences, their timeless and everlasting genuine friendship. Special thanks also to Nicole, with whom I shared most of the PhD experience between Rome and Rennes, difficulties, successes and baguettes, and many precious moments in time since more than 10 years.

Finally, I would like to thank Andrea, for coming into my life during this special period of the life, for his enthusiastic and limitless support, and for his love. I want to thank my sister Luigia and my parents Mimma and Sebastiano for their unique place in my life and their priceless support in all these years.

Pink Floyd albums deserve to be mentioned, as they filled up all the emptiest moments of the soul.

Contents

List of figures

List of tables

Chapter 1

Introduction

More than one century of technology exploitation can be traced in the history of Remote Sensing technique. In 1855, the French photographer Nadar (Gaspard-Félix Tournachon), believing in the utility of aerial view for military purpose and cartography, took the first aerial photographs in the sky of Paris from a balloon. Soon, the adventure of sky's eyes started to spread the enthusiasm all over Europe and in different application domains. At the very beginning of 1900, while Mr. J. Neubronner was equipping his pigeons with miniature cameras, the archaeologist G. Boni embarked on a military balloon to photograph Forum Romanum ruins, giving rise to the very first remote sensing documentation of archaeological excavations.

After more than one century, the history of Remote Sensing for archaeology, which started with aerial photography, soon recognised as the most effective and non - invasive technique par excellence, points at optical satellite data, and looks with inspiring curiosity at radar satellite data. LANDSAT-TM and SPOT sensors before, and very high spatial resolution sensors as IKONOS and QuickBird later, all of them conceived for several land applications far from archaeology, have been used in time for the realisation of cartography and for the study of ground anomalies that could be linked to anthropic phenomena. These data, analysed in the wake of the archaeologists' proven aerial photography know-how, provide a high spatial resolution analysis, granting the recognition of small archaeological

features, and a high temporal resolution analysis, assuring a constant monitoring of the conservation state of a site and of the changes occurred in its environment. The PhD research here discussed represents an example of the challenge to which archaeological investigation can takes on today, in a field that the "initiated" call "Space Archaeology". The study, in fact, wants to extend the current knowledge on remote sensing application for archaeology, principally based on optical data analysis, to a particular kind of radar satellite application: SAR (Synthetic Aperture Radar) polarimetric data analysis for the detection of surface and subsurface archaeological features of the UNESCO World Heritage site of Gebel Barkal (Sudan).

1.1 Background and motivation

The interest in such topic originates from the studies on Ancient Topography, and in particular on the subject of Archaeological Aero topography, carried out during the last years of University (University of Rome "La Sapienza", Faculty of Archaeology). In that occasion, a first knowledge on aerial remote sensing for archaeology addressed the interest towards a study beyond aerial photographs, and, in particular, in the applicability of optical and SAR satellite data analysis in the archaeological domain, focusing on the study of SAR Polarimetry technique.
The not enough spatial resolution and the complexity of SAR polarimetric data have, often, prevented the exploitation of such technique for the archaeological investigation. Nevertheless, the 24-hours acquisitions SAR sensors provide, independently from an external illumination source (Sun) and from cloud covering, the possibility to penetrate ground (especially in dry environments and at given wavelengths) as well as the possibility to derive information on the dielectric properties of the target, make SAR polarimetric data a potential and powerful World Heritage investigation tool. Moreover, SAR data often supply to the lack of optical acquisitions in certain areas of the World, and they provide a remote monitoring of those unreachable (natural constraints) or inaccessible (politic situation) heritage areas.

All these aspects are at the origin of the integration of a pure humanistic background with SAR remote sensing knowledge, started at the Italian Establishment of the European Space Agency (ESA/ESRIN) in 2008, when

thanks to the collaboration between ESA and the University of Rome "La Sapienza" the work reached its first identity in the Master Degree thesis. The experience continued over years, resulting in a joint PhD project between the Faculty of Engineering of the University of Rome "La Sapienza" (Italy) and the Institut d'Electronique et de Télécommunications de Rennes (IETR) of the University of Rennes 1, France, where the expertise on Polarimetry has been deepened during the second year of the PhD research.
The multidisciplinary synergy between the archaeological background and the application of a so specific technology culminated in a dedicated GIS (Geographic Information System) project for Gebel Barkal, realised at the University of Turin (Geositlab - Dipartimento di Scienze della Terra) in the last months of the third year of PhD. Thanks to this tool, the possibility of observing an overall view of an archaeological site, as well as details linked to the specific aspects characterizing it, meets the need of communication between archaeology and engineering technology.

1.2 The research

Nowadays, SAR applications for archaeology focus on high spatial resolution SAR sensors, which allow the recognition of structures of small dimension and give information of the surface topography of sites. This is the case of TERRASAR-X or COSMO-SkyMed sensors, working in X-band and in dual-polarisation.
Given the potential of fully polarised SAR data, the research focuses on a polarimetric multi-frequency analysis of ALOS PALSAR (L-band) and of RADARSAT-2 (C-band) sensors for the detection of surface and subsurface archaeological structures of Gebel Barkal archaeological site, inscribed in the UNESCO World Heritage List since 2003.
In addition, a multi-incidence angle analysis, intended as evaluation of the potential of diverse incidence angle configurations for the detection of archaeological features, is illustrated analysing the different configuration mode selected for RADARSAT-2 acquisitions.

The polarimetric sensor PALSAR ceased operation in 2011, thus providing acquired data that can be considered "historic", even though quite recent, polarimetric satellite acquisitions. RADARSAT-2 polarimetric data have been

specifically acquired in the frame of the last two years of the PhD research, and have been scheduled to achieve a multi-temporal observation of the archaeological area.

Selection criteria of both satellite sensors and archaeological site are based on specified needs. Sensors spatial resolution (ALOS PALSAR ca. 20 m and RADARSAT-2 ca. 10 m), archaeological structures' dimensions, the dry environment characterizing the site and the great potential L-band and C-band demonstrated in such context, make the research suitable for the monitoring of the archaeological area, as well of the possible threatening factors that can affect the integrity of a cultural site.

The research develops towards the need of finding a suitable methodology, based on the use of SAR polarimetric data, which can be applied to the study of archaeological sites. On the subject of remote sensing for archaeology, an unequivocal method capable of an automatic detection of archaeological features is still not existing. Hence, objective of the presented work is to exploit the potential of such complex but meaningful technique as SAR polarimetry is, and to individuate investigation guidelines that can be useful for the archaeological community.

1.3 Thesis outline

The arguments discussed in the thesis are listed in the following chapters' structure:

- **Chapter 2.** "Archaeology below Earth's surface: State of Art". This chapter presents the history of photointerpretation and its development to the use of satellite data for the archaeological research, focusing on some applications example of SAR data analysis applied to the ancient sites study.
- **Chapter 3.** "SAR Remote Sensing Technique and Polarimetry". Basic principles of SAR and Polarimetry are given, explaining related concepts and illustrating SAR characteristics and the theoretical polarimetric descriptors analysed in the research.
- **Chapter 4.** "Spaceborne sensors". A brief list of used sensors introduces to ALOS PALSAR and RADARSAT-2 polarimetric sensors, fulcrum of

the research activity, and to QuickBird and KOMPSAT-2 optical sensors, only used as optical basis for the comparison of data.

- **Chapter 5.** "Case study: Gebel Barkal archaeological site". In this chapter, the archaeological area is presented, highlighting the selection criteria of the site, strictly depending on the special interest this ancient context originates. Following, the UNESCO World Heritage List, in which the site is inscribed, is presented.
- **Chapter 6.** "Data set presentation". The chapter provides a complete overview of data analysed. Data are not only presented for the different sources they come from, but also illustrated explaining the choice related to the typology of satellite acquisitions and the purpose data analysis aimed to.
- **Chapter 7.** "Polarimetric SAR Multi-frequency analysis". The applied data processing chain, the analysis of the obtained results and their discussion are illustrated. The chapter concludes with the description of the ground truth campaign performed.
- **Chapter 8.** "Polarimetric SAR Multi-incidence angle analysis". The multi-incidence angle analysis presented in this chapter is conceived as a support-analysis as well as an autonomous study for archaeological investigation, previously carried out by means of the multi-frequency approach.
- **Chapter 9.** "GIS: A potential application". This chapter focuses on the importance of managing data coming from different sources in a unique tool, the Geographic Information System, for archaeological purposes. The dedicated GIS project for Gebel Barkal is illustrated as an example of useful communication between technology and archaeology.
- **Chapter 10.** "Conclusion and Outlooks". A critic summary of the whole research and its most interesting points, as well as the originality of such a non – invasive approach in the archaeological scientific field introduce to future applications and developments in the remote sensing monitoring of World Heritage sites. Different outlooks are proposed for a future continuation of this research subject.

This page intentionally left blank

Chapter 2

Archaeology below Earth's surface: State of the Art

This chapter wants to show the ascending curve of remote sensing in archaeology. Some historical details are shown about the history of the first approaches of remote sensing applied to archaeology, dating back to XIX century and going through the two World Wars, which left an indelible mark in the development of photointerpretation. Following, an explanation of natural indicators is presented. It is shown how archaeological underground ruins can be detected by airplane in the optical remote sensing domain. As conclusion to this chapter, some examples of the state of art based both on optical and SAR images are reported.

2.1 Historical introduction

Before starting with a brief historical introduction, it is important to define what remote sensing is.

Remote sensing is the science of obtaining and interpreting information from a distance, using sensors that are not in physical contact with the object being observed [1]. It includes aerial, spacecraft and satellites observations.

According to this definition, here below is given an illustration of the first attempts in the European panorama, going from '800 to the Second World War, when the importance of the photography from airborne applied to the study of archaeological environment became clear to archaeologists and historians.

2.1.1 The Beginnings

The beginnings of the aero photointerpretation started in XVIII century with the philosopher and politician C.L. De Montesquieu who, during his stays in Italy was used to go on the top of bell towers to observe the landscape. Already in XVII and XVIII centuries, crop marks were known with the name of "devil path" by Italians and subsequently correctly defined as crop marks by British writers. These marks, well visible in crop fields, were conveniently interpreted as ancient cities viability.

As known, photography was developed at half of the XIX century. Ancient cameras were not easy to be carried on board of balloons and the exposure time was too long. Even though these restrictions, in 1858 the first photograph over Paris was shot by "Nadar" (Gaspar Felix Tournachon).

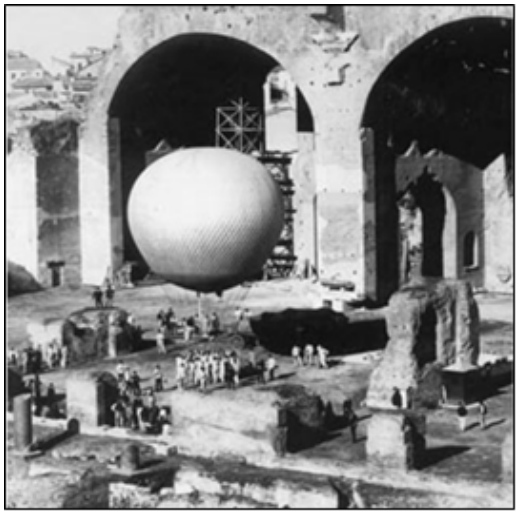

Figure 2.1 : Military balloon tied to ground used by Giacomo Boni (1900) © Piccarreta 1994

In 1879, Franz Stolze documented Persepoli's excavations (Iran) by means of airborne photographs. It is the first example of an archaeological application of remote sensing. Twenty years later, in Italy, Giacomo Boni thanks to a collaboration with Scuola Reale di Ingegneri in Rome, assembled a camera on a balloon used by Brigata Specialisti del Genio Militare to support excavation at Forum Romanum in Rome, (Figure 2.1). This collaboration has to be seen as a proof of exchange of favours, as archaeologists took advantages of Military

Forces to perform the acquisitions they were interested in, while Military Force used archaeology as justification for recognising sensible targets.
It was after these first attempts that aerial remote sensing for archaeology was born.
Concerning the Italian scenario, in 1907 Aeronautica Militare took shots of Fiumicino (RM, Italy) and Isola Sacra (RM, Italy), while in 1910 an aerophotographic relief of Pompei (NA, Italy) was realised. In 1911, Ostia Antica (RM, Italy) was documented and an interesting detail of the area was the discovery of the mark of an ancient cove of Tiber River. Importance of this anomaly is especially linked to the benefit given by remote sensing in understanding how ancient environments were and how they changed across centuries.
A new era for the airborne photography started when, in 1903, Wright brothers took the first flight on board of a plane. It is some years later this flight experience that an Italian official understood the importance of sum up cameras and airplanes. This intuition, then, was extensively adopted during the First World War [2].

2.1.2 The World War I and post-war period

First World War gave a big impulse to sectors such as aviation, cameras, film evolution to be employed for strategical aims. In this period, apart from the big quantity of photographic material, many professional personalities such as pilots and observers were available for archaeological purposes.
The most important period was the one immediately after the war. After some years, in fact, many photographic acquisitions taken first for military purposes were made available to archaeologists. These allow the identification of Roman cities in Palestine during aerial reconnaissance missions organised by Th. Wiegand, chief of the Turkish-German archaeological commission in Middle East (1919).
Among the personalities of that period, O.G.S. Crawford played an important role in the English panorama. In 1920, he became the official archaeologist of the Ordnance Survey, the institute in charge of the cartographic realisation. In three years, he was able to provide proofs about the ancient agriculture organisation near Winchester by means of military photographs.

During these years, England made a step forward thanks to the Major G.W.G. Allen that bought himself an airplane. Between 1932 and 1939, he acquired regularly oblique photos. This made possible the availability of several acquisitions over the same archaeological sites in the same periods of the year. Excavations confirmed observations of what noticed from airplane. This made possible to refine observation already carried out by Crawford.

One of the biggest pioneers for the aero photointerpretation in the Middle East was Padre Antoine Poidebard. After serving the French church for several years, he became aviator and soldier in Armenia. In 1924, he was transferred to Labanon as Professor at the University of Beirut. He started to study Syria landscapes, starting to understand the importance linked to climate and soil. He went in depth with this topic and in 1926 started to investigate Roman and Byzantine ruins noticed during his first flights.

In Italy as well, between these years, several experiments were carried out. Istituto Geografico Militare and other authorities developed photogrammetric restitutions during 1920s. At the end of 1930s, Giuseppe Lugli undertook an important initiative. He understood the informative potential of aerial photographs, especially for central and southern Italy. Unfortunately, this systematic documentation did not ensue because of the beginning of the Second World War aggravated by the creation of an Italian law (July 1939) that ratified to Italian citizens, companies and governmental bodies to obtain necessary authorisations and to be available for inspections and official approvals for the planning, acquisition and utilisation of photographs taken from aerial platform [3].

2.1.3 The World War II and post-war period

The Second World War represents a pause in this direction. During the conflict millions of photographs were shot, primarily vertical. A good part of them was destroyed at the end of the war, but a good percentage is still traceable in archives. Many photos with strategic purposes were taken by RAF (Royal Air Force).

It was only after 1945 that the research started again in all Europe. Among the researchers, John Bradford, official of the British aerial forces, took pictures during the war. These were reused after the conflict for archaeological purposes. He was able to detect a big amount of Neolithic villages in Puglia (Italy), Roman

centuriation in North of Italy and important studies over Tanquinia and Cerveteri (RM, Italy).

Noteworthy is Giulio Schmiedt, supervisor of the archaeological section at Istituto Geografico Militare (IGM). Between the two wars, he had the assignment of realise national covering over Italy. This activity started before the Second World War, continued after it. The first coverage date back to 1954-55. These acquisitions were all followed by methodological publications.

Eminent figure in the field of Ancient Topography was Ferdinando Castagnoli. His research was dedicated to the study of the Roman centuriation and of all those cities with an orthogonal map, typical of the Roman times. It is thanks to a collaboration between Castagnoli and Giulio Schmiedt that in 1956 the first application of aerophotogrammetry finalised to archaeology was realised. Starting from 1960s, the interest towards techniques finalised to an archaeological use grew up and as results had the X International Congress of Photogrammetry in Lisbon (1964) and the II International Symposium of photo interpretation in Paris (1966).

The enthusiasm towards the new discipline brought to a big interest enlarged in other European countries [4].

2.2 The archaeological marks

Although satellites aroused curiosity since 1970's, it is only thanks to the launch of higher spatial resolution sensors that the discipline of remote sensing was applied to the humanistic field, making it more and more independent by aerial photographs that, however, continue to keep their importance from an historical point of view. Of course, optical satellites revenge a very important role in the research thanks to platforms (such as IKONOS, QUICKBIRD, WORLDVIEW, etc.) that allow the individuation of archaeological ruins thanks to the very high spatial resolution.

Possibility of detecting archaeological structures in the optical domain is made possible thanks to natural indicators that interact with finds still underground, thus drawing buildings' shape revealing the nature of the findings (villas, villages, streets and so on).

The soil is modified on the surface on the base of the differences in humidity content and on the base of different influences that the buried structures exercise on vegetation growing above. Thus, humidity, humus, relief and vegetation are the mediators that help in recognising structures not visible to an observer standing on the ground.

Marks are divided into six classes, each one associated to the element that gives rise to them: 1) humidity; 2) vegetation; 3) alteration of soil composition; 4) microrelief; 5) anomaly; 6) continuity marks [4].

2.2.1 Humidity marks

Moisture marks are typical of soils without vegetation (Figure 2.2). They arise after rain precipitations because of changes in colour that are due to differences in water content in the humus. The time available for detecting them is quite short considering the whole cycle of water drying up. By considering this factor, the first and the last period of the cycle are not useful for detecting changes in colour because the terrain will be saturated by water or because too much dry. Furthermore, it has to be taken into account that also the structures depth influences the visibility of this category of marks, in fact, if too much in deep, different humidity content will not be appreciable.

Figure 2.2 : Moisture marks © Piccarreta 1994

2.2.2 Vegetation marks

Vegetation marks (Figure 2.3) are visible on vegetated terrains, mainly where domestic plants or spontaneous grass are cultivated. This anomaly is due to the roots growth disturbed because of structures presence underneath that prevent their regular growth, modifying both vegetation colour and development. The period involved in this phenomenon goes from seeds germination to the first

phase of plants development. After this period, the phenomena flags till its disappearance. As in the previous example, also in this case structures size and depth play an important role. Tone inversions are possible. Instead of a bright colour due to the difficulties of growth, this colour inversion can appear when the archaeological structure is located near an area with a high content of humidity, supporting thus, a major vegetation growth.

Figure 2.3 : Vegetation marks © J. Dassié

2.2.3 Alteration of soil composition marks

The marks due to alteration of soil composition are visible in terrains with no vegetation and are detectable because of variation in ground colour, as visible in Figure 2.4. These can be due to materials that alter the terrain surface, with consequential changes in light reflection or because of materials that influence terrain coloration. One example is ascribable to fields work. Agricultural instruments, in facts, erode ruins not in deep (e.g. walls) and fragments of them are brought to the surface, changing thus the superficial colour.

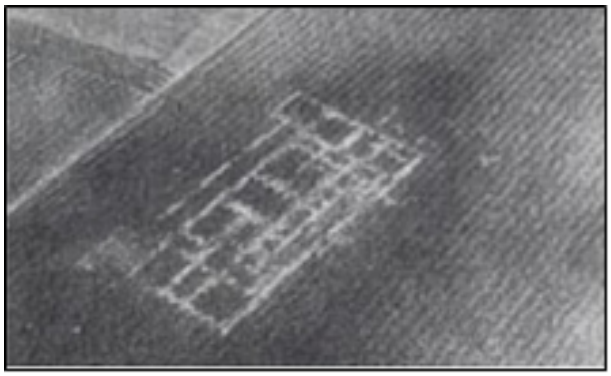

Figure 2.4 : Surface alteration marks © Piccarreta 1994

2.2.4 Microrelief marks

Microrelief marks are due to terrain height variations, visible with a stereoscopic observation or in specific moments of the day, as sunrise and sunset, thanks to the visibility of the shadows created by underground structures emerging on the ground, as visible in Figure 2.5.

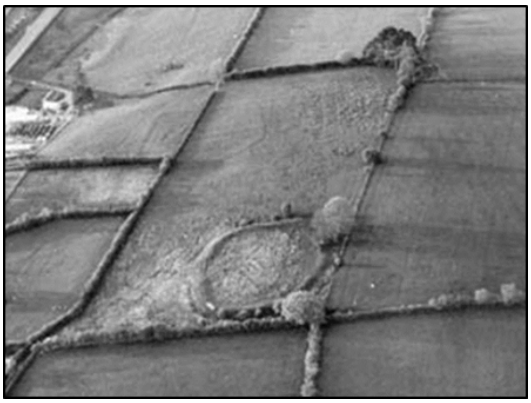

Figure 2.5 : Microrelief marks © Musson et al, 2005

2.2.5 Anomalies marks

Anomalies marks (Figure 2.6) are linked to archaeological evidences known to be ancient ruins, but by observing them in the global contest, they create a clashing evidence. Examples of this mark typology are cultivated fields where, the presence of obstacle elements reproduces the shape of the archaeological ruins. Among them, some examples are human activities in a field concealed by the time that look-like natural elements of the environment; anomalies in the terrain morphology; irregular trend of water drainage due to the presence of ancient ruins.

Figure 2.6 : Anomalies marks © Piccarreta 1994

2.2.6 Continuity marks

Outliving marks, visible in Figure 2.7, is the last class to be listed. Among this category, there are archaeological marks not buried, whose material persistence is lost, but its function (partial or total) is still existing. Two well-known examples are: Roman centuriation and ancient urban viability. These elements, even if anomalous, have coherence among them and help archaeologists in recognise them.

Figure 2.7 : Continuity marks © Musson et al, 2005

2.3 Last decades in remote sensing for archaeology

Thanks to the great potential aerial photography demonstrated for the archaeological investigations, the interest for a new complementary remote source of research began to increase at the beginning of 2000. In fact, satellite remote sensing acquisitions, especially the optical ones with their high spatial resolution, constituted soon a new possible tool for a remote observation of anthropic elements on the ground. Marks of Prehistoric huts, Roman ditches and Medieval fortresses started to be recognized from archaeologists also on this new promising data, following the same principles of ground surface alterations aerial reconnaissance provided.

Besides the LANDSAT-TM (Thematic Mapper) first studies of satellite data analysis for archaeology, the availability of KVR-1000 imagery, declassified after the end of the Cold War, lead to the identification of crop and soil marks in the Stonehenge site as well as to the study of the ancient city of Zeugma, crossing

point on the Euphrates river from Mediterranean to Mesopotamia. Moreover, also the imagery of the American strategic reconnaissance satellite Corona become available, thus permitting the spread of archaeological remote observations, as the case of Early Bronze Age ancient road systems of Ur [5].

Starting from 2000s, thanks to the launch of VHR (Very High Resolution) satellite data as IKONOS in 1999 and QuickBird in 2001, the monitoring and observation of archaeological complexes increased, therefore opening new perspectives in archaeological research. The already high spatial resolution has increased then with Worldview and GeoEye, with a spatial resolution of 50 cm in the panchromatic acquisition (0,41 and 0,46 cm for military purpose only) and 2 m in the multispectral (1,65 m and 1,80 m for military purpose). The contribution of VHR satellite data showed, and still shows, its usefulness in the study of ancient landscapes, not only due to the possibility to have stereoscopic view and the realisation of Digital Elevation Models, but also thanks to its role of complementary non – invasive source of information for the traditional archaeological research.

Many studies have been carried out to monitor and document ancient complexes using optical data, although archaeological pattern recognition and classification by means of satellite data is a quite recent method of investigation in the field of cultural heritage.

Different archaeological periods have been investigated by means of remote sensing techniques. Masini et al. [6] focused the attention on the medieval village of Yrsum, located in Basilicata, Southern Italy, to analyse and identify archaeological crop marks, micro relief and geomorphological features. Pansharpening, edge detection algorithms and vegetation indices over QuickBird data showed ground features caused by archaeological deposits, detectable thanks to difference in soil moisture content and changes in colour and height of vegetation in the area.

More recently, the archaeologist Sarah Parcack showed how thanks to the optical infrared wave, is possible to detect ancient structures, in certain conditions. During a project which aim was to look for Egyptian sites via satellite, Parcak uncovered 17 potential new pyramids, more than 1,000 tombs and more than 3,000 ancient settlements. On location, she and a team of archaeologists were able

to confirm and unearth many of those discoveries. The effects population growth, looting, urban expansion, and war have on archaeological sites, especially in in Egypt, can be recordable by analysing multispectral imagery (Figure 2.8) [7].

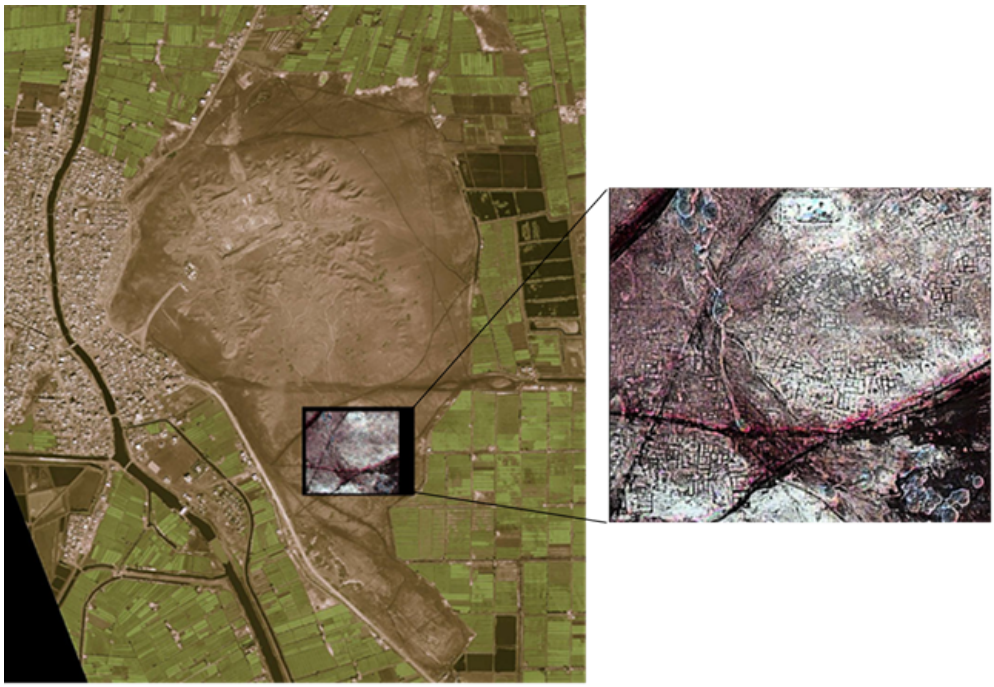

Figure 2.8 : The NASA satellite image shows an infrared image of a pattern of streets and houses in the buried ancient city of Tanis, Egypt. © University of Alabama

Concerning the applications of satellite SAR remote sensing in this field, the situation appears more complex. The great limit of a not enough high spatial resolution for archaeological contexts prevented a so deep development of knowledge in this sense, although their 24 hours acquisitions, independent from the day light, represent a decisive benefit respect to optical data in general. However, some scientists exploited the capability of such a data in very dry environments and in specific morphological and meteorological conditions. In the last decades, SAR remote sensing increased its application field, as is the case of archaeology.

The first applications did not convince the academic archaeological community because of the complexity of a visual interpretation of data, which is immediate and easier with optical imagery, and due to the spatial resolution, still not suitable for the recognition of archaeological patterns. From this last point of view, the more recent launch of satellite radar sensors with a higher spatial resolution as

COSMO-SkyMed (2007-2010) and TerraSAR-X (2007) opened new perspectives in the observation of ancient complexes. In relation to the subsurface observation of archaeological marks, we need to refer to SAR polarimetric sensors. As already introduced, SAR sensors could have a very high potential in the detection of underground structures as a result of their penetration capabilities, according to their wavelength, potential that increases with polarimetric SAR sensors, which are able to derive electromagnetic properties of the target. This real new quality of the polarimetric technique shows its capability to look underneath the surface in precise conditions and in specific environment, giving information about the geometry of the structure, the orientation of the target as well as its geophysical properties. This characteristic, often considered a limit due to its restrictive applications, represents, on the contrary, a capable tool of investigation, especially in those areas where traditional field archaeology is impracticable for some reasons and optical aerial and satellite data are limited to day-time acquisitions and affected by cloud coverage. In this scenario, the present work demonstrates the promising capabilities of SAR polarimetric technique (see §7 and §8).

The proved effectiveness of polarimetric applications for different land studies, as the evaluation of RADARSAT-2 quad-pol data for functional assessment of wetlands for the Fougeres wetlands in Brittany (France) [8], or the detection of sub-soil moisture for the identification of paleo hydrology [9], does not exclude the possibility of a full positive exploitation of polarimetry also for archaeological investigations. Still many steps have to be done in this direction, considering the link between spatial resolution and structures dimensions and the penetration capability for each specific site. To this end, the development of a study towards a semi - automatic extraction of archaeological features from SAR data in a user-friendly methodology is required, also for a future spread of these promising remote sensing data in the whole archaeological community.

2.4 Overview of SAR Remote Sensing applications for archaeology

Satellite Synthetic Aperture Radar in archaeology provides a new and powerful tool in the study of Cultural Heritage, especially thanks to the possibility to

extract, in specific cases, information about ancient complexes behind the contemporary landscape.

Compared to optical imagery, SAR data require a more complex data processing, particularly evident for archaeology users. However, the very first applications of SAR for archaeology date back to the 1980s, when the first shuttle imaging SAR SIR-A allowed NASA researchers to identify unknown paleo-channels under the desert sand in Northern Sudan and Southern Egypt, discovery that lead to implications in the geo-archaeology of prehistoric environments of the Sahara [10]. SIR-C data allowed to detect a portion of the Great Wall of China [11] and to identify the convergence of several ancient roads in the city of Ubar, desert of Oman [12].

SIR-A and SIR-B wavelengths and multi polarization technology was then overcame by the NASA SIR-C/X-SAR, that lead to the discovery of a vat water management system under tropical forests in the archaeological complex of Angkor, Cambodia [13].

The Shuttle SAR Topography Mission SRTM (2000) provided and still provides SAR-based products that are used in archaeology and landscape studies, thus assuring a virtual survey of large areas for the detection of huge archaeological features. SAR satellite for archaeology are still in an experimental stage, even though it offers a great potential for applications ranging from the detection of ancient features and sites, the reconstruction of former landscape, the monitoring and the preservation of archaeological remains.

The reason for using SAR in archaeology is based on the different scattering characteristics that different surfaces and features present. Moreover, based on the given SAR observation parameters (wavelength range (band), polarization and incidence angle), the backscattering coefficient provides information about roughness, geometry and dielectric properties of the target.

The advent of the quite new generation of space borne radar sensors, such as ENVISAT/ASAR (2002-2012, C-band, dual pol), ALOS PALSAR (2006-2011, L-band, quad pol), Radarsat-2 (2007, C-band, quad pol), COSMO-SkyMed (2007, X-band, dual-pol), TerraSAR-X (2007, X-band, dual pol) opened new application possibilities for archaeology. In particular, COSMO-SkyMed and TerraSAR-X

sensors offered a very high spatial resolution, even though they both have a limited penetration capability [14] (Table 2.1).

SAR sensors	Band	Polarisation	Incidence angle	Spatial resolution (mt)	Organisation	Launch year
SIR-A	L	HH	45°	30	NASA	1981
SIR-B	L	HH	20° - 60°	30	NASA	1984
ERS-1	C	VV	24°	25	ESA	1991
JERS-1	L	HH	35°	18	NASDA/JAXA	1992
SIR-C	CL	All	17° - 60°	25	NASA	1994
X-SAR	X	VV	17° - 60°	25	DLR/ASI	1994
ERS-2	C	HH	24°	25	ESA	1995
ENVISAT ASAR	C	VV, HH, VV/HH, HV/HH, VH/VV	20° - 45°	30	ESA	1998
ALOS PALSAR	L	HH, HV, VH, VV	20° - 55°	10 - 100	JAXA	2006
RADARSAT-1	C	HH	10° - 60°	8 - 100	CSA	1995
RADARSAT-2	C	HH, HV, VH, VV	18° - 52°	1.6x0.8 – 160x100	MDA/CSA	2007
COSMOSkyMed	X	HH, VV / H, HV/ VV, VH	20° - 60°	1 - 100	ASI/MUR/MOD	2007 - 2010
TerraSAR-X	X	Single, dual	20° - 60°	1 - 16	DLR/ BMBF	2007

Table 2.1 : SAR Systems parameters

2.5 Examples of SAR applications for archaeology

In the following section, the more recent examples of SAR applications for archaeology are shown. They give an idea of the current state of the art in the field.

2.5.1 Archaeological site detection: a case study from Egypt

L-band HH polarization of ALOS PALSAR sensor capability for archaeology has been studied in a joint research by the University of Tokai, the National Authority for Remote Sensing and Space Science (NARSS) and the Japan Aerospace Exploration Agency (JAXA). The L-band is known to be able to penetrate the

sand layer of the extremely arid desert, thus permitting the discovery of previously unknown ruins buried in the ground. In particular, two ancient Egyptian complexes ruins (Site No. 29 and Site No. 39), buried in the desert at the Necropolis of Memphis, were successfully discovered. The discovery of these ruins demonstrates the effectiveness of detecting ruins in the desert by means of satellite L-band HH polarization.

With the aim of establishing if space borne SAR could be an effective general system for detecting ruins, clarifying the relationship between the SAR system parameters and the ones of the target, in this case the ruins, the research group focused the attention on SAR incident angle, which has been noted to have a great impact on the detection of ruins.

A visual interpretation of L-band HH polarization PALSAR images at different incident angles and observation directions was performed, and together with ground truth results of the actual ground structure, composition, and moisture content, the influence factor of each parameter on the search for ruins was investigated. One of the most difficult obtaining parameter they considered is the one of the contemporaneity of acquisition of data and ground survey, which in this case, was possible as PALSAR data observation was carried at the same time as ground truth.

The analysed data of this case study were five ALOS PALSAR images acquired between August 2006 (50.8° and 36.9° ascending mode) and August 2007 (off-nadir angle: 34.3° descending mode), one SIR-C image of 1994 (April) and two JERS-1/SAR of 1994 (August/November), used as validation of ALOS PALSAR results. Moreover, ground truths of soil moisture content were carried out between February 2006 and July 2007, so to investigate the relation between soil moisture content and SAR backscattering strength. From February 21st, 2006, the soil moisture content of the target area was measured four times. Of these, the three measurements on August 12th and 14th, 2006, and July 27th, 2007, were scheduled to coincide with PALSAR observations. The measured soil moisture content was in the range from 0% (Site No. 39: July 27th, 2007) to 6.3% (Site No. 29: August 14th, 2006).

According to previous observation results from JERS-1/SAR and SIR-C, the so called Site No. 29 is identifiable in images acquired at JERS-1/SAR's off-nadir

angle of 35.0°, while Site No. 39 is identifiable in images acquired at only SIR-C's off-nadir angle of 61.5° (Figure 2.9). Hence, the researchers stated that incident angle is considered to have a strong impact on the detectability of buried ruins.

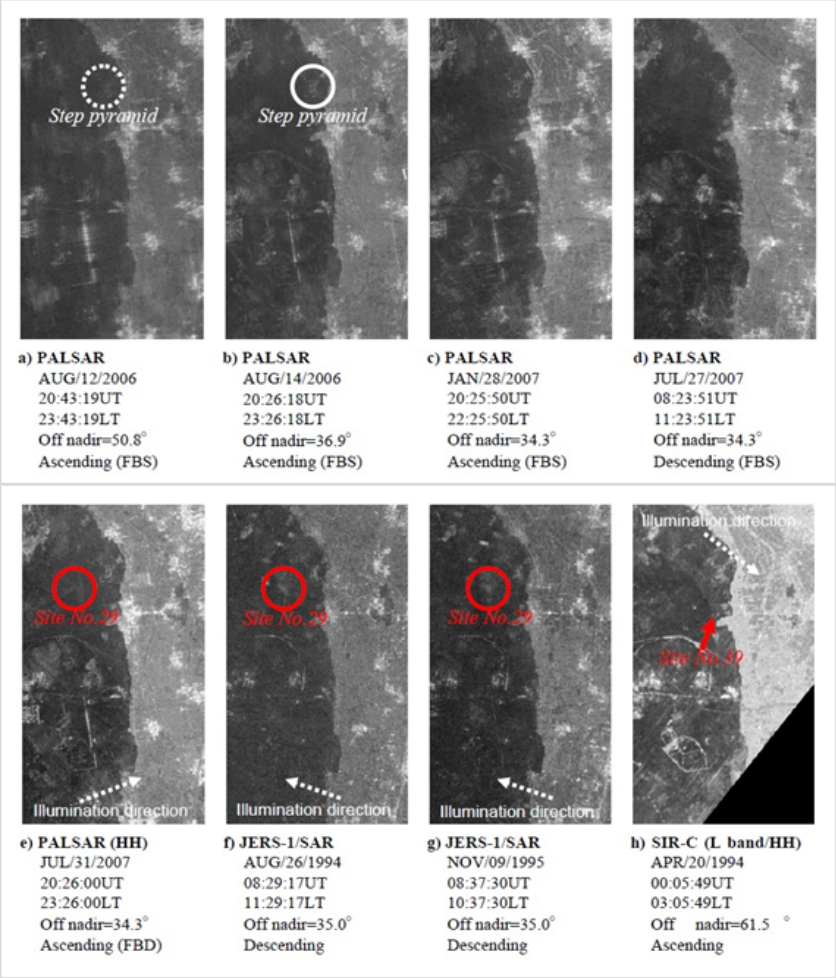

Figure 2.9 : Archaeological structures in the data collection © Masahiro et al.

They observed two PALSAR images of August 2006, at off-nadir angles of 50.8° and 36.9° (both with only HH polarization). Generally, since L band SAR can penetrate a layer of sand under arid conditions, the back scattering coefficient is small for empty desert, which appears dark in the images; on the other hand, the back scattering coefficient is comparatively large for most artificial structures such as buildings and roads, which appear light in the images. PALSAR data obtained from an observation mode with an off-nadir angle of more than 41.5° suffer from range ambiguity due to the transceiver characteristics of the sensor, and it is considered that removing this noise is not possible. Nonetheless, the most well-known of the large ruins, the pyramids, are visible in the image acquired on July

31st, 2007, at an off-nadir angle of 34.3°. This data differs from other data in that the image was taken in the HH/HV fine beam double (FBD) polarization mode.
A further factor they consider was both the illumination and the orientation effect. The illumination direction of JERS-1/SAR, which contributed to the discovery of Site No. 29, was approximately WNW (descending mode); however, the existence of Site No. 39 could not be identified from this image. On the other hand, the illumination direction of SIR-C, which contributed to the discovery of Site No. 39, was approximately SE (ascending mode), but the existence of Site No. 29 could not be identified.
This is likely attributable to the influence of illumination direction of SAR. Site No. 29 was identifiable in 2 scenes from JERS-1/SAR that were acquired in descending mode, as well as from PALSAR in ascending mode (July 31st, 2007), and thus the influence of the SAR observation direction on the discovery of the ruins is considered small (Figure 2.9) [15].

2.5.2 The Archaeological Heritage of Nazca, PERU

Nazca lines and their environment are investigated since long time by archaeologists and specialists of remote sensing techniques. EO optical imagery already provided information about anomalies attributable to buried settlements, looting activities over the area, hydraulic infrastructure. The researchers of British Geological Survey of NERC (Natural Environmental Research Council, UK), the Institute for the Conservation and Valorization of Cultural Heritage (ICVBC-CNR), the Institute for Archaeological and Monumental Heritage (IBAM-CNR, Tito Scalo, Italy) and the Institute of Methodologies for Environmental Analysis (IMAA-CNR, Tito Scalo, Italy), exploited eight ENVISAT ASAR IS2 descending images (February 2003 - November 2005) and five corresponding ascending imagery (July 2005 – November 2007) [16].
The nominal ground range resolution of about 30 m is not the suitable one for archaeological pattern recognition. Nevertheless, it gave information about the former environment of the observed area, including ancient waterways and sources of irrigation (strategic for such an arid region) and about the preservation conditions, as well as the monitoring of looting activities and their effects on cultural heritage.

The analysis performed over a sector of Nazca lines and other ancient features (the *puquios* of Rio Taruga and the archaeological site of Cahuachi) confirmed that the identification of surface marks analyzing SAR amplitude could help in recognition of ancient patterns. The time series extracted from a Multilook Intensity (MLI) generation, as well as the observation of σ^0 (sigma nought) values variations, helped in distinguish over the sites geoglyphs from the surrounding bare soil or a *puquio* (horizontal water wells aqueducts) from neighboring vegetation, underlining the helpfulness of SAR amplitude information for archaeology (Figure 2.10). Moreover, other remote sensing studies carried out by Lasaponara et al 2012, already suggested the presence of illegal excavation in the site of Cahuachi, highlighted by a variation of σ^0 values in the more recent study of Tapete et al, 2013 [17].

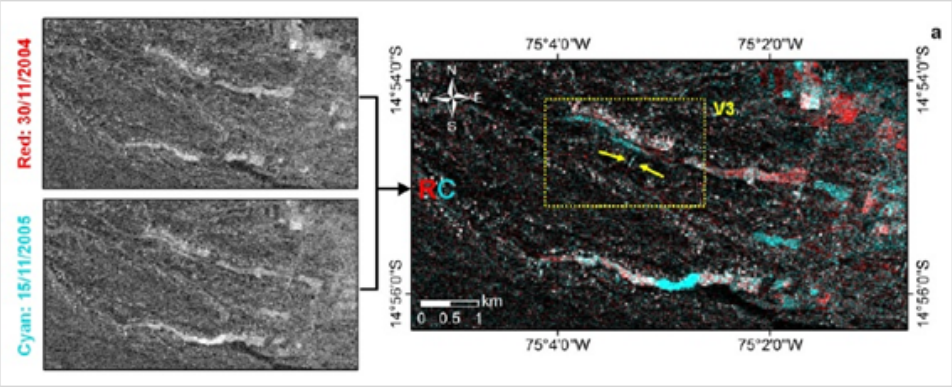

Figure 2.10 : RC colour composite of the ASAR MLIs acquired on 30/11/ 2004 and on 15/11/ 2005. The yellow arrows indicate the location of an ancient puquios. © Tapete et al, 2013

Earth Observation techniques can help to reconstruct environmental and cultural lasdscape, their evolution in time, climate factors that affect them and to evaluate the natural processes impact over the cultural heritage. This is truer in those areas where the construction material of ancient buildings is made of the same local natural material. The previous studies over the Nazca region were based on a change detection approach based on interferometric coherence, which offered an effective indication of ground changes between two different SAR images. To complete this approach, limited by vegetation cover, Cigna et al. proposed to apply a change detection approach based on SAR amplitude, that can provide further insights in changes occurred over an area, by observing temporal

variations of the backscattering coefficient of the target surface. The temporally averaged radar signatures of the observed targets highlighted the signatures of different surfaces, as well as colour composite between different scenes showed modification occurred in time over the area. Indeed, γ^0 changes can be related to the movements of surface materials producing a consequent variation of the local incidence angles of newly developed radar-backscattering surfaces.

2.5.3 The case study of the Roman Fortress of Qreiye, SYRIA

TerraSAR-X applications for archaeology are quite new in the remote sensing for archaeology scenario.

Although the technical characteristics of TerraSAR-X sensor are not the suitable one for archaeological prospection, apart from its spatial resolution of up to 1m, an exploitation attempt of this kind of data has been carried out by Linck et al, over the archaeological site of Qreiye, Syria. Antoine Poidebard already investigated the archaeological area in 1929 by means of aerial photographs, showing the presence of the ancient Roman fortress of Qreiye, in the framework of his systematic survey of Syrian Desert.

The disadvantage of this sensor is that its X-band waves have a wavelength of around 3 cm. According to electromagnetic theory, the penetration depth is inversely proportional to the wavelength, so only a limited penetration of the subsoil is possible at this wavelength. However, Linck et al, have tried to demonstrate the ground penetration capabilities of X-band, using as guideline the results of a ground-penetrating radar campaign performed over the area.

The area of interest, located on the right bank of the river Euphrates, presents a various morphology, interested by alluvial flooding ancient phenomena and sedimentary rocks. The researchers analysed seasonal climate conditions, noting not so intense rain phenomena especially in summer time, and absence of precipitation for the considered acquisition period, the spring of 2012. These considerations led the researchers to conclude that the conditions of the area would have been suitable for testing the penetration depth of TerraSAR-X signal [18].

The researchers tested a stacking series of nine consecutive TSX images between February and May 2012. The images were acquired in a horizontal polarization

and the experimental 300MHz bandwidth high-resolution Spotlight mode. By using the first acquisition as reference, the other eight have been resampled with a cubic resampling method to the image bounds and the pixel spacing of this master image and compiled in a multichannel stack. From this stack different multitemporal (three, six and all nine dates) average images are calculated by evaluating the unweighted average of the scenes on the basis of the radar brightness $\square_0$ with consideration of the inclination angle, calibration constant and intensity.

The researchers stated that as the optical image of OrbView-3 observed does not show any superficial archaeological remains in the area of the fortress, except the enclosure wall as a slight elevation, all structures visible in the SAR image have to be due to buried ancient structures.

Analyzing then the available results GPR survey provided, they follow the same archaeological features over TerraSAR-X data, affirming that all the detected marks belong to structures appearing for the first time at a depth of 20 cm, as the GPR can detect further anomalies at a depth of 30 cm (Figure 2.11). On these bases, Linck et al proposed a shallow penetration of X-band waves in dry desert soils.

Figure 2.11 : TerraSAR-X of the Roman Fortress overlaid with the digital interpretation of the visible remains. © Linck et al, 2012

2.6 Conclusions

Since the XVIII century, the aerial observation of landscapes provided a different point of view for the study of territorial analysis. Soon, aerial photographs became the new method of investigation for archaeologists, who started to derive information about ground anomalies linked to ancient features. Different kind of ground anomalies were thus classified and became the basis of the aero photography interpretation. With the arrival of satellite images, investigation possibilities increased in archaeology, first with optical data, then with SAR sensors. The exploitation of optical data for archaeological purposes has been widely applied, thanks to the very high spatial resolution they present. Concerning SAR sensors, which today still present a not enough spatial resolution, the analysis is still at its initial level. Their capability to penetrate ground and provide 24h acquisitions constitutes a high potential for archaeological investigation. Case study from different areas of the world have been here presented to show how SAR data analysis for archaeology requires a specialized knowledge and a not-immediate visual interpretation.

Today, there is still a lack of correspondence between the great amount of SAR data and effective methods to extract information linked to past human activity in the environment. The future scientific challenge could be the communication between them for the conservation and preservation of Cultural Heritage. The promising usefulness of SAR sensors for archaeological investigation is to be exploited and spread among archaeologists as well as Earth Observation users to manage World Heritage sites.

This page intentionally left blank

Chapter 3

SAR Remote Sensing and Polarimetry

In the present chapter, an overview about SAR systems and the polarimetric technique employed for the research are presented.

3.1 Radar remote sensing advantages

As already pointed out, definition of remote sensing is linked to the science of obtaining and interpreting information from a distance, using sensors that are not in physical contact with the object being observed [1]. This term is generally used for methods that detect and measure electromagnetic energy (Figure 3.1). Images acquired by airborne are an important source of information for aspects that go from the monitoring of natural and human disasters, to urban expansion, to the study of the environment in general. According to the necessity, dedicated sensors are realised, whose characteristics are strictly linked to the scope they are built for. For example, in case of environmental changes, where a huge area is involved in the observation, satellites with a very high spatial resolution will not be necessary. At the contrary, in studies such as archaeology, a high/very-high spatial resolution will be essential in order to identify ground anomalies or structures already surfaced to be studied by a remote approach.

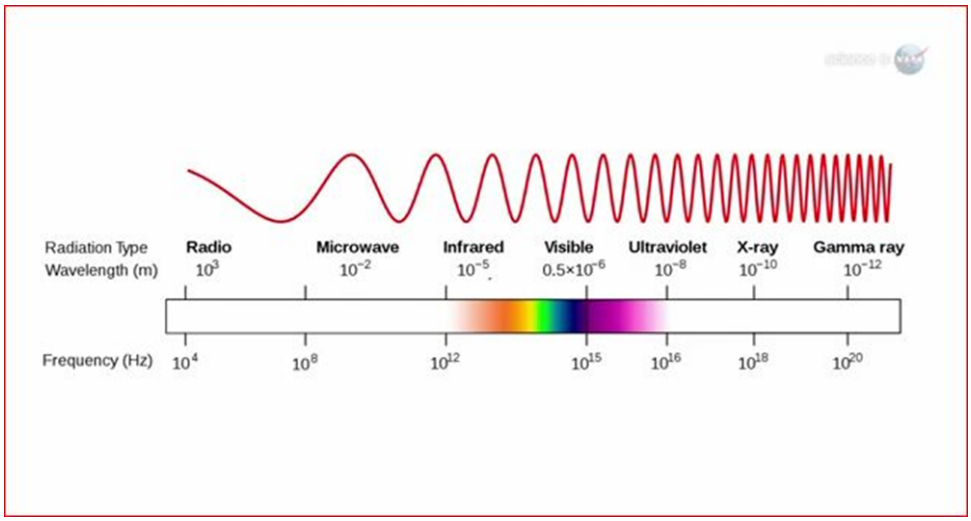

Figure 3.1 : Electromagnetic spectrum

These general characteristics above indicated are valid both for radar and for optical sensors. While optical sensors need the light for illuminating the Earth surface, radar sensors have the peculiarity of illuminating themselves the scene by electromagnetic waves transmitted toward the ground and backscattered to the sensor. Radar systems present several advantages that render this instrument of analysis very attractive. These advantages, varying according to the system frequency, are listed below:

- small sensitivity of clouds and light rain (low frequency);
- independence of Sun illumination;
- no effects of atmospheric elements (high frequency);
- sensitivity to surface roughness (high frequency);
- capability in distinguishing dielectric properties;
- accurate measurements of distances;
- ground and vegetation penetration (low frequency).

In spite of all these positive aspects, there are some characteristics that make its use exclusive only to a part of the scientific world. This is due to:

- data of not immediate comprehension, as it is not what we are used to watch in an image;
- speckle noise effects that makes the image difficult to be analysed;
- distortions of the image that falsify the reality.

In this scenario SAR (*Synthetic Aperture Radar*) is placed. SAR is intrinsically the only viable and practical imaging radar technique to achieve high spatial resolution, also from space-platforms. SAR synthesizes a long aperture by the motion of the radar platform. Synthetic Aperture Radar imaging is a well developed coherent and microwave remote sensing technique for providing large scaled 2-D high spatial resolution images of the Earth's surface reflectivity.

The imaging SAR system is an active radar system operating in the microwave region of the electromagnetic spectrum, usually between P-Band and Ka-Band. It is usually mounted on a moving platform (airplane, UAV, space-shuttle or satellite) and operates in a side-looking geometry with an illumination perpendicular to the flight direction [19].

3.2 Radar viewing geometry

Imaging geometry in a radar system is different from the optical one (Figure 3.2). A radar platform flights forward *a flight direction* (A) with the *nadir* under the platform (B). The antenna transmits the microwaves in a *side-looking* way to the ground, illuminating a ground portion called *swath* (C). This oblique view is typical of radar systems.

The signal coming back to the sensor (echo) is backscattered and recorded in a fraction of second later by the same transmitting antenna. According to the time delay between the transmission of the electromagnetic waves and their returns to the sensor, distance from the sensor and their locations are determined, creating thus, a two-dimensional image of the surface.

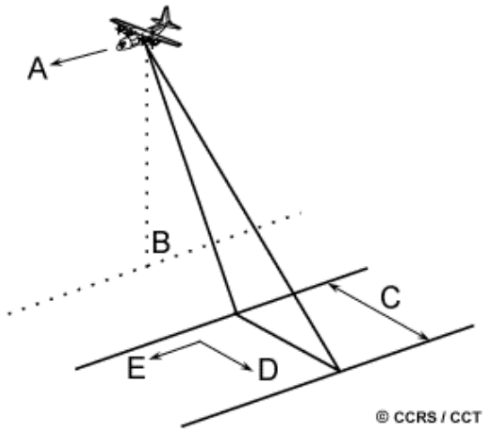

Figure 3.2 : Radar viewing geometry

The local *incidence angle* (□) is referred to the angle between the radar line of sight and the normal to the surface (Figure 3.3, A). The radar *look angle* (Figure 3.3, B), increases moving across the swath. In the *near range* (the portion of the swath closest to the sensor) the viewing geometry is considered to be steep, while in the *far range* (the farther part of the swath) the viewing geometry is shallow.

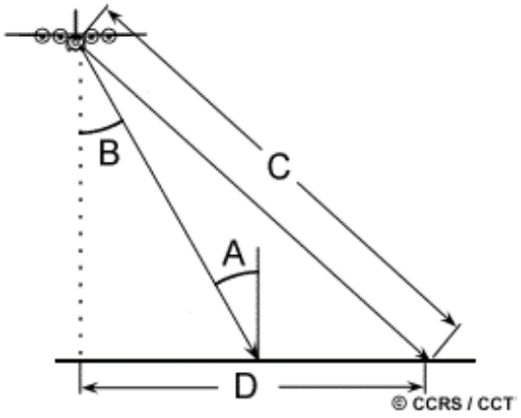

Figure 3.3 : Incidence angle

At all ranges the radar antenna measures the radial line of sight distance between the radar and each target on the surface. This is the *slant range* distance in the image (Figure 3.3, C), different from the *ground-range* (Figure 3.3, D) that is the true horizontal distance along the ground corresponding to each point measured in the slant-range.

3.3 SAR resolution

Range or *across-track* resolution is dependent on the pulse length (Figure 3.4, P).

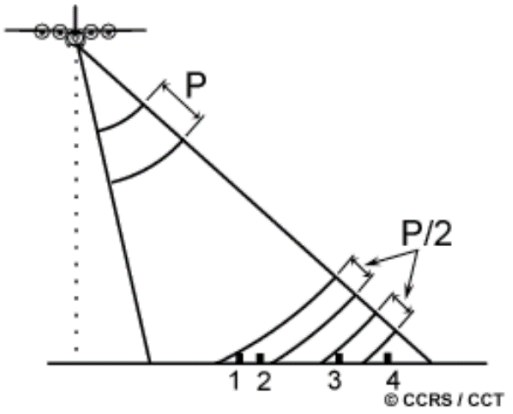

Figure 3.4 : Range or across-track resolution

Two separated targets will be distinguished in the range dimension if their distance on the ground is bigger than half the pulse length. An example is given in

Figure 3.4, where targets 1 and 2 will not be detected as separated, while targets 3 and 4 will be well distinguished.

Azimuth or *along-track* resolution is determined by the angular width of the radiated microwave beam and the slant range distance. This beam-width (Figure 3.5, A) is a measure of the width of the illumination pattern. As visible, radar illumination propagates as the distance from the sensor increases. As consequence, the azimuth resolution decreases. Targets 1 and 2 are separable (near range) while targets 3 and 4 will not.

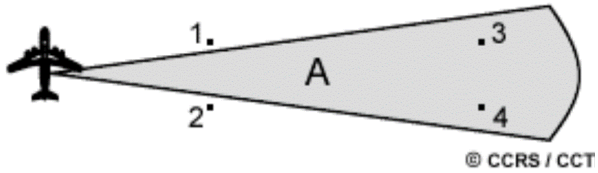

Figure 3.5 : Radar illumination propagation

As azimuth resolution in azimuth requires large antennas, the solution to achieve high resolution without the use of large antennas is given by the concept of "synthetic aperture", which is based on the construction of a longer effective antenna by moving the real sensor antenna along the flight direction. The azimuth resolution is determined only by the physical site of the real antenna of the radar system and is independent of range and wavelength. Therefore, the azimuth resolution is equal to half the length of the real antenna on board. Apart from these resolutions mentioned above there are other three important characteristics of a SAR system to be considered. These are the spatial, spectral, temporal and radiometric resolutions. Each of them provide important information that can be selected according to the necessities of the research.

Spatial resolution places limits on which information we can derive from remotely sensed images. Spatial resolution, in fact, is a measure of the spatial details perceived in an image, depending on technical properties of the sensor and altitude of the sensor. In digital images, spatial resolution is expressed as ground dimension of an image pixel. The smaller is the target distinguishable in the image, the higher is the spatial resolution of the sensor.

Temporal resolution is linked to the time-interval separating successive acquired images. This kind of resolution is very useful especially considering the dynamic

surface environment of the Earth. It is important for the study of changes occurring in time, especially considering the necessity of repeated observations over area interested, as instance, by floods or earthquakes.

Radiometric resolution is referred to the range of brightness of the system that, in the case of a radar sensor, amounts to 100.000 levels distinguishable. It is related to the sensor sensitivity in measuring the electromagnetic energy coming back to the sensor from each target of the scene. However, as the human eye is able to detect only 40 levels, radar images are sampled at 16 or 8 bits [20].

3.4 SAR geometric distortions

As optical images, also radar is affected by distortions. These distortions have to be taken into account according to the morphology of the area analysed.

The first distortion mentioned is the one due to radar sensors geometry of acquisition : the *slant-range scale distortion* (Figure 3.6). This distortion is due to the way of observation of the sensor that is side-looking. Because of this configuration, the sensor does not measure the real distance of the objects, thus targets in the near range will appear compressed compared to the ones located in the far range.

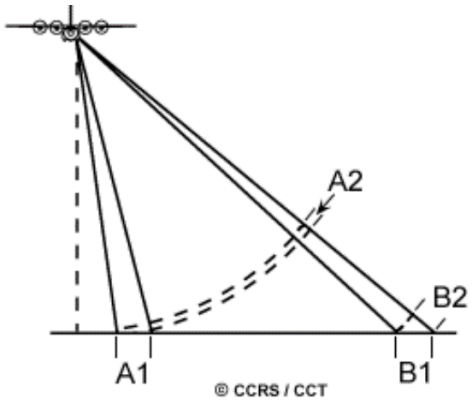

Figure 3.6 : Example of slant-range scale distortion

A second distortion is the *relief displacement*. This displacement occurs perpendicular to the flight path and is typical for targets of outstanding height that assume a laid down position. Consequence of this distortion are the *foreshortening* and the l*ayover*.

The first one is probably the most striking feature in SAR images concerning the geometry effects in range direction. This effect is visible as "compression" of the

image. This is caused because the SAR measures signal travel time and not angles as optical systems do. As basics of SAR measuring, the time delay between the radar echoes received from two different points determines their relative distances in the image. This effect is displayed when radar microwaves reach first the base (Figure 3.7, C, A) and then the peak of it (D, B). The slope will appear compressed and its length falsify (Figure 3.7, C'D', A'B'). Depending on the angle of the mountain and on the radar incidence angle, the severity of the foreshortening varies, until the overlapping between the base and the peak of the mountain (Figure 3.7, C'D'). Foreshortening effects are greatest in the near range and less pronounced in the far range.

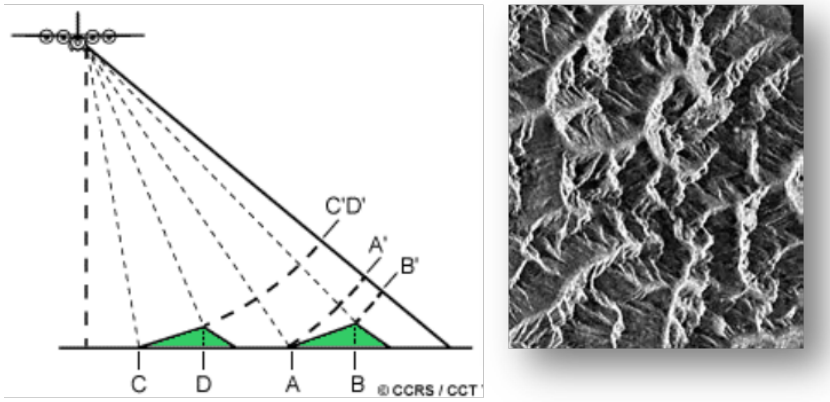

Figure 3.7 : Example of foreshortening

Layover (Figure 3.8) occurs when, in the case of a very steep slope, targets in the valley points of mountains have a larger slant-range than the mountain top, then the foreslope is reversed in the slant range image.

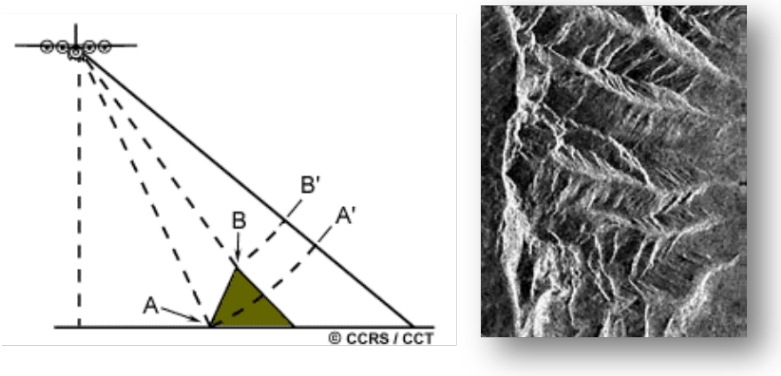

Figure 3.8 : Example of layover

Thus, the ordering of surface elements on the radar image is the reverse of the ordering on the ground: radar microwaves reaches the top of a tall target before its base. The signal coming from the top of the feature will be received first. The result is a mountain, for example, displaced towards the radar and "lays over" the base of the target.

Radar shadow (Figure 3.9) is the last distortion in radar images. This distortion occurs when radar microwaves are not able to illuminate the ground. It is visible for those high targets (e.g. mountains) beside which radar signal does not arrive. Therefore, this distortion corresponds to an absence of information and on the radar image is detectable as a black feature that remembers the shadow visible on optical images. The radar shadow can help us in understanding where the microwaves are coming from and the relief height observed [20].

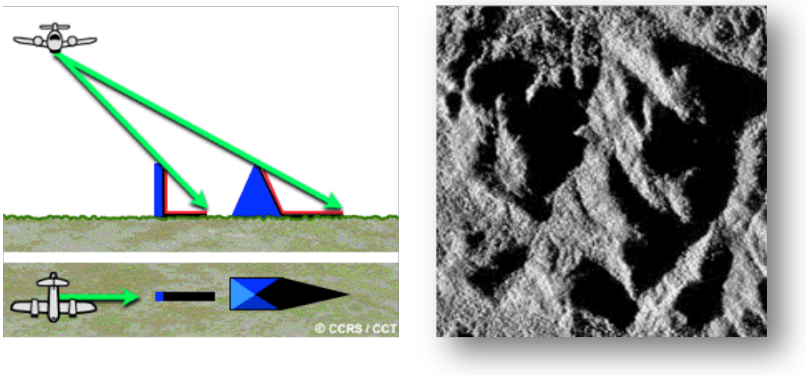

Figure 3.9 : Example of radar shadow. Black parts in the image and in the drawing do not contain information

3.5 Image appearance

Targets inside an image can vary in brightness. This variation depends on the quantity of the backscattered energy to the radar. Brightness intensity depends on how the microwaves interact with the surface depending, however, on several parameters. These parameters are linked, in fact, both on the characteristics of the radar system (polarization, viewing geometry, frequency…) and on surface characteristics (land cover type, relief, topography…). Among these lasts, the most important are surface roughness, radar viewing and surface geometry relationship, moisture content and electrical properties of the target.

Surface roughness varies according to the average height variations of the surface. One surface can be defined rough or smooth on the base of the wavelength and

the incidence angle. For example, a surface is defined smooth if the variations in height are smaller than the radar wavelength, while it is said rough if the height variations are larger than the wavelength. A smooth surface causes specular reflections and, as consequence, only a small part of the transmitted energy is backscattered to the sensor. A rough surface, at the contrary, scatters the energy equally in all the directions and a significant part of it is backscattered to the sensor.

3.6 Target interaction

There exist different kinds of reflection and they depend on the surface characteristics of the target, on the position of each target and on the shape of the illuminated targets. According to the typology of interactions between the target and the signal, different reflections are possible. A corner reflection (*double bounce*, Figure 3.10) occurs when two or more surfaces are positioned at right angles.

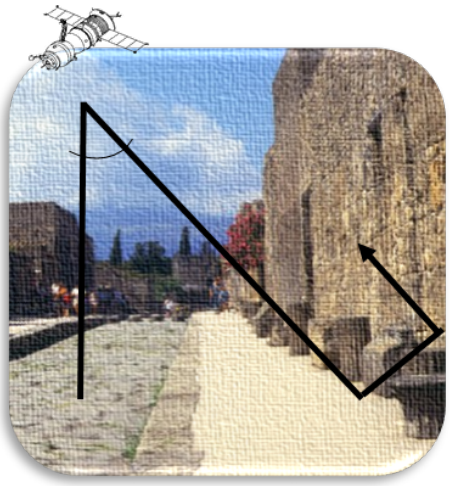

Figure 3.10 : Example of double bounce

This surface disposition causes most of the radar energy reflected back to the antenna due to the double bounce (or more) reflection. This kind of scattering mechanism is typical of urban environments (e.g. buildings, streets, bridges…) and appears in the image as very bright targets.

In the case of forests or areas where vegetation is present, a different scattering mechanism occurs. This is the *volume scattering* (Figure 3.11). It consists of multiple bounces and reflections from different components within the volume. In a forest, for example, this scattering mechanism may come from leaf canopy at the

top of the trees, the leaves and branches further below, tree trunks and soil at the ground level. Related to this scattering mechanism, brightness in the images varies according to quantity of the energy scattered out of the volume and back to the radar.

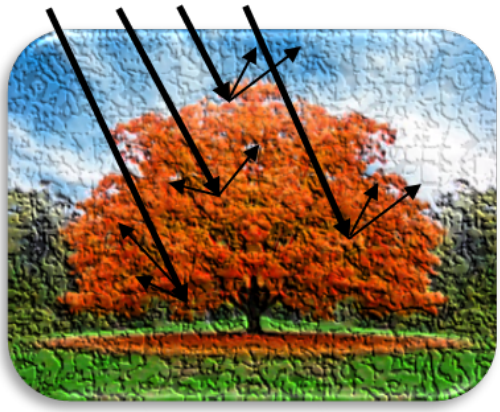

Figure 3.11 : Example of volume scattering

The last typology of backscatter is the surface scattering mechanism (*single bounce*, Figure 3.12). This backscatter occurs when a target is moist, wet or rough. In this case, if the reflection is specular, little of the energy sent by the sensor comes back. The signal will be mostly or totally lost according on how rough the material appears to the radar [20]

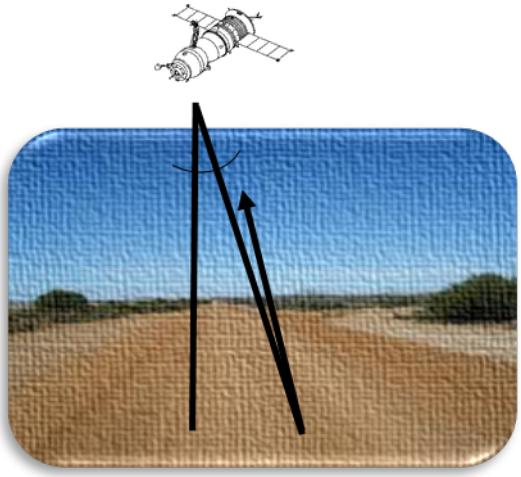

Figure 3.12 : Example of single bounce

Following the dissertation on Radar Remote Sensing, next paragraphs focus on the basic concepts of Polarimetry technique. The different polarimetric descriptors analysed in the PhD research are here presented and discussed.

3.7 Electromagnetic waves and Polarisation

As electromagnetic waves have intrinsic vector nature, the concept of "wave polarization" is necessary for the comprehension the complete description of propagation and of scattering phenomena.

An electromagnetic plane wave is composed of Electric and Magnetic Field vectors varying in time and space in a plane perpendicular to the direction of propagation.

In free space, these two fields propagate at the speed of light and according to the Maxwell's equations are orthogonal. For this reason, the electromagnetic wave behaviour can be observed taking into account the electric field vector as a function of time and space and takes the vectorial form:

$$\vec{\boldsymbol{E}}(z,t) = \begin{bmatrix} E_{0x}\cos(\omega t - kz + \delta_x) \\ E_{0y}\cos(\omega t - kz + \delta_y) \\ 0 \end{bmatrix}$$

At a fixed time $t = t_0$, the electric field is composed of two orthogonal sinusoidal waves with, in general, different amplitudes and phases at the origin, as shown in Figure 3.13.

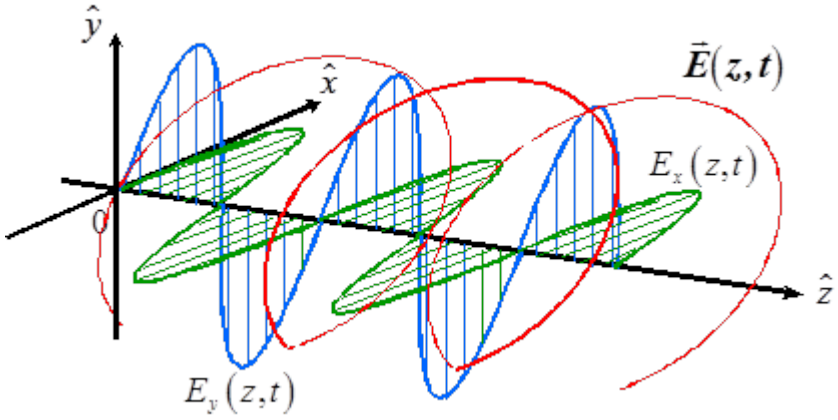

Figure 3.13 : Spatial evolution of a circularly polarized plane wave © Lee-Pottier 2009

In the general case, the spatial evolution of a plane monochromatic wave follows a helical trajectory along the $\hat{\mathbf{z}}$ axis. From a practical point of view, three-dimensional helical curves are difficult to represent and to analyse. This is why a

characterization of the wave in the time domain, at a fixed position, is generally preferred [21] [22].

The temporal behaviour is then studied within an equi-phase plane, orthogonal to the direction of propagation and at a fixed location along the $\hat{\mathbf{z}}$ axis. As time evolves, the wave propagates «through» equi-phase planes and describes a characteristic elliptical locus as shown in Figure 3.14, which is called the polarisation ellipse that describes the wave polarisation [19] [23].

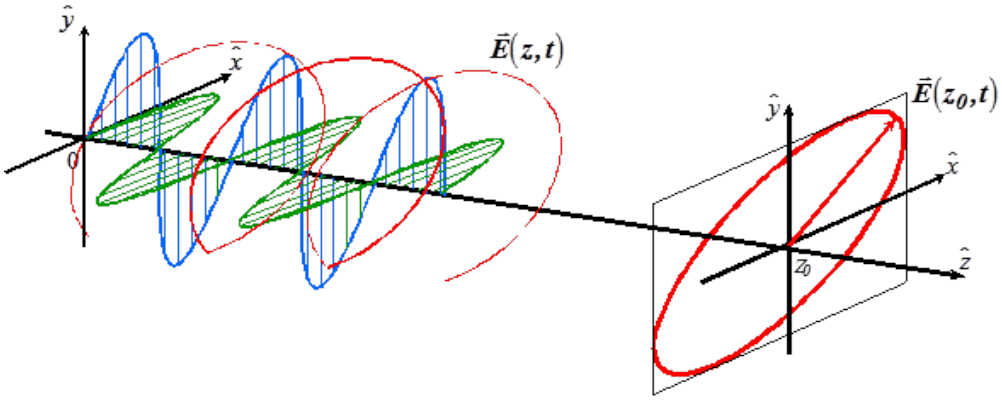

Figure 3.14 : Temporal trajectory of a monochromatic plane wave at a fixed abscissa $z = z_0$ © Lee-Pottier 2009

3.8 Scattering matrix

An electromagnetic plane wave traveling in time and space can reach a particular target, and then interacts with it, as shown in Figure 3.15.

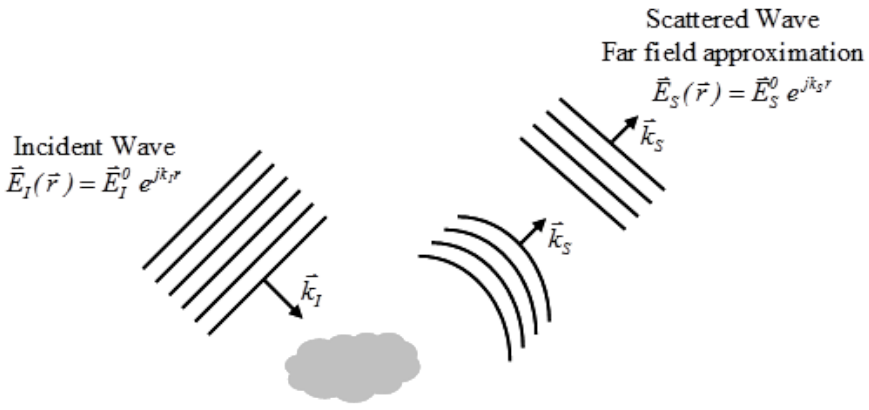

Figure 3.15 : Interaction of an electromagnetic wave and a target © Lee-Pottier 2009

The most fundamental form to describe the interaction of an electromagnetic wave with a given target is the so-called radar equation [24][24]. This equation establishes the relation between the power that the target intercepts from the

incident electromagnetic wave and the power reradiated by the same target in the form of the scattered wave.

The radar cross-section □, determines the effects of the target of interest on the balance of powers established by the radar equation given by

$$\sigma = 4\pi r^2 \frac{\left|\vec{E}_S\right|^2}{\left|\vec{E}_I\right|^2}$$

If we denote by p the polarization of the incident field and by q the polarization of the scattered field, we can define the following polarization dependent radar cross section

$$\sigma_{qp} = 4\pi r^2 \frac{\left|\vec{E}_{S_q}\right|^2}{\left|\vec{E}_{I_p}\right|^2}$$

The elements of the scattering matrix can be related with the radar cross section of a given target as follows:

$$\sigma_{qp} = 4\pi \left|S_{qp}\right|^2$$

It follows that In the Cartesian basis or in the Horizontal-Vertical basis, the 2x2 complex back-scattering S matrix can be expressed as [25]

$$\boldsymbol{S}_{(\hat{x},\hat{y})} = \begin{bmatrix} S_{XX} & S_{XY} \\ S_{YX} & S_{YY} \end{bmatrix} = \boldsymbol{S}_{(\hat{u}_H,\hat{u}_V)} = \begin{bmatrix} S_{HH} & S_{HV} \\ S_{VH} & S_{VV} \end{bmatrix}$$

The elements S_{HH} and S_{VV} produce the power return in the co-polarized channels (HH = horizontal transmitting and horizontal receiving, VV = vertical transmitting and vertical receiving) and the elements S_{HV} and S_{VH} produce the power return in the cross-polarized channels (HV = vertical transmitting and horizontal receiving, VH = vertical transmitting and horizontal receiving). If the role of the transmitting and the receiving antennas are interchanged, the reciprocity theorem (in case of reciprocal propagation medium) requires that the back-scattering matrix be symmetric, with $S_{HV} = S_{VH}$ [19].

3.9 Polarimetric Coherency T matrix

The concept of "distributed target" arises from the fact that not all radar targets are stationary or fixed, but generally are situated in a dynamically changing environment and are subject to spatial and temporal variations. This can be analysed more precisely by introducing the concept of space and time varying stochastic processes where the target or the environment can be described by the second order moments of the fluctuations, which will be extracted from the polarimetric coherency T matrix given by [19]

$$\mathbf{T}_3 = \frac{1}{2}\begin{bmatrix} \left\langle |S_{XX}+S_{YY}|^2 \right\rangle & \left\langle (S_{XX}+S_{YY})(S_{XX}-S_{YY})^* \right\rangle & 2\left\langle (S_{XX}+S_{YY})S_{XY}^* \right\rangle \\ \left\langle (S_{XX}-S_{YY})(S_{XX}+S_{YY})^* \right\rangle & \left\langle |S_{XX}-S_{YY}|^2 \right\rangle & 2\left\langle (S_{XX}-S_{YY})S_{XY}^* \right\rangle \\ 2\left\langle S_{XY}(S_{XX}+S_{YY})^* \right\rangle & 2\left\langle S_{XY}(S_{XX}-S_{YY})^* \right\rangle & 4\left\langle |S_{XY}|^2 \right\rangle \end{bmatrix}$$

3.10 Polarimetric descriptors

The present paragraph describes and illustrates the most significant polarimetric descriptors that have been analysed in this research activity.

3.10.1 Pauli Decomposition

Pauli decomposition constitutes one of the first polarimetric descriptors that visualises polarimetric information coded as a colour.

This decomposition expresses the scattering S matrix as the complex sum of the Pauli matrices, where an elementary scattering mechanism is associated for each basis matrix, with:

$$\boldsymbol{S} = \begin{bmatrix} S_{HH} & S_{HV} \\ S_{VH} & S_{VV} \end{bmatrix} = \frac{a}{\sqrt{2}}\begin{bmatrix} 1 & 0 \\ 0 & 1 \end{bmatrix} + \frac{b}{\sqrt{2}}\begin{bmatrix} 1 & 0 \\ 0 & -1 \end{bmatrix} + \frac{c}{\sqrt{2}}\begin{bmatrix} 0 & 1 \\ 1 & 0 \end{bmatrix} + \frac{d}{\sqrt{2}}\begin{bmatrix} 0 & -j \\ j & 0 \end{bmatrix}$$

where a, b, c, and d are all complex and are given by

$$a = \frac{S_{HH}+S_{VV}}{\sqrt{2}} \quad b = \frac{S_{HH}-S_{VV}}{\sqrt{2}} \quad c = \frac{S_{HV}+S_{VH}}{\sqrt{2}} \quad d = j\frac{S_{HV}-S_{VH}}{\sqrt{2}}$$

The application of the Pauli decomposition to deterministic targets may be considered the coherent composition of four scattering mechanisms: the first being single scattering from a plane surface (single or odd-bounce scattering), the second being diplane scattering (double or even-bounce scattering), the third corresponding to volume scattering (random scattering) or oriented target scattering, and the final element being all the antisymmetric components of the scattering S matrix [19].

In the monostatic case, where $S_{HV}= S_{VH}$, the Pauli matrix basis can be reduced to the three first matrices, leading to d=0.

Consequently, an RGB image can be formed (Figure 3.16) with the intensities $|a|^2$, $|b|^2$ and $|c|^2$, which correspond to clear physical scattering mechanisms: respectively single bounce, double bounce, and volume scattering, with

$$|a|^2 = T_{11} = \frac{1}{2}|S_{HH} + S_{VV}|^2 = single\ bounce$$

$$|b|^2 = T_{22} = \frac{1}{2}|S_{HH} - S_{VV}|^2 = double\ bounce$$

$$|c|^2 = T_{33} = \frac{1}{2}|S_{HV}|^2 = volume\ scattering\ or\ oriented\ target$$

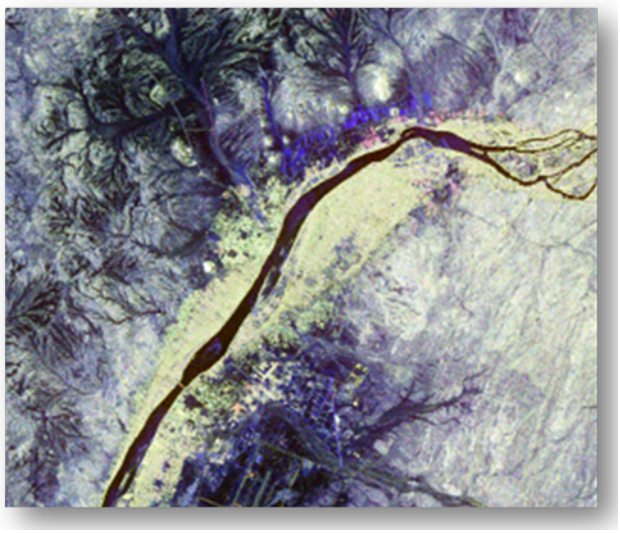

Figure 3.16 : Pauli decomposition RGB image : $|S_{hh} + S_{vv}|$ $|S_{hh} - S_{vv}|$ $|S_{hv}|$

Thus, the resulting colour image (Figure 3.16) can be employed, from a qualitative point of view, to interpret the physical information related to the scattering mechanisms that occurs in each pixel.

3.10.2 Entropy (H) and Alpha angle (□) polarimetric descriptors

In 1997, S.R. Cloude and E. Pottier proposed a method for extracting average parameters from experimental data using a smoothing algorithm based on second order statistics [26]. This method does not rely on the assumption of a particular underlying statistical distribution and so is free from the physical constraints imposed by such multivariate models. An eigenvector analysis of the 3x3 coherency T3 matrix is used since it provides a basis invariant description of the scatterer with a specific decomposition into types of scattering processes (the eigenvectors) and their relative magnitudes (the eigenvalues). From the eigenvalues, the entropy polarimetric descriptor (Figure 3.17, left) is defined with values ranging from $0 < H < 1$. This polarimetric descriptor provides information about the randomness of scattering mechanisms associated to the T_3 matrix.

If the polarimetric entropy H is low ($H < 0.3$), then the system may be considered weakly depolarizing and the dominant scattering mechanism in terms of a specifically identifiable equivalent point scatterer may be recovered. However, if the entropy is high, then the scatterer ensemble is depolarizing and there no longer exists a single equivalent point scatterer. In the limit case, when *H=1*, the polarization information becomes zero and the target scattering is truly a random noise process.

From the eigenvectors, it is possible to define a parameter named alpha angle (Figure 3.17, right) describing the backscattered phenomenon of the target, with values ranging from $0 < \square < 90°$.

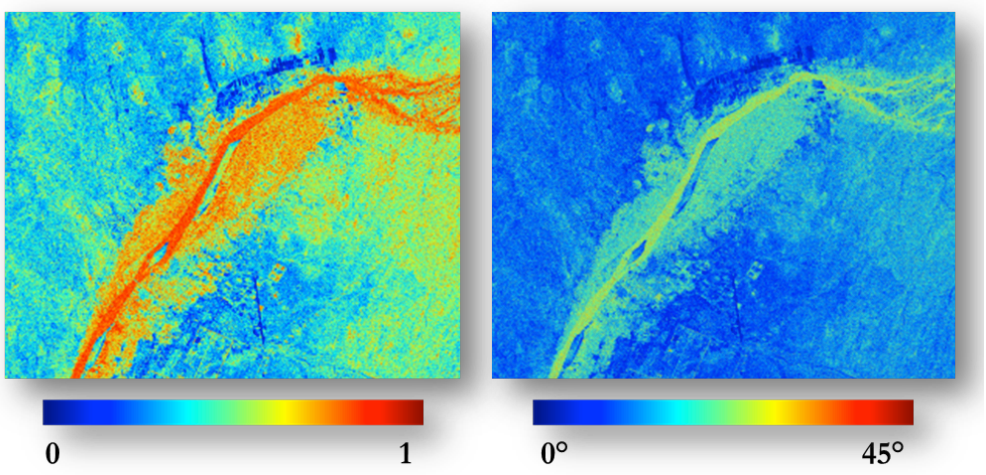

Figure 3.17 : Entropy (H) and Alpha Angle (□) visualisation

With □ = 0 the scattering mechanism corresponds to single bounce, while with □ = 90° the scattering mechanism corresponds to double bounce. Intermediate values (□ = 45°) corresponds to random scattering or volume scattering mechanism. In 1997, Cloude and Pottier proposed an unsupervised classification scheme based on the use of the two-dimensional H / □ plane, where all random scattering mechanisms can be represented [26]. The key idea is that entropy arises as a natural measure of the inherent reversibility of the scattering data and that the alpha angle (□) can be used to identify the underlying average scattering mechanisms. The H / □ plane is sub-divided into nine basic zones characteristic of classes of different scattering behaviour, in order to separate the data into basic scattering mechanisms, as shown in Figure 3.18.

The location of the boundaries within the feasible combinations of H and □ values is set based on the general properties of the scattering mechanisms. There is of course some degree of arbitrariness on the setting of these boundaries, which are not dependent on a particular data set.

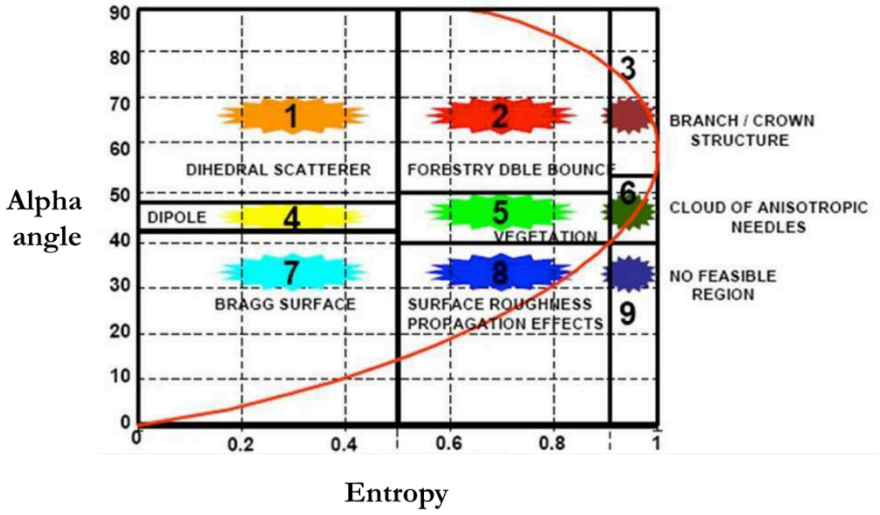

Figure 3.18 : H/Alpha plane © Lee-Pottier 2009

3.10.3 Shannon Entropy polarimetric descriptor

Since the publication of the H / A /□ decomposition in 1997, it is amazing to have seen all the research activities that have been conducted, based on the use of this original approach. Among them, one interesting approach has been selected,

revealing a specific scientific interest and presenting an important starting point for future development: the Shannon Entropy.

The *Shannon Entropy* (*SE*) has been introduced by J. Morio [27] [28] as a sum of 2 contributions related to: *intensity* (SE_I) and *polarimetry* (SE_P), given by

$$SE = \log\left(\pi^3 e^3 |\mathbf{T}_3|\right) = SE_I + SE_P$$

where SE_I is the intensity contribution that depends on the total backscattered power, and SE_P the polarimetric contribution that depends on the Barakat degree of polarization p_T. These two terms are given by:

$$SE_I = 3\log\left(\frac{\pi e I_T}{3}\right) = 3\log\left(\frac{\pi e \,\mathbf{Tr}(\mathbf{T}_3)}{3}\right)$$

$$SE_P = \log\left(1 - p_T^2\right) = \log\left(27\frac{|\mathbf{T}_3|}{\mathbf{Tr}(\mathbf{T}_3)^3}\right)$$

Figure 3.19 shows the Shannon Entropy (SE) parameter and the intensity (SE_I) and polarimetric (SE_P) contribution terms when applied on the Gebel Barkal site PolSAR image.

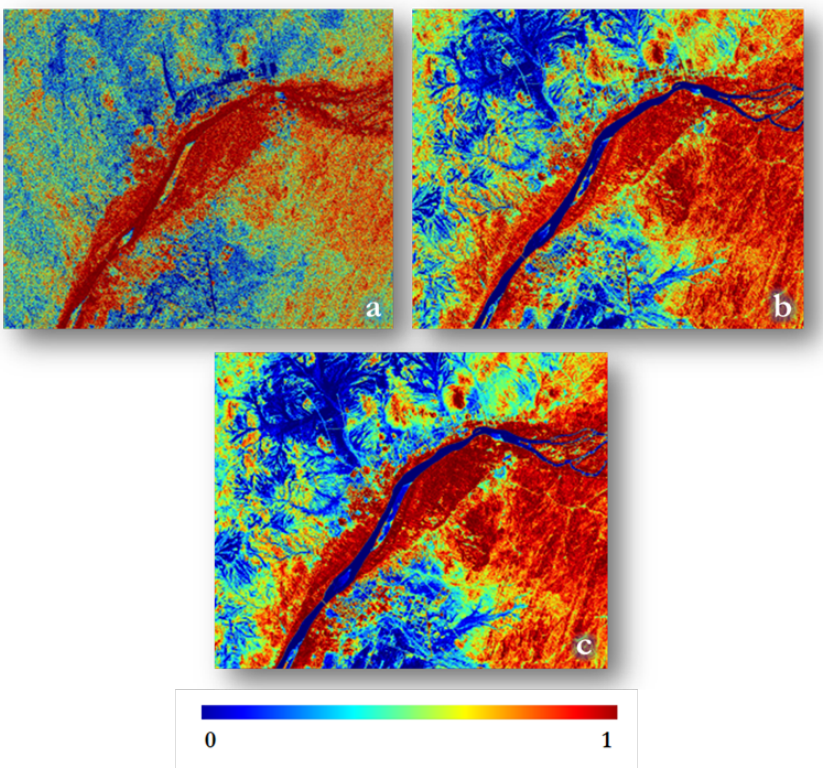

Figure 3.19 : Shannon Entropy descriptors : Polarimetry (a) ; Intensity (b) ; Shannon Entropy (c)

3.10.4 Model based Decomposition

The Freeman-Durden decomposition is a technique for fitting a physically based, three-component scattering mechanism model to the polarimetric SAR observations without utilizing any ground truth measurements [29] [30]. The mechanisms are canopy scatter from a cloud of randomly oriented dipoles, even- or double-bounce scatter from a pair of orthogonal surfaces with different dielectric constants, and Bragg scatter from a moderately rough surface.

This three-component scattering power model can be applied successfully to decompose SAR observations under the reflection symmetry condition (Figure 3.20).

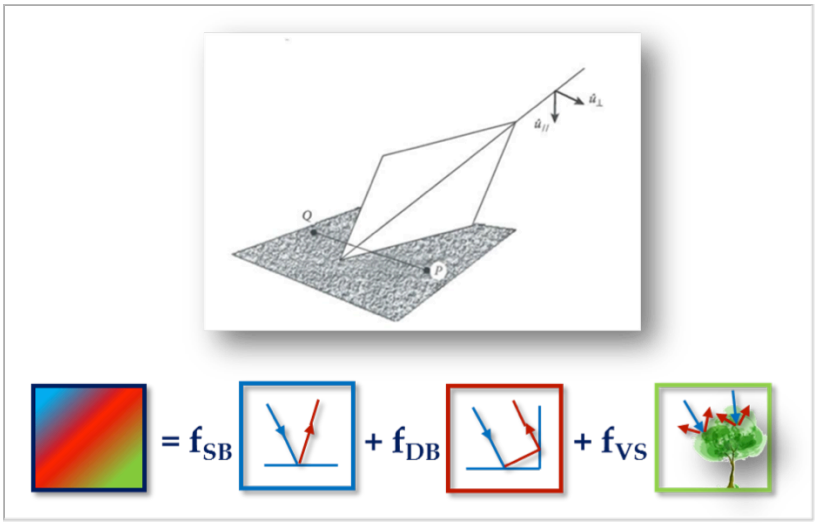

Figure 3.20 : Model – based Freeman decomposition

The Freeman-Durden model-fitting approach has the advantage that it is based on the physics of radar scattering, not a purely mathematical construct. This model can be used to determine to first order what are the dominant scattering mechanisms that give rise to observed backscatter in polarimetric SAR data.

While this decomposition can always be applied, it contains one important assumption which limits its applicability : the reflection symmetry that is not always valid [19].

Scattering symmetry assumptions about the distribution of the scatterers lead to a simplification of the scattering problem and allow quantitative conclusions about their scattering behaviour [26]. If the scattering matrix S for a target is known,

then the scattering matrix of its mirrored or rotated image in certain symmetrical configurations can be immediately derived [19].

Considering a distributed target that has reflection symmetry in the plane normal to the line-of-sight, whenever there is a contribution from a point P there will always be a corresponding contribution from its image at point Q (Figure 3.20).

It can be possible to find some areas in a SAR image for which the reflection symmetry condition does not hold, like in urban areas. Based on the 3-component scattering model approach, Yamaguchi et al. proposed, in 2005, a 4-component scattering model by introducing an additional term corresponding to non-reflection symmetric cases [19]. In order to accommodate the decomposition scheme for the more general scattering case encountered in complicated geometric scattering structures, the fourth component introduced is equivalent to a helix scattering power. This helix scattering power term appears in heterogeneous areas (complicated shape targets or man-made structures) whereas disappears for almost all natural distributed scattering (Figure 3.21).

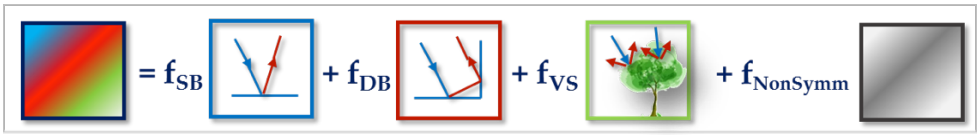

Figure 3.21 : Model –based Yamaguchi 4 component decomposition

This decomposition has a result a RGB image where the red channel corresponds to the double-bounce scattering, the green channel corresponds to volume scattering and the blue channel corresponds to single-bounce scattering. The fourth scattering mechanism, helix, can be considered in a separate channel.

The decomposition allows an interpretation of the physics behind the colours represented in three resulting RGB decompositions: Yamaguchi4 Y4O, Yamaguchi4 Y4R and Yamaguchi4 G4U1 [31] (Figure 3.22).

The Yamaguchi Y4O (Figure 3.22, top) represents the classical decomposition of the three above mentioned, in which the oriented targets present a volume scattering contribution and urban areas appears still saturated [31].

Applying a de-orientation for each pixel, Yamaguchi defines the second decomposition: Y4R, in which case a wave rotation is applied along the radar line of sight (Figure 3.22, middle), resulting in a better distinction of urban areas (double bounce) [31].

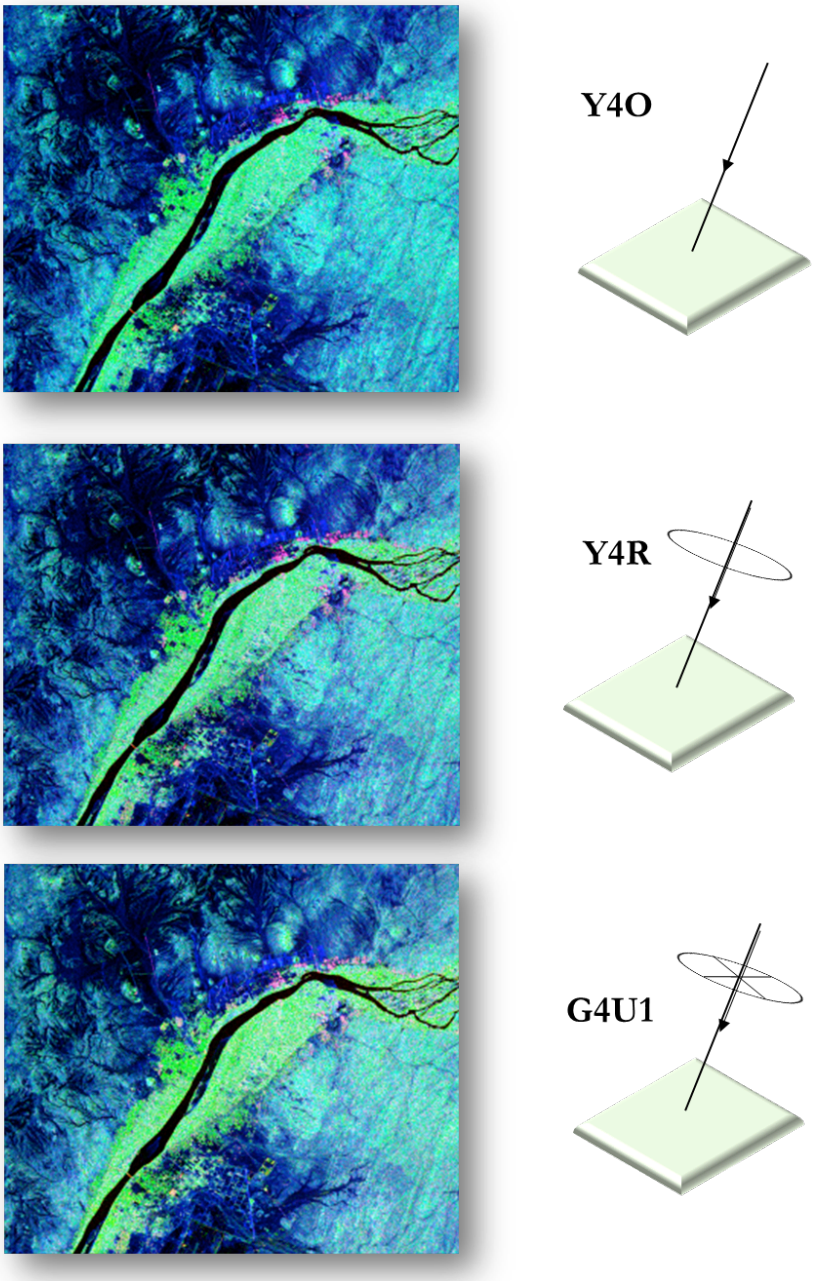

Figure 3.22 : Yamaguchi Y4O (top), Yamaguchi Y4R (middle) and Yamaguchi G4U1 (bottom) decomposition RGB images

The last step in development of Yamaguchi decomposition is then represented by the Yamaguchi G4U1 descriptor. Redefining the Freeman model, in which the asymmetry coming from different kind of forest trees was not contemplated (trees are represented by 3 different models), Yamaguchi includes different kind of responses for different kind of targets applying a complex rotation matrix, equivalent to a polarimetric basis change along the line of sight of the radar (Figure 3.22, bottom) [31]

This page intentionally left blank

Chapter 4

Spaceborne sensors

The present research focuses on the use of satellite SAR polarimetric ALOS PALSAR and RADARSAT-2 data for the study of the archaeological site of Gebel Barkal (Sudan). The objective of this analysis is to exploit the potential of SAR wave penetration in the ground and to monitor the archaeological area in time, both for subsurface and for surface features, independently from cloud coverage conditions that on the contrary represent a limit for the optical acquisitions. Nevertheless, also some optical sensors are used, where available, in order to evaluate the conservation state of the surface archaeological structures and to observe the effects urban sprawl and agricultural activity have on the Heritage. Optical images, in fact, provide a very high spatial resolution visualisation of archaeological structures and the environment surrounding them. Moreover, they are used as master images for the georeferencing process of ALOS PALSAR data. A brief overview of both SAR polarimetric and optical sensors used in this research is illustrated below.

4.1 SAR polarimetric sensors

SAR polarimetric data analysed in this research are represented by ALOS PALSAR archived data and by RADARSAT-2 specifically acquired data. The availability of different frequency and different incidence angle acquisitions makes possible to carry out multi-frequency and multi-incidence angle analysis that will be described, respectively, in Chapter 7 and in Chapter 8.

4.1.1 ALOS PALSAR

The *Phased Array type L-band Synthetic Aperture Radar* (PALSAR) is an active microwave sensor using L-band (central frequency 1.270 GHz, Table 4.1) of the *Advanced Land Observing Satellite* (ALOS), which was launched in January 2006 by the Japanese Aerospace Exploration Agency (JAXA) and ceased operations in 2011 [32]. PALSAR sensor achieved day-and-night and cloud free observation. The development of the PALSAR comes from a joint project between JAXA and the Japan Resources Observation System Organization (JAROS). Observation modes of ALOS PALSAR are illustrated in Figure 4.1.

Mode	Fine		ScanSAR	Polarimetric (Experimental mode)*1
Center Frequency	1270 MHz (L-band)			
Chirp Bandwidth	28MHz	14MHz	14MHz,28MHz	14MHz
Polarization	HH or VV	HH+HV or VV+VH	HH or VV	HH+HV+VH+VV
Incident angle	8 to 60deg.	8 to 60deg.	18 to 43deg.	8 to 30deg.*
Range Resolution	7 to 44m	14 to 88m	100m (multi look)	24 to 89m
Observation Swath	40 to 70km	40 to 70km	250 to 350km	20 to 65km
Bit Length	5 bits	5 bits	5 bits	3 or 5bits
Data rate	240Mbps	240Mbps	120Mbps,240Mbps	240Mbps
NE sigma zero *2	< -23dB (Swath Width 70km) < -25dB (Swath Width 60km)		< -25dB	< -29dB
S/A *2,*3	> 16dB (Swath Width 70km) > 21dB (Swath Width 60km)		> 21dB	> 19dB
Radiometric accuracy	scene: 1dB / orbit: 1.5 dB			

Table 4.1 : Technical characteristics of ALOS PALSAR © *JAXA*. Only the 25.5deg incidence angle beam was calibrated for the polarimetric mode.

Other two ALOS onboard instruments were the Panchromatic Remote-sensing Instrument for Stereo Mapping (PRISM), dedicated mostly to digital elevation mapping with a spatial resolution of 2.5 m (at nadir), and the Advanced Visible and Near Infrared Radiometer type 2 (AVNIR-2) for precise land coverage observation, with a spatial resolution of 10 m (at nadir). Nevertheless, these last two sensors are not illustrated in detail as the images available for the research

present some acquisition errors (images present stripes in the visualization) that cannot be fixed [32].

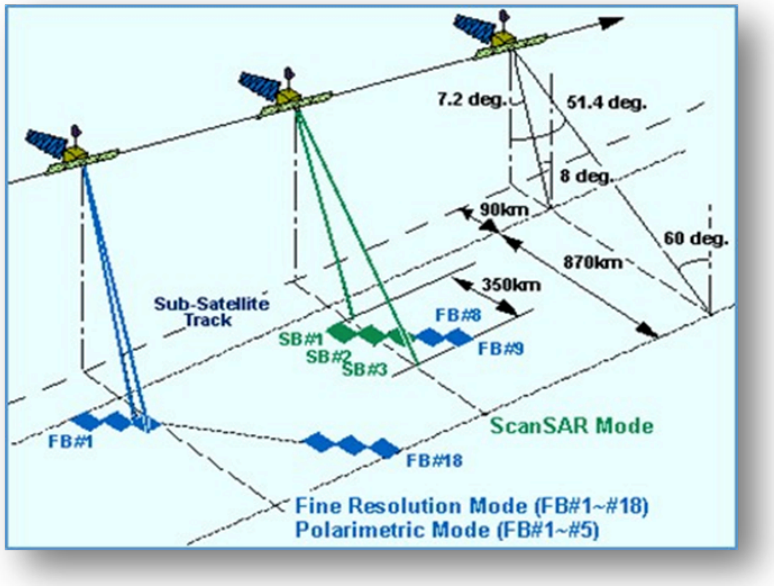

Figure 4.1 : Observation modes of PALSAR © *JAXA*

4.1.2 RADARSAT-2

RADARSAT-2 is a jointly-funded satellite mission of CSA (Canadian Space Agency) and MDA (MacDonald Dettwiler Associates Ltd. of Richmond, BC). RADARSAT-2, launched on 4 December 2007, is an advanced state-of-the-art technology follow-on satellite mission of RADARSAT-2 [34].

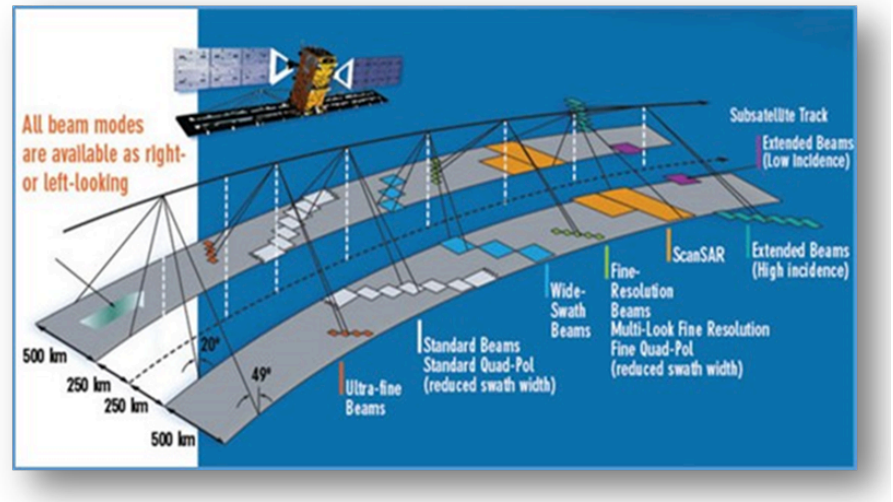

Figure 4.2 : Observation mode of RADARSAT-2 © *CSA*

The objective of the mission is to provide several services among which ice monitoring, disaster management, environmental monitoring, mapping

applications and so on. One of the reasons that drove the research to use RADARSAT-2 data is linked to the flexibility of the sensor. It is possible to reprogram the sensor, for example, according to resolution and swath width. Thanks to this flexibility, two different configuration modes were selected for the present research (see §6.3), in a Fine Quad Polarisation mode (Figure 4.2).

The Wide Fine Quad-Polarisation Beam modes have a wider swath width of about 50 km (compared to 25 km for the regular beams, Table 4.2) and the same spatial resolution as for the original beams. There are 21 beams with overlaps of 50% between the swaths, covering an incidence angle range between 18-42°. The sensor works in C - band with a central frequency of 5.405 GHz [33].

Beam Modes		Nominal Swath Width (km)	Nominal Resolution (m)
Selective Polarization Transmit H or V receive H and/or V	Fine	50	10 x 9
	Standard	100	25 x 28
	Low incidence	170	40 x 28
	High incidence	75	20 x 28
	Wide	150	25 x 28
	ScanSAR narrow	300	50 x 50
	ScanSAR ScanSAR wide	500	100 x 100
Polarimetric Transmit H and V on alternate pulses / receive H and V on any pulse	Fine Quad-pol	25	11 x 9
	Standard Quad-pol	25	25 x 28
Selective Single Polarization Transmit H or V receive H or V	Ultra-Fine	20	3 x 3
	Spotlight	18	3 x 1
	Multi-Look Fine	50	11 x 9

Table 4.2 : Technical characteristics of RADARSAT-2 © *CSA*

4.2 Optical sensors

For the present research, optical data serve as reference images for the georeferencing process and they contribute to the creation of a multi-temporal dataset to be compared and integrated with SAR polarimetric one. A detailed description about data recruitment and use will follow in Chapter 6.

4.2.1 QuickBird

QuickBird optical satellite (Figure 4.3), launched in October 2001, provides sub-meter resolution imagery (Table 4.3), high geolocation accuracy, and large on board data storage. With global collection of panchromatic and multispectral imagery, Quickbird has been designed to support a wide range of geospatial applications [35].

Figure 4.3 : QuickBird Satellite © *ATLISVUE*

Launch date	October 18, 2001
Launch Location	Vandenberg Air Force Base, California
Orbit Altitude	450 km
Orbit Inclination	97.2 degree, sun-synchronous
Speed	7.1 km/second
Equator Crossing Time	10:30 a.m. (descending node)
Orbit Time	93.5 minutes
Revisit Time	1-3.5 days depending on latitude (30° off-nadir)
Swath Width	16.5 km at nadir
Metric Accuracy	23-meter horizontal (CE90%)
Digitalization	11 bits
Resolution Pan	61 cm (nadir) to 72 cm (25° off-nadir)
MS	2.44 m (nadir) to 2.88 m (25° off-nadir
Image Bands	
Pan	450 - 900 nm
Blue	450 - 520 nm
Green	520 - 600 nm
Red	630 – 690 nm
Near IR	760 - 900 nm

Table 4.3 : Technical characteristics of QuickBird © *DigitalGlobe*

4.2.2 KOMPSAT-2

KOMPSAT-2 (*Korea Multi-Purpose Satellite-2*, Figure 4.4), launched in July 2006 (Table 4.4), has been developed by KARI (Korea Aerospace Research Institute) to continue the observation program of the KOMPSAT-1 mission [36].

Figure 4.4 : KOMPSAT-2 Satellite © *EOPortal*

Space vehicle name	KOMPSAT-2
Country	South Korea
Designers	KARI, Astrium
Operator	KARI
Booster	Rokot-KM
Launch date	July 28th, 2006
Orbit **Altitude, km** **Inclination, deg** **Sidereal period, min** **Revolution number per day**	Morning sun-synchronous 685 98,1 98.5 10:50
Platform **Survey equipment** **Deviation angles, deg**	MSC ±45
Active lifetime, years	5
Repeated surveillance period, days	3
Power, Wt	955
Size, m x m	2.6×2.0

Table 4.4 : Technical characteristics of KOMPSAT-2

The satellite provides a surveillance of large-scale disasters and its countermeasure, acquisition of independent high-resolution images for GIS (Geographic Information Systems), composition of printed maps and digitized maps for domestic and overseas territories, survey of natural resources.

Chapter 5

Case study : Gebel Barkal archaeological site

The present chapter presents the study area of the archeological site of Gebel Barkal (Sudan). The selection of the site, strictly depending on the special interest this ancient context originates, results from a previous feasibility study carried out on several potential case studies. The selection criteria range from the relationship between sensors spatial resolution and structures' dimension to the threatening factors that can affect the integrity of a cultural site.

Starting from this premise, the UNESCO World Heritage List in which the site is inscribed, a historical introduction to the site as well as the history of the international excavations missions until present are illustrated. A final section is then dedicated to a general overview of geology in Sudan, so that the archaeological site can be contextualized in its so characterizing and specific morphology.

5.1 The UNESCO archaeological site of Gebel Barkal

The World Heritage List of UNESCO (United Nations Educational, Scientific and Cultural Organization) includes 759 cultural, 193 natural and 29 mixed properties in 160 States Parties. Cultural and natural sites of outstanding value must meet at least one out of ten selection criteria to be included in the World Heritage List (Figure 5.1).

Figure 5.1 : World Heritage List © *UNESCO*

The protection, management, authenticity and integrity of properties are key factors in maintaining sites belonging to the List. War conflicts, earthquakes and other natural disasters, pollution, poaching, looting, uncontrolled urbanization and unchecked tourist development pose the major problems to World Heritage sites. For these reasons, the World Heritage Committee can inscribe in the World Heritage List in Danger properties whose protection requires immediate operations and constant assistance. The factors threatening cultural and natural sites can be either 'ascertained', referring to specific and proven imminent threats, or 'potential', when threats could have negative effects on the World Heritage values of the site [37].

Archaeological sites of both Gebel Barkal and the Napatan region are located in the Northern Sudan, Province of Meroe. Since 2003, these sites are inscribed in the World Heritage List, covering a property of 183ha and a buffer zone of 47ha, this last one still not definitively established (Figure 5.2). Gebel Barkal and the sites of the Napatan region represent, in fact, the exceptional example of the Napato-Meroitic (Kushite) civilization that prevailed in the Nile Valley from the 9th Century BC to the Christianization of the country in the 6th Century [38].

The high degree of intactness of the archaeological structures expressing Outstanding Universal Value gives the serial site's great integrity. The archaeological buildings are, in last years, only very slightly affected by modern urban extensions.

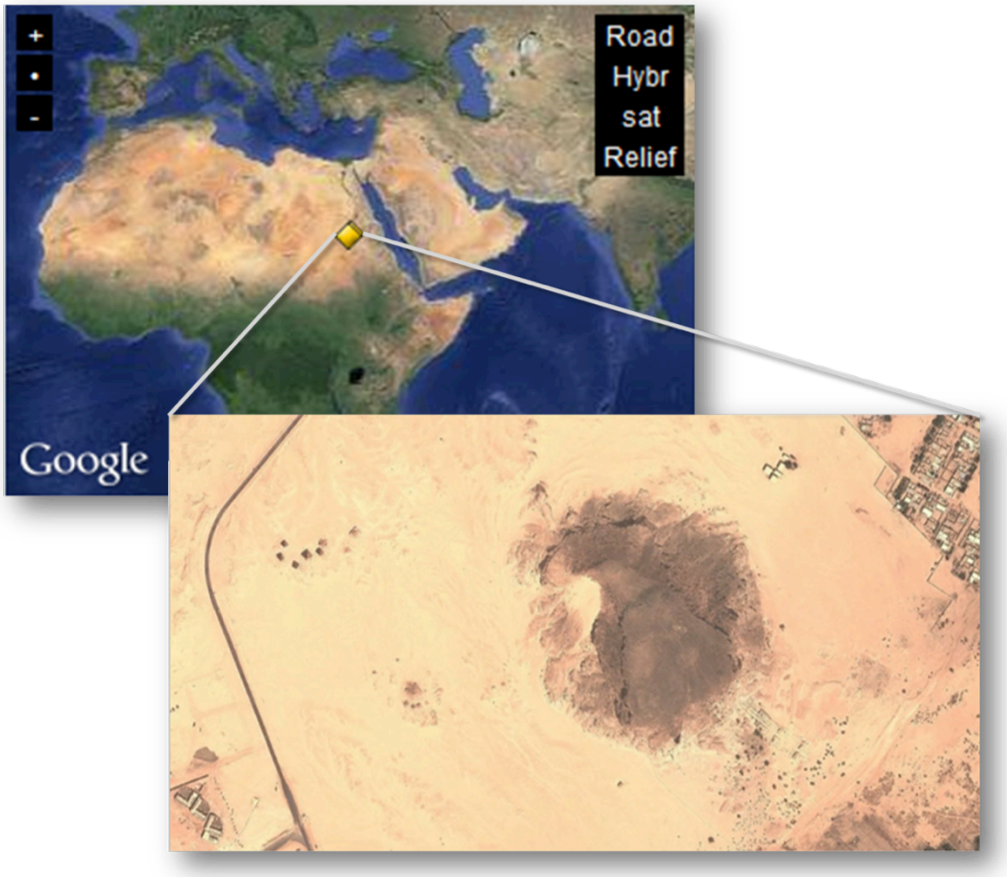

Figure 5.2 : Gebel Barkal archaeological site © Google Earth

However, careful monitoring of the developments around the property needs to be carried out, especially concerning the urban extension on the Desert side, which could become one of the major threats for the site.

5.1.1 A historical introduction to the site

Gebel Barkal (18° 32' N, 31° 49' E, WGS84) constitutes one of the five Napatan (900 to 270 BC) and Meroitic (270 BC to 350 AD) archaeological sites located on both sides of the Nile river in an arid area considered part of Nubia (Sudan). The sites (Gebel Barkal, Kurru, Nuri, Sanam and Zuma) stretch over more than 60 km along the river (Figure 5.3). Gebel Barkal is the modern Arabic name of a lone sandstone hill rising on the SW edge of Karima, about 365 km N/NW of Khartoum and 23 km downstream from the Merowe Dam at the fourth cataract of the Nile [38].

This Napatan civilization had strong links with the northern Pharaonic and other African cultures. When the Egyptians conquered northern Sudan (kingdom of

Kush) in the early Eighteenth Dynasty (ca. 1504 BC), they identified *Jebel Barkal* as the birthplace and chief southern residence of their state god Amun.

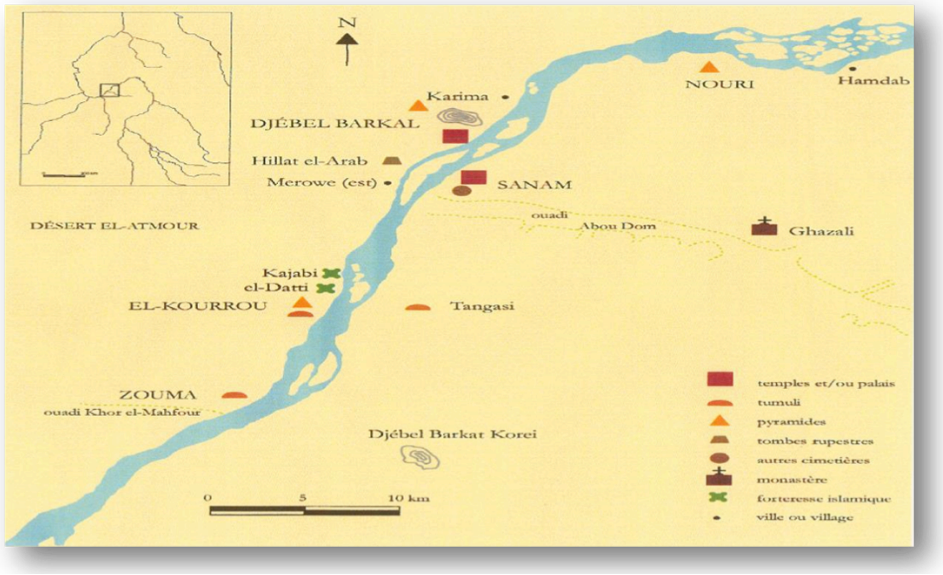

Figure 5.3 : Gebel Barkal and the sites of the Napatan region © *UNESCO*

Gebel Barkal seems to have had a unique importance for them as a creation site and home of a primitive aspect of the god Amun who renewed life each year with the Nile inundation. Beneath the Gebel Barkal cliff the Egyptians constructed a major religious centre and gave it the same name as Karnak (Ipet-Sut), Amun's great sanctuary at Thebes. The settlement that grew up around it was called Napata, which became the southernmost town in their African empire. Since antiquity, the hill of Gebel Barkal has been strongly associated with religious traditions and local folklore. For this reason, the largest temples (Amon Temple for example) were built at the foot of the hill and are still considered by the local people as sacred places.

Gebel Barkal has thus been a sacred mountain since New Kingdom times (ca. 1500 BC). Today, this "Holy Mountain" is locally named Gebel Wad el-Karsani after a Muslim sheikh was buried near the 100m high, flat-topped sandstone rock. The mountain is closely associated with religious traditions, since the local people for blessings are still visiting the tomb of this sheikh.

Excavations and surveys of the hill and its surroundings have revealed nine temples, all at the foot of the hill and facing the Nile, palaces, administrative

structures, pyramids and other kinds of tomb. The largest temple, whose remains can are shown in Figure 5.4, is that dedicated to the god Amon [39].

Figure 5.4 : The Holy Mountain and the temple of Amun (B1500). © Max Farrar

Figure 5.5 : Pyramids at Gebel Barkal (Courtesy of L. Perotti)

Unlike the temples, which are built from stone, many of the palaces were made from earthen, sun-dried bricks, very sensitive material presenting a low weather-

resistance. Pyramids and tombs are unique in their typology and building technique, still preserving their original shape and height, being also part of the special desert border landscape. The field of pyramids constitutes the necropolis, part of the royal Napatan-Meroïtic cemetery (Figure 5.5).

Many differences exist between Napatan pyramids and the well-known Egyptian ones, like distinctive construction styles (Napatan pyramids are maximum 30m high presenting different stone-finishing technique) as well as different purposes. While the Egyptian pyramids were built to enclose the funerary chamber, the Napatan ones were rather commemorative monuments, in which the deceased was buried in a hypogeum underneath. A small temple was built in the entrance of the pyramid for offerings [38].

The Gebel Barkal site presents a vast archaeological area that has been neither excavated nor studied [40]. Archaeological excavations at Gebel Barkal still have not reached the earliest strata, and in the surroundings of the site excavations revealed human activity dating back to the 3rd millennium BC. For the Egyptians of the New Empire, Gebel Barkal was a holy place: they made it a religious centre, and probably an administrative one as well. Napata or Gebel Barkal was the capital of the Kushite kingdom, probably already at the end of the 9th century BC, and kept its religious and administrative role until the 4th century [39].

Figure 5.6 : Muslim cemetery in the SW part of the archaeological area © Google Earth

Although Gebel Barkal pyramids are the best preserved royal funerary monuments in Sudan, temples and palaces are in very poor condition due to very soft nature of the building stone, to the severity of the local environment (floods and sandstorms), and to the long-term looting of the site by local villagers seeking cut stone blocks for use in the lining of the graves of the Muslim cemetery, immediately west of the temples (Figure 5.6).

5.1.2 Historical excavations and modern academic expeditions

Travellers of the last century had a strong interest for the "Sacred or Pure Mountain" and the associated monuments. History of excavations starts with exploration and documentation by Prussian expedition (1842 - 1845) headed by Karl Richard Lepsius. Nevertheless, the most important archaeologist for the archaeology of Sudan was George Andrew Reisner who excavated on behalf of the Harvard University and the Boston Fine Art Museum (MFA), from 1907 until 1920. Currently expeditions still continue on the basis of Reisner's work and are dedicated to the excavation of temples and palaces and to the collection of all the documentation already existing, as well as to more detailed archaeological research purposes, as the delineation of urban model, contemporaneity of structures and their mutual relationships.

After the conclusion of Reisner's work in 1920, no further excavations were undertaken at Jebel Barkal until 1973, when an Italian Mission held by the University of Rome "La Sapienza", under the direction of Prof. F. Sergio Donadoni, reopened work at the site. When Donadoni retired in 1992, he turned over his Mission to his colleague Prof. Alessandro Roccati, and in 2006, the Mission received a new institutional sponsor from the University of Torino (Figure 5.7). The current Italian Mission in Gebel Barkal is nowbeing carried out by Emanuele M. Ciampini (University of Venice, "Ca' Foscari").

In 1986, the Italian Mission was joined at Gebel Barkal by a small team from the Museum of Fine Arts, Boston, led by Timothy Kendall, whose research area was restricted to Reisner's former concession. His expedition was then temporarily merged, at Prof. Roccati's invitation, with the Italian Mission.

Between 1995 and 1997, a team from the Fundacio Clos of Barcelona, Spain, under the direction of Dr. Francesca Berenguer renewed excavations in Gebel

Barkal cemetery and discovered two previously unknown royal tombs of the late Napatan Period.

Figure 5.7 : Local workers 2006 excavation missions (Courtesy of L. Perotti)

In 2003, at the request of Hassan Hussein Idriss, Director General of the Sudan's National Corporation for Antiquities and Museums (NCAM), Kendall's mission was designated an official NCAM Mission, with new US sponsorship from the African-American Studies Dept., Northeastern University, Boston. This expedition has worked nearly each season to the present [41].
In the frame of the last Italian excavation mission (November- December 2013), carried out by Prof. E. Ciampini (University of Venice, "Ca' Foscari"), a verification in situ related to the results of the present research, illustrated later in detail in Chapter 7, have been performed.

5.2 Geology and geomorphology

A brief presentation of the geology of Sudan is here reported in order to locate the site in its natural and very specific environment.

The Sudan plain consists partly of dark clays and partially of red and brown sands, and is so flat that railways have been laid on it for dozen of miles without embankments or cuttings. Apart from some well-known chains, the Sudan plain is only occasionally broken by isolated "jebels" which rise sharply from the flat surface. In particular, the part of Sudan relevant to Nubia is divided in zones

called Nile Cataracts (First, Second, Third, Fourth, Fifth, and Sixth). These granite outcrops formed, in past time, a sufficient impediment to travellers to detect the expansion of the Egyptians, leaving the land in the possession of its indigenous Nubian population. As Egypt was, Nubia is called "the gift of the Nile", even if beyond its floodplain, through most of the region, there is nothing but lifeless desert. The river is bordered by the same rich black soils as in Egypt, but here they occur only in discontinuous patches interrupted by areas where the river is directly bordered by cliffs or dunes. Moreover, through most of Nubia, in contrast with what happened in the past, the Nile does not regularly overflow its high banks during the flood season, and water for irrigation must always be raised by artificial means [42].

Unlike to others Cataracts, the land between the Third and Fourth Cataracts, where the archaeological site of Gebel Barkal is located, is the most fertile part of Nubia. It is a sandstone region geologically and topographically similar to Lower Nubia, but it has in addition two fairly sizable basins where the river regularly overflows its banks during the flood season, making possible the kind of basin irrigation practiced throughout most of Egypt. This region was always, and remains today, the most populous part of Nubia [43]. In the area of Gebel Barkal, during Ground Penetrating Radar campaigns, carried out in occasion of excavation missions, layers of historical activities of Nile flooding have arisen, thus demonstrating how the river flow activity influenced also the ancient urban organization. This characteristic makes more complex the precise topographic reconstruction of the ancient environment.

Figure 5.8 : Erosion pebble conglomerate © Max Farrar

Layers of sand are mixed to pebble conglomerate and smoothed rocks, whose surface portions are shaped by strong winds and sand storms (Figure 5.8). The activity of atmospheric agents determines also the current shape of archaeological structures and represent a threat affecting their conservation. Although the mud-bricks pyramids of the Royal cemetery are well preserved, some of them show noticeable signs of erosion effects.

5.3 A multidisciplinary approach for Gebel Barkal site

The integration of a very specific and technical topic like SAR remote sensing with a humanistic field of research like archaeology can be considered an interesting challenge. Besides the already proven capabilities of optical remote sensing for cultural heritage, SAR applications for archaeology make these two scientific fields converging in a productive and non-invasive collaboration, ideally made of archaeologists and scientists to whom specific knowledge is required.

This synergy of humanistic and technological fields offers great opportunities for a worldwide heritage mapping and consciousness. The research here presented originates from this idea of multidisciplinary synergy and continues in the next chapters with the discussion of the topics above mentioned, following the logic of the combined exploitation of SAR polarimetric data and archaeological knowledge.

Chapter 6

Data set presentation

The present chapter provides an overview of the data selected for the research activity. Data are not only presented for the different sources they come from, but also illustrated explaining the choice related to the typology of satellite acquisitions and the purpose data analysis aimed to. In the last paragraph, the attention is focused on the meteorological condition of the area of Gebel Barkal, ancillary but fundamental information.

Data are not listed in order of importance, but following the classical research scheme used in what we call "Space Archaeology": starting from the cartographic documentation, analysing aerial and optical satellite images and available radar data, in this case focusing on the study of SAR polarimetric images and concluding with meteorological information, crucial for the comprehension of electromagnetic wave interaction with structures.

6.1 Data set overview

Traditionally, cartography is considered to be at the basis of a well-documented topographic archaeological study. The recording of both existing and supposed ancient urban division, as well as of complexes or single structure location and site overall topography, is the basis of the archaeological documentation, and it could constitute the starting point of a non-destructive investigation like the one presented in this work (Figure 6.1).

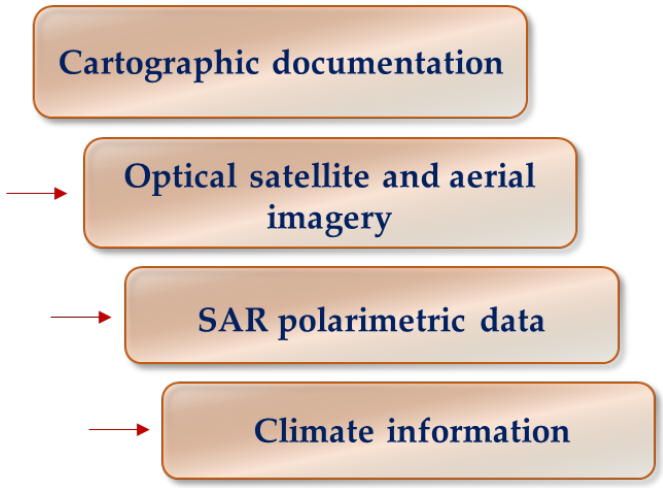

Figure 6.1 : Complete dataset overview

Since one century and few decades, respectively aerial photography and very high-resolution optical satellite data gave a great aid to documentation purposes. Optical satellite data are more and more used as principal remote sensing source of information for archaeological sites observation, providing precious information about vegetation and moisture changes occurred in time presenting also an historical, even if quite recent, multi-temporal documentation. This aspect turned out to be the most representative for the monitoring of urban sprawl as well as for the identification of looting activities in the investigated areas. Satellite SAR data, and especially SAR polarimetric data, are quite new investigation tools in this field. Nevertheless, their great potential, mostly linked to soil penetration capabilities and to 24h acquisitions, neither affected by sun illumination nor by meteorological conditions, make them a perfect sensor for future exploitation of both surface and subsurface archaeological patterns reconnaissance.

Ancillary data like geomorphological information and archived meteorological records are crucial, as shown later in paragraph 6.4, for the comprehension and reliability of remote sensing data analysis.

6.2 Cartographic documentation and optical images

The archaeological map used as topographic reference in the present research, which dates back to 1995 (Figure 6.2), represents the unique cartographic document available from UNESCO reports [38], documents describing the state of conservation of the area inscribed in the World Heritage List and collect the

related documentation. Unluckily this map [44], due to some restitution errors occurred at the time of its realisation, both for the general topography of the site and for the geographic location and relative measurements of excavated temples and palace, presented several problems in the georeferencing process as well as in the geographic comparison with remote sensed data. It is worth, in fact, to remark the importance of a well georeferenced archaeological map, which is linked not only to the possibility of locating archaeological features on the map, but also to the precise correspondence between cartography and satellite images when overlapping them. This is truer when working with SAR data, in which pattern recognition still constitutes a complex operation.

Figure 6.2 : Gebel Barkal archaeological area, 1995. © E. Mitchell

Thanks to the collaboration with the Geological Sciences Department of the University of Turin (Dott. L. Perotti), it has been possible to work on a Quickbird image acquired on 3rd September 2003, coming from a previous optical and cartographic research over Gebel Barkal area he carried out [45] (see §9.2). The original purpose of his work was the exploitation of several image-processing techniques in order to highlight the archaeological structures that archaeologists needed to map and to realize a more detailed high-resolution cartography. L. Perotti processed QuickBird and ASTER data acquired in 2006 to generate a high scale multispectral orthoimage of the area, in order to realize a more recent

cartographic basis for the archaeological documentation. The high scale orthoimage obtained, has been thus used in the present research as geographic basis for all the other data (Figure 6.3).

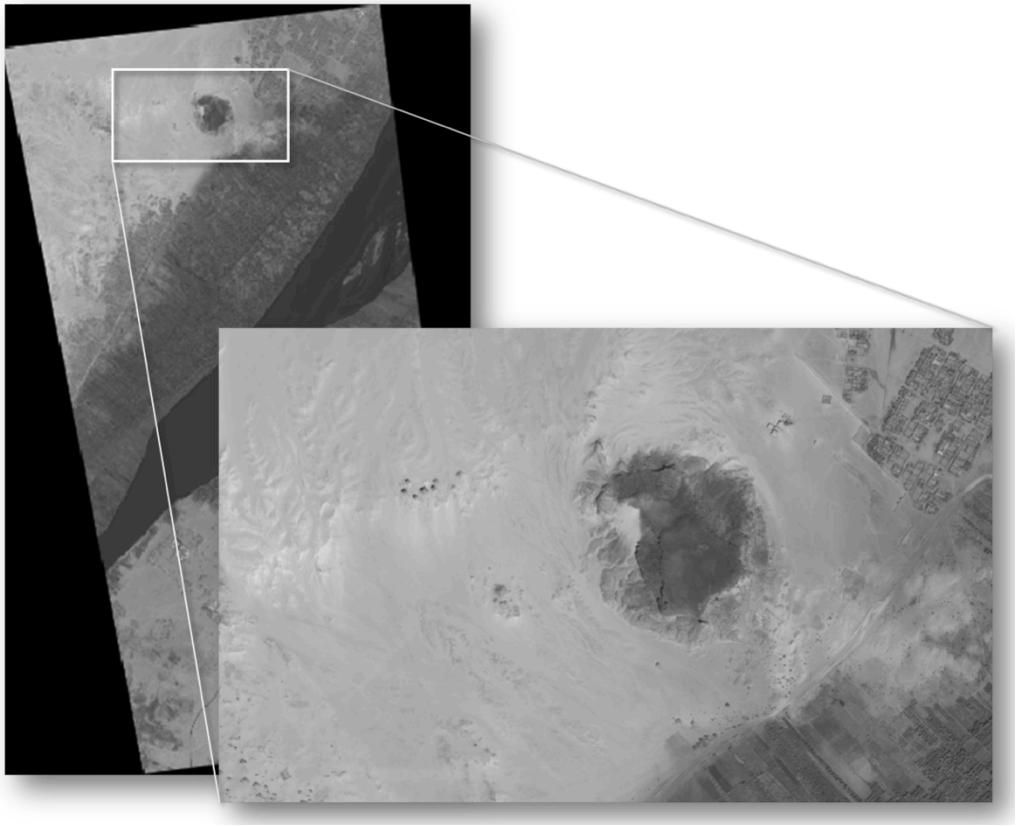

Figure 6.3 : Quickbird orthophoto derived from the image acquired on 2003/09/03. In the detail, the archaeological area

Satellite data were retrieved from ESA/ESRIN (Italian establishment of the European Space Agency) Eoli-SA catalogue [46] in the frame of the joint PhD collaboration between the University of Rome "La Sapienza" (Italy) and the University of Rennes 1 (France). Two optical ALOS PRISM (panchromatic) and two ALOS AVNIR (multispectral) images were the first data requested but, unfortunately, both presented some acquisition errors (images presents stripes in the visualisation) and for this reason, they have not been included in this research. The only high-resolution optical image available for the area of interest is a KOMPSAT-2 image acquired on 16th May 2008 (Figure 6.4). The KOMPSAT-2 image is used, initially, as a master image in the geocoding process of SAR data. Later, a qualitative analysis is carried out to record the overall state of conservation of Gebel Barkal area in 2008, when most of the modern current

infrastructures, very close to the site, were not yet completely built, and the urban area of Karima, in the NE part of the archaeological site, was slowly growing up towards the ruins.

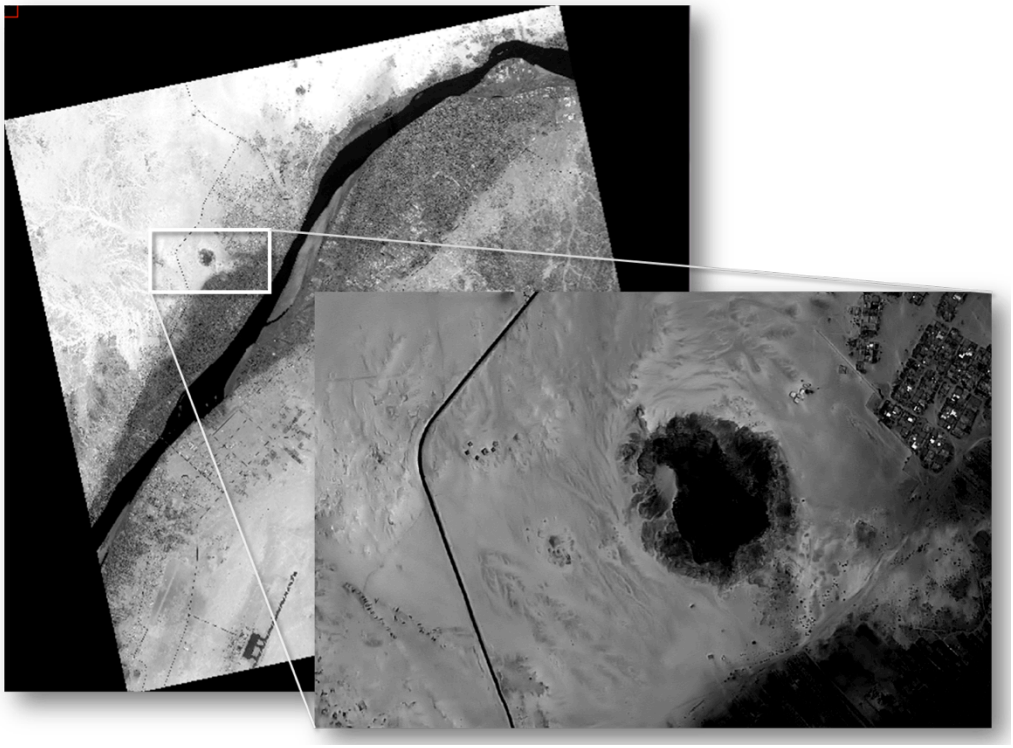

Figure 6.4 : KOMPSAT-2 acquisition (2008/05/16) and the detail of the archaeological area

In addition to QUICKBIRD (2003) and KOMPSAT-2 (2008) acquisitions, three more optical images were then derived from Google Earth (respectively on 3rd January 2004, 8th March 2006 and 7th November 2012) in order to obtain an exhaustive historical overview of Gebel Barkal site. Thanks to these images, spreading over a period of nine years, it has been possible to create a multi-temporal dataset based on five different acquisitions, thus providing a seasonal mapping of the urban and agricultural changes occurred in time over the area (Figure 6.5).

Concerning the aerial optical dataset, images from two aerial photography campaigns, carried out over the archaeological area in the last 20 years, are also taken into account. The first campaign was realised in 1984 for a preventive investigation of the Nile river before the construction of dams and realization of water ducts (Figure 6.6). Only few vertical photographs remains of this first campaign (the archaeological area is highlighted by the white frame in Figure 6.6)

giving, however, a broad evidence of the agricultural and contemporary urban organization that, in that period, were not threatening the archaeological zone.

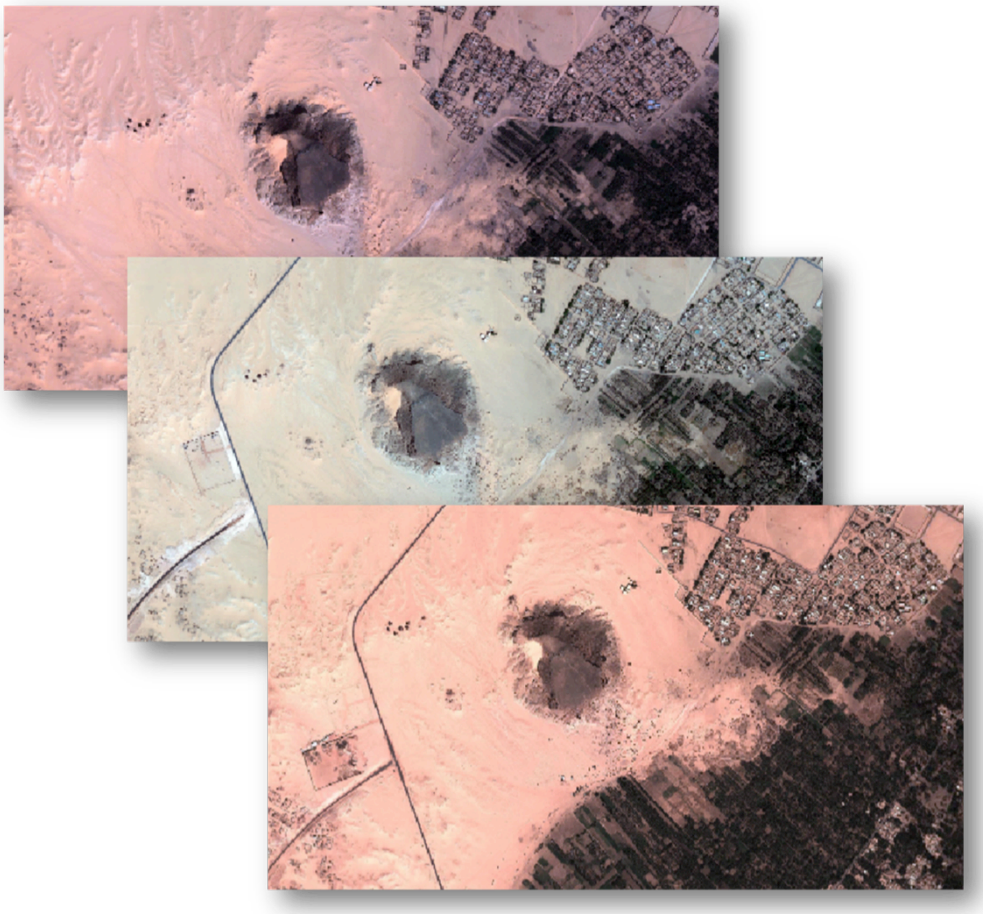

Figure 6.5 : Google Earth acquisitions (2004/01/03; 2009/10/14; 2012/11/07)

Figure 6.6 : Ortophoto collection of 1984

Professor A. Roccati, head of excavations for previous archaeological missions from the University of Rome "La Sapienza" at Gebel Barkal, carried out the second campaign in the frame of 2005 mission excavations, with the aim to observe and document the temples of the SE portion of the archaeological area, granted to the Italian University. During this campaign, several oblique photographs were taken, providing an updated source of information for the observation and comparison of the different state of conservation of the surface structures in a more detailed low-altitude visualisation (Figure 6.7).

Figure 6.7 : Oblique aerial photograph, 2005. Courtesy of A. Roccati

6.3 SAR polarimetric dataset

The exploitation of SAR polarimetric data for archaeological research is still in a very preliminary stage of development, although it constitutes a promising non-invasive technique for the management of Cultural Heritage of the World. The great potential given by this kind of data for Earth Observation is known (see §6.1), but some characteristics, as the medium spatial resolution they present (around 10 meters, today the highest spatial resolution for full-polarimetric sensors), prevent the spreading in the scientific community of the in-depth analysis of SAR applications for archaeology. For this reason and for this specific application, SAR polarimetric data exploitation requires skilled interpreters who

are able to combine both SAR technical knowledge and archaeological expertise, which combination allows the identification of features linked to archaeological structures or complexes in SAR data.

As known, backscattering can vary with incidence angles. Therefore, the selection of the most appropriate incidence angle is very important for precise target recognition. This is why in two images acquired with different incidence angles, archaeological structures can result enhanced only in the one with a precise configuration angle: Elachi and Granger [47] found that the discrimination of paleo - drainage features was allowed by wider incidence angle configurations (wider than 50°).

The polarimetric dataset was selected on the basis of a multi – frequency analysis approach (see §7.1), comparing ALOS PALSAR L-band, with a central frequency of 1.27 GHz, with RADARSAT-2 C-band sensor, whose central frequency is 5.405 GHz.

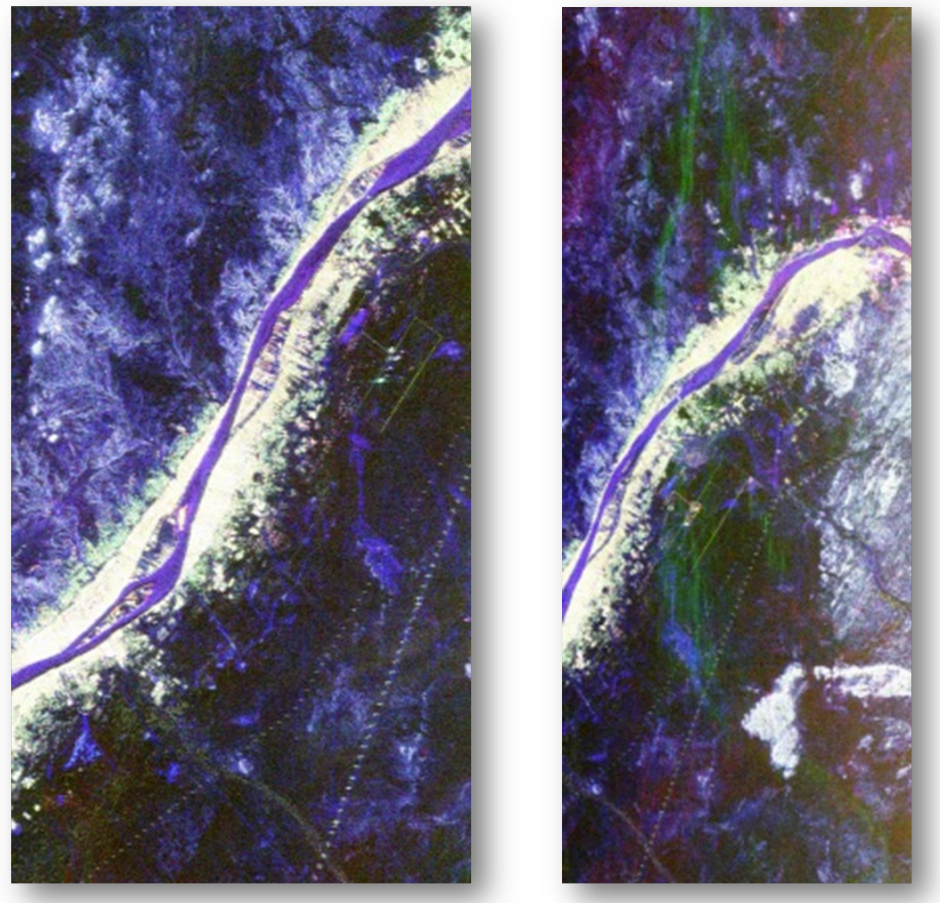

Figure 6.8 : ALOS PALSAR SLC products (2006/08/14, 26.07° - 2009/11/05, 23,10°) in the RGB visualisation of the Pauli decomposition

All the polarimetric images selected in the research activity are in SLC format with a 1.1 level of processing (see §7.3.1). A so-called Single Look Complex (SLC) product, is generated starting from the raw SAR data that cannot be displayed as an image. It presents the minimum number of interpolation and corrections on the data and it contains all the phase and amplitude information, which can be extracted by means of specific processing operations [48].

The multi-frequency analysis takes into account the possibility to compare the fixed incidence angle configuration mode of ALOS PALSAR acquisitions (between 23° and 26° incidence angle) and the selective (not-fixed) configuration mode of RADARSAT-2 acquisitions.

The ALOS PALSAR dataset is, hence, composed of two full-polarimetric archived images acquired respectively on 14th August 2006 and on 5th November 2009, provided by ESA through Eoli-SA catalogue, with respectively an incidence angle configuration of 26.07° and 23.10° (Figure 6.8). The RADARSAT-2 dataset is composed of four Fine Quad polarimetric mode (see §4.2) images acquired on 28th April and 6th November 2012, and on 1st January and 4th July 2013 (Figure 6.9).

In addition, a multi-incidence angle analysis has then been performed (see §8.1), based on the flexibility of RADARSAT-2, analysing the 27° and the 45° acquisitions of the polarimetric sensor. To this purpose, four further RADARSAT-2 Fine Quad polarimetric images have been acquired, on the 1st May and 11th November 2012 and 20th January and 7th July 2013 (Figure 6.10).

RADARSAT-2 27° and 45° incidence angle images have been specifically scheduled and acquired for the present research by the VigiSAT [49] ground station of Brest (France) in the frame of GIS BRETEL [50]. Being archived data, the selection of the acquisition dates of ALOS PALSAR imagery is not related to a a season or a month specifically required, while for RADARSAT-2 data it has been been possible to select the acquisition date on the basis of the average of seasonal precipitations, assuring the lowest possible influence of humidity effect coming from precipitation phenomena, on the electromagnetic wave. To this end, the climate information corresponding to the date of acquisition were derived, as shown in

Figure 6.13 and in Figure 6.14.

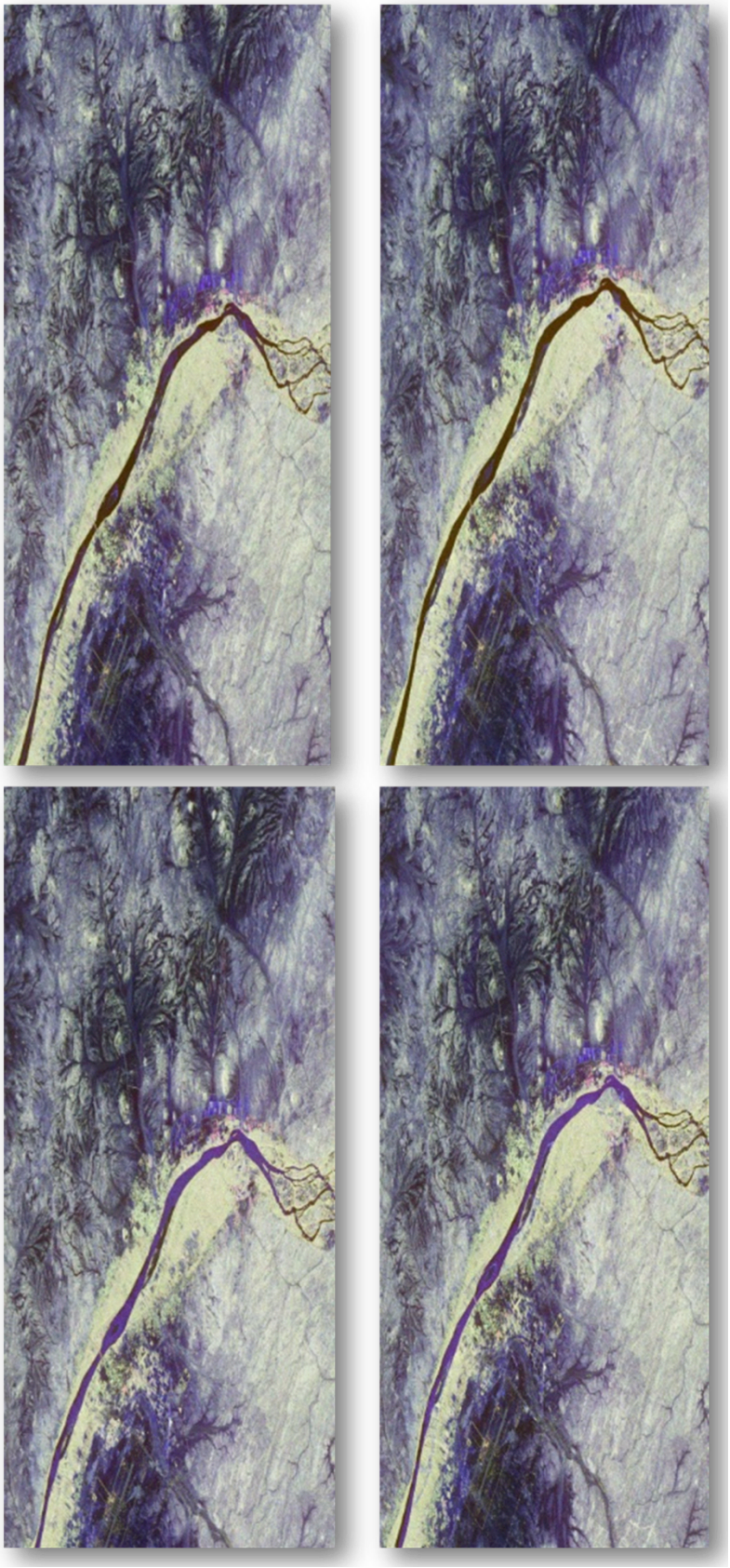

Figure 6.9 : RADARSAT-2 SLC Pauli decomposition (□ = 27,06°). Clockwise order: 2012/04/28; 2012/11/06; 2013/01/17; 2013/07/04 acquisitions

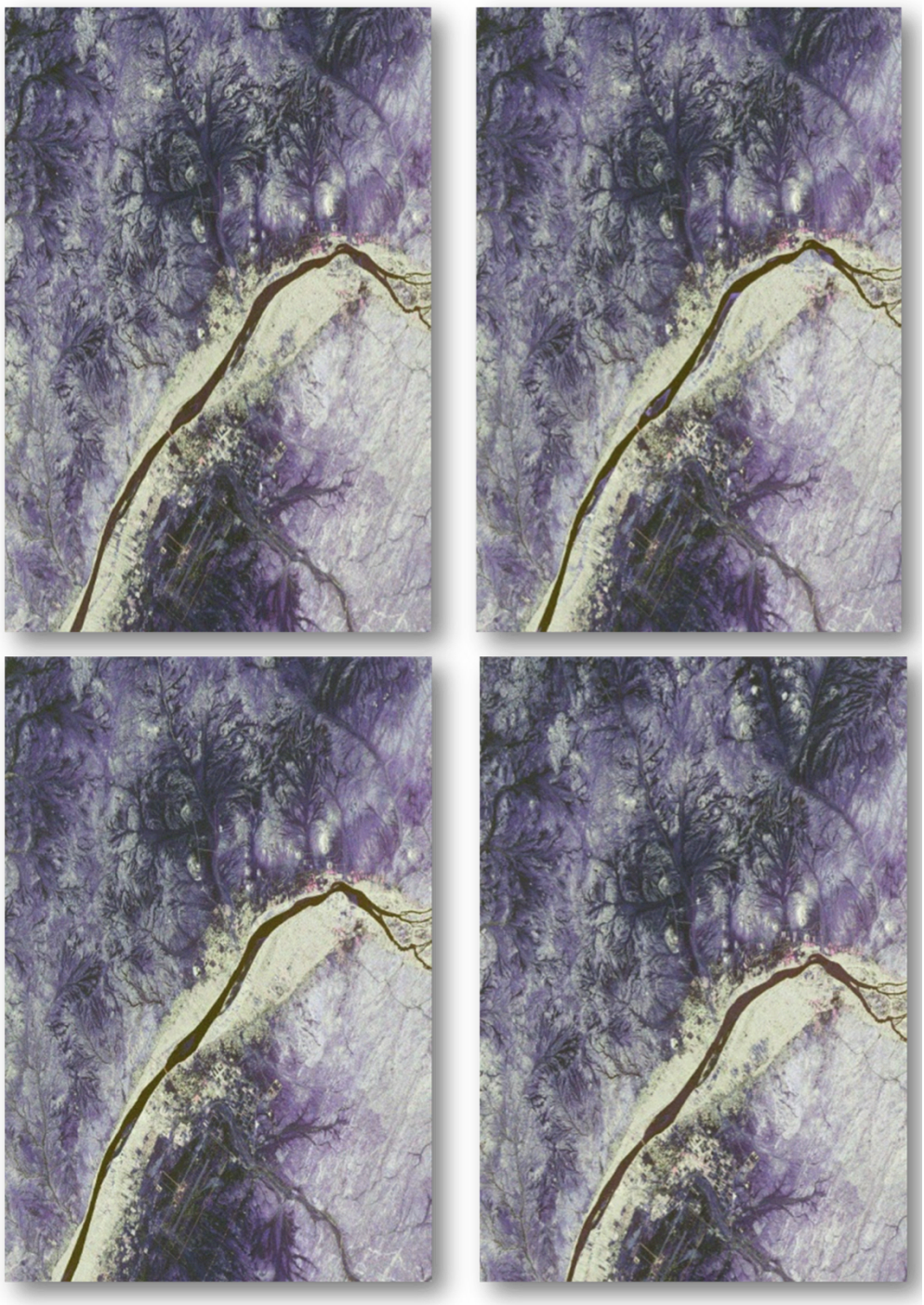

Figure 6.10 : RADARSAT-2 SLC Pauli decomposition descriptor (□ = 45.41°). In clockwise order: 2012/05/01; 2012/11/11; 2013/01/20; 2013/07/07 acquisitions

6.4 Climate information

Even if meteorological conditions of the area of interest are considered as ancillary information, their importance is crucial when performing satellite data analysis. While optical acquisitions could be affected by cloud coverage, SAR

sensors overcome this limit. Collecting weather information related to the days of the acquisitions, as well as general climate condition of the area can help in evaluating the wave penetration capability in the soil (Figure 6.11). It has to be reminded that this capability is influenced, however, by several factors like, among the others, soil's typology and moisture content.

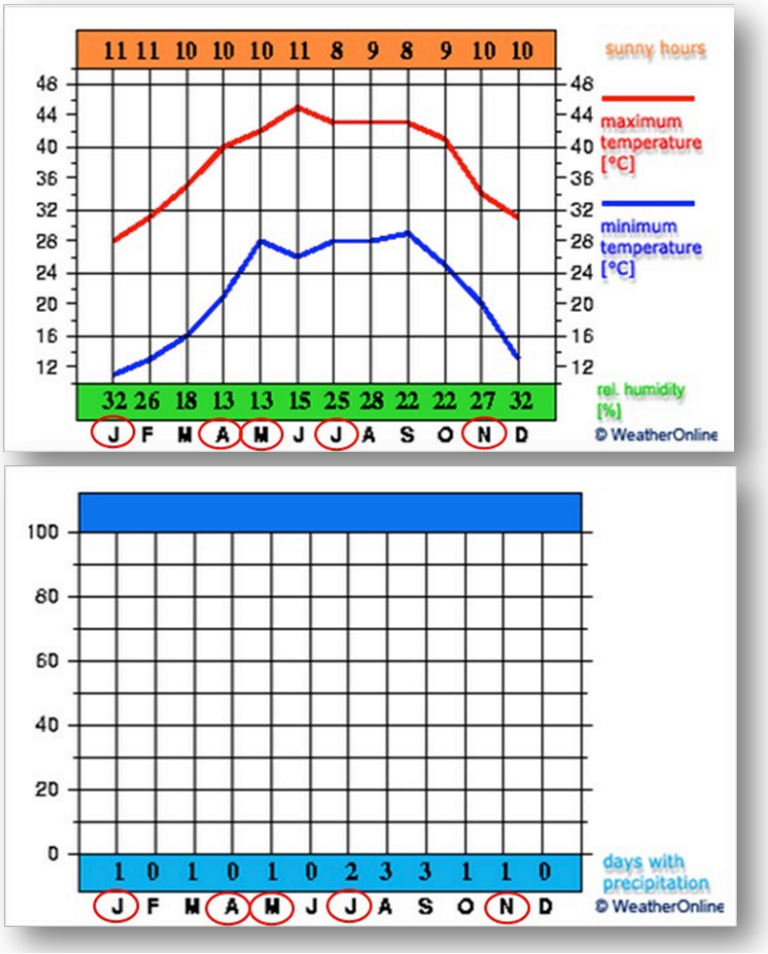

Figure 6.11 : Average of Gebel Barkal seasonal climate and precipitations corresponding to the months of the acquisitions. In the lower graph, millimetres of precipitation are indicated in the light blue row. © WeatherOnline

This is the reason why, especially for RADARSAT-2 images, the acquisition time was selected also considering the seasonal precipitation average, apart from the availability of the acquisition time of the sensor itself.

All the information concerning the general meteorology of the area, humidity percentage, temperature (min/max), precipitations and their periodicity are retrieved from the History Climate section of the Weather Online [51] and of the

Weather Underground [52] websites, by setting the city of Karima as reference weather station (Figure 6.12).

Figure 6.12 : GeoMap of Karima weather station © WeatherOnline

After the observation of the average climate at Gebel Barkal, a deeper analysis of precipitations occurred in the days of interest is necessary.

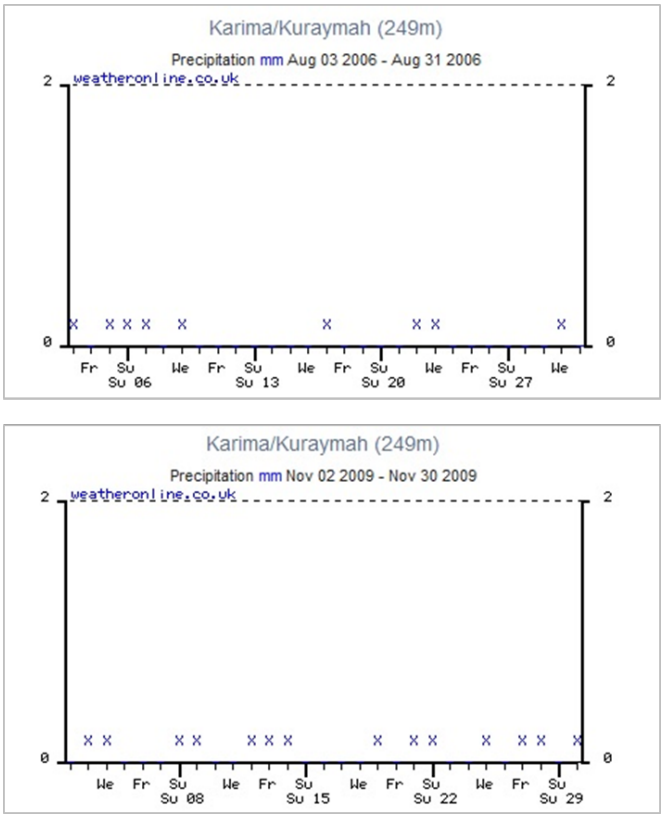

Figure 6.13 : Precipitation phenomena corresponding to ALOS PALSAR acquisition dates © WeatherOnline

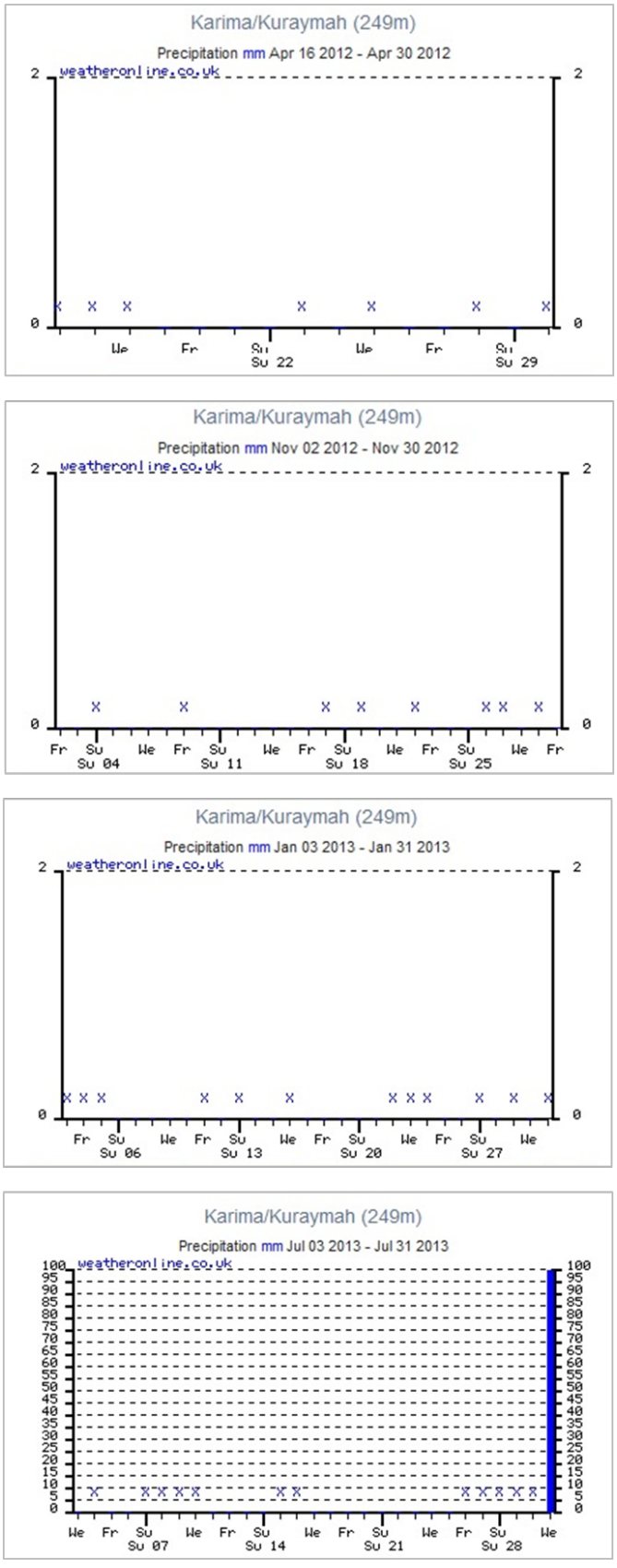

Figure 6.14 : Precipitation phenomena corresponding to RADARSAT-2 acquisition dates © WeatherOnline

Precipitation phenomena for every acquisition date are analysed, both for the days of the acquisitions and for the previous days, as reported in

Figure 6.13 and in Figure 6.14 (crosses indicate the absence of precipitation phenomena).

The absence of precipitation phenomena was registered in the dates of both ALOS PALSAR and RADARSAT-2 acquisitions, thus driving the research to the following conclusion: any meteorological event influenced the wave penetration in the ground or altered the soil moisture content, element which turned out to be decisive in the final evaluation the results obtained (see §7 and §8).

This page intentionally left blank

Chapter 7

Polarimetric SAR Multi-Frequency Analysis

After the presentation of the purpose and the selection of data set according to the designated analysis of the present research, illustrated in previous chapters, the study pursues the workflow represented in Figure 7.1. The presentation of the methodology performed in the research activity conducted for this PhD thesis focuses, in this chapter, on a polarimetric multi-frequency analysis, then completed with a multi-incidence angle analysis illustrated in the next chapter (see §8). The applied data processing chain, the analysis of the obtained results and their discussion are presented and illustrated. In the conclusive part, the description of the subsequent ground truth campaign, carried out in the frame of the last archaeological excavation mission at Gebel Barkal (November-December 2013), is described. Potential developments derived from this analysis, as data integration in a dedicated GIS project, are mentioned in the first paragraph to complete the workflow general overview, and will be presented in details in Chapter 9.

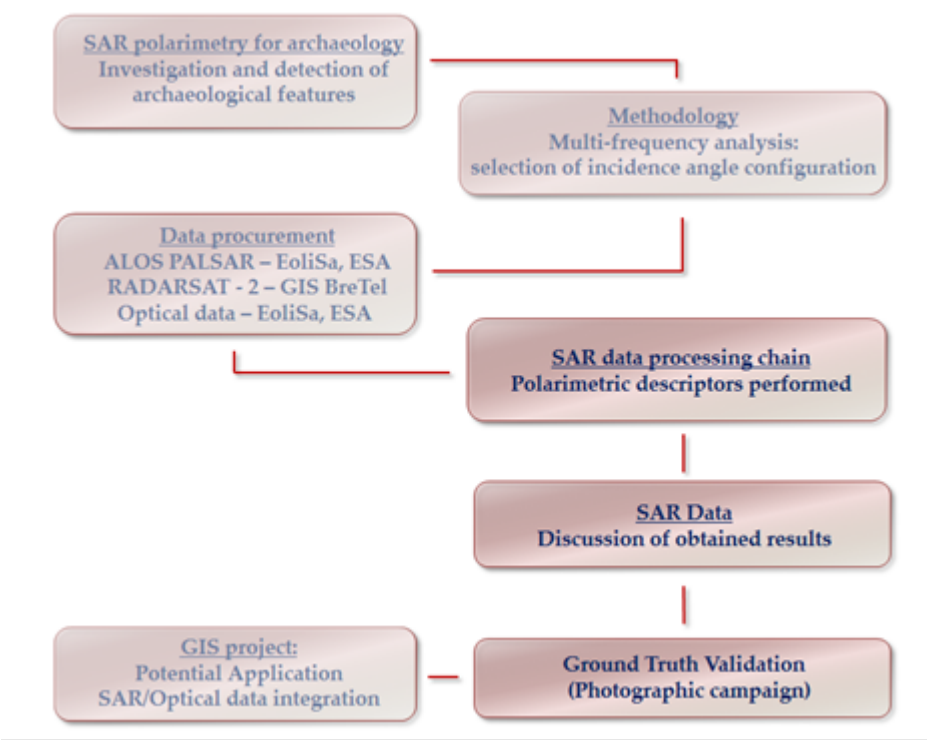

Figure 7.1 : Research workflow

7.1 A polarimetric multi-frequency and multi-temporal analysis

As already mentioned in the previous chapter (see §6.3), the approach followed in the present research is based on a multi-frequency analysis by means of the two different SAR polarimetric sensors ALOS PALSAR and RADARSAT-2. In order to compare L-band and C-band sensors at different central frequency (1.27 GHz and 5.405 GHz) but with a similar incidence angle configuration, RADARSAT-2 data were acquired in a compatible configuration mode (27.06°) compared to ALOS PALSAR (26.7° and 23.10°). As a further and more complete analysis, also the RADARSAT-2 45° incidence acquisition mode was selected, representing the most sensitive incidence angle configuration to "double bounce" scattering mechanism, compared to 27.06° incidence angle configuration, which is more sensitive to "single bounce" scattering mechanism (see §8). Moreover, the two configurations are analysed to understand which of the selected incidence angles could be the most suitable one for the detection of different archaeological features, according to the different response ancient structures could backscatter to the sensor (inclination, orientation and so on).

With regards to ALOS PALSAR data, provided by EoliSa archive of the European Space Agency (ESA) and RADARSAT-2 polarimetric data, provided by the GIS (Scientific Interest Group) BreTel (Bretagne Télédetection, see §6.3), all the images are processed by means of PolSARpro software [53]. Concerning optical dataset, the available KOMPSAT-2 image (EoliSa, ESA) and GoogleEarth acquisitions are integrated with a Quickbird imagery derived from the previous cartographic study over Gebel Barkal conducted by L. Perotti in 2005 [45] (see § 8.1).

In addition to the SAR multi-frequency analysis, a multi-temporal dataset has been collected and analysed. Moreover, available data allow an integrated multi-seasonal observation by means of the different configuration SAR polarimetric data present (Aug, 2006 ; Nov, 2009 ; Apr, 2012 ; May, 2012 ; Nov, 2012 ; Jan, 2013 ; July, 2013) and the optical images (Sep, 2003 ; Jan, 2004 ; Mar, 2006 ; May, 2008; Nov, 2012).

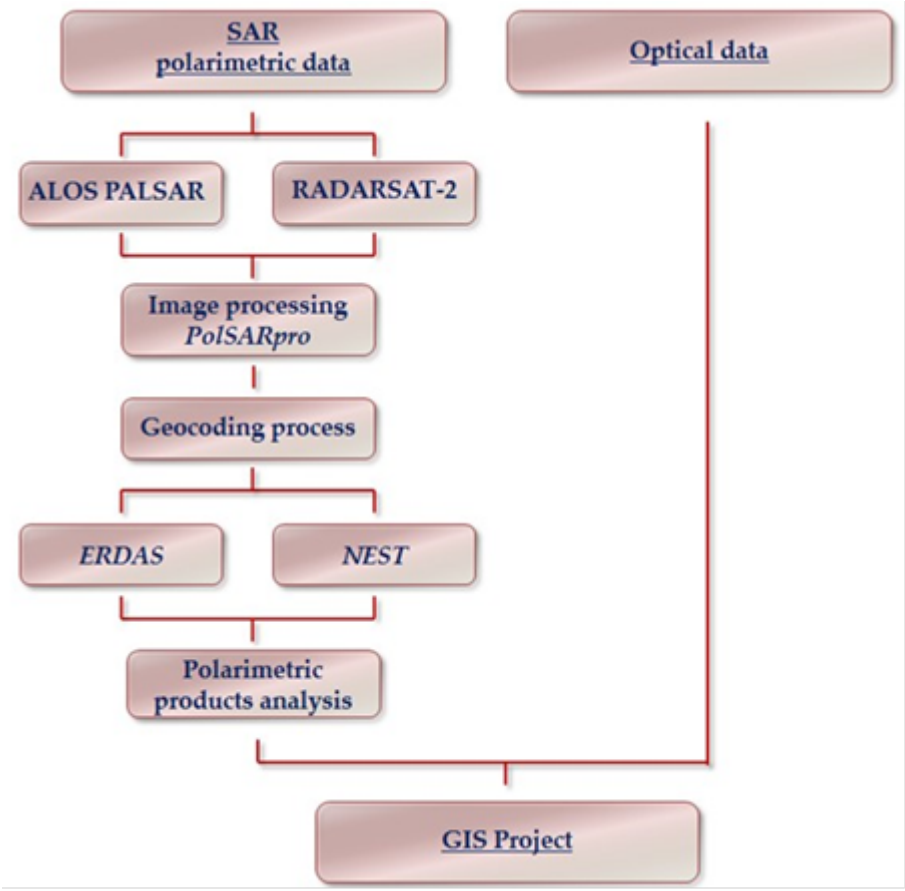

Figure 7.2 : Data collection and image processing

In fact, the acquisition dates, covering a period of ten years, allow the identification and observation of persistent and non-persistent ground anomalies in the archaeological area, for which a ground truth validation by means of a photographic campaign has been then carried out, thanks to the current Italian excavations of the University of Venice. As a conclusive step, all the satellite data are implemented in a Geographic Information System (Figure 7.2), together with Aerial photographs and cartography, and a 3D restitution of the Royal Cemeteries is performed (see §9.5), in order to complete the already existing digitalisation of the temples of Gebel Barkal. The GIS project (see §9.3) will be used in the future to perform an updated high-resolution cartography that includes all the archaeological structures, and will be carried out in the frame of the collaboration with the University of Turin (Prof. L. Perotti, Geological Sciences department) and of the already mentioned University of Venice (Prof. E. M. Ciampini, head of excavation missions to Gebel Barkal).

7.2 Data acquisition: the 26 deg incidence angle configuration

The choice to focus the attention towards a 26° incidence angle configuration is due primarily to the multi-frequency approach selected for the present PhD research, which gives priority to the use of SAR polarimetric sensors with different frequency (see §7.1).

L-band and C-band sensors, with respectively their capability to penetrate the soil and their medium spatial resolution, can constitute the most suitable SAR polarimetric instruments for the detection of anthropic complexes and archaeological structures today available from satellite. In fact, wave penetration in the soil represents a challenging factor for the modern archaeological research, based on the observation of ground anomalies that are verifiable only through surveys activities on the site.

In this scenario, thanks to the opportunity of selecting the incidence angle acquisition mode for RADARSAT-2 polarimetric sensor, it has been possible to dispose of RADARSAT-2 (specifically scheduled) and ALOS PALSAR acquisitions (archived data) with a compatible configuration mode, respectively 27.6° and 26.7°/23.1° (Figure 7.3). By keeping the same incidence angle at

different frequency, it is possible, in fact, to investigate the scattering mechanisms of the surface archaeological features illuminated by L-band (longer wavelength) and by C-band (shorter wavelength), as well as the scattering mechanisms related to target generating both persistent and sporadic anomalies.

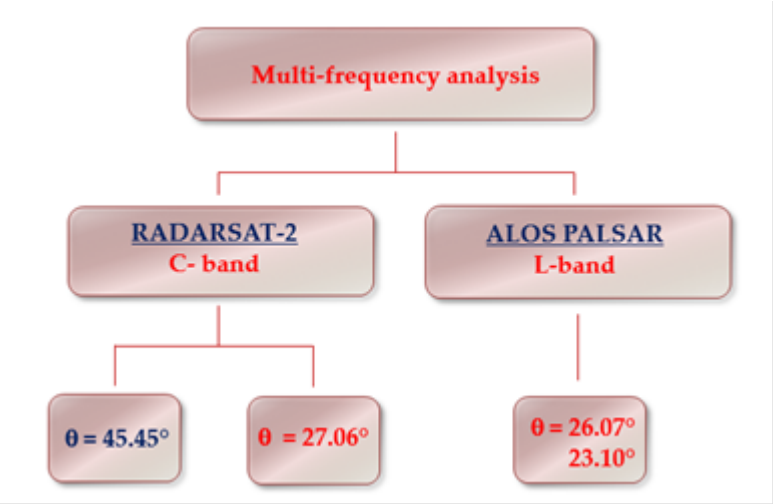

Figure 7.3 : Multi-frequency analysis

To this end, the 45° incidence angle configuration of further RADARSAT-2 acquisitions was later considered with the aim to compare the same backscattering responses noticed in the 26° acquisitions as well as to identify further scattering mechanisms as the ones defined by a double bounce backscatter (see §8).

As will be shown, the 26° configuration mode turned out to be the most suitable one for the detection of some of the temples and palaces at Gebel Barkal, as well as pyramids, whose varying walls are detectable both by a 45° and a 26° incident wave, but also for the detection of highlighted backscattering due to the probable presence of subsurface features. Information derived from this kind of analysis helped also in understanding the type of backscattering coming from structure rather than from the light morphology characterizing Gebel Barkal site, at different frequency and at different incidence angle configurations.

7.3 SAR polarimetric analysis over the archaeological area of Gebel Barkal

Before entering in the details of the polarimetric descriptors analysis, a recall on the archaeological structures and their environment is necessary to understand the steps and the choices selected in the study workflow.

The central archaeological area of Gebel Barkal expands for about 3 square kilometres without being affected by natural or artificial constraints. However, beyond this limits, several archaeological remains have been localised both in the urban area of Karima, the modern city located at NE of the archaeological zone, and along the palm cultivation belt that follows the west bank of Nile river (Figure 7.4, a). Nevertheless, archaeologists think that many of the ancient structures have to be still unearthed.

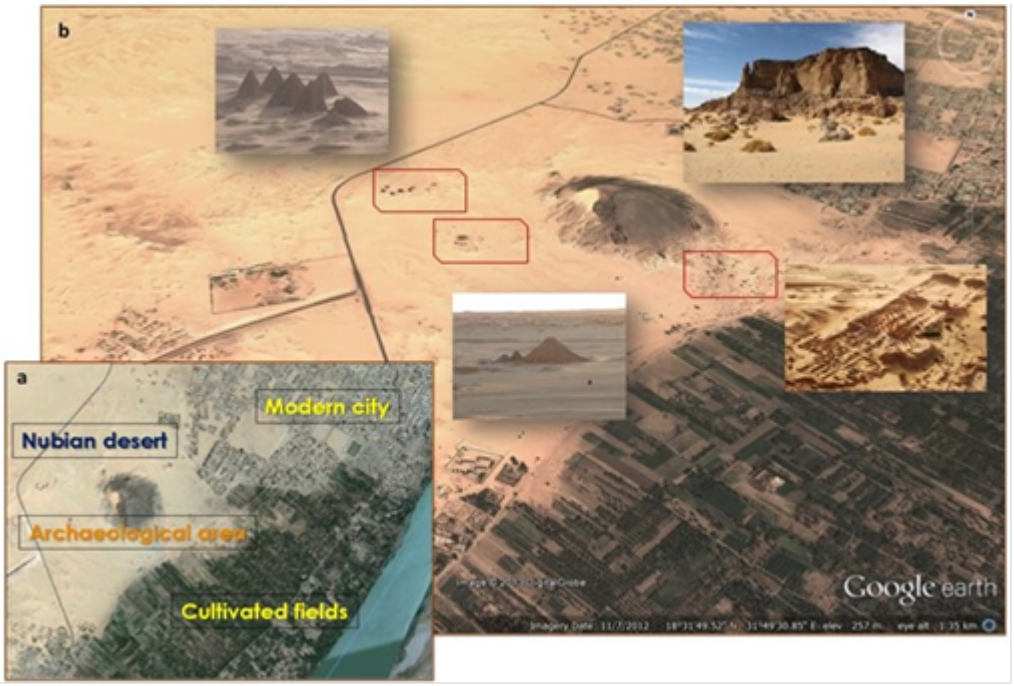

Figure 7.4: (a) Gebel Barkal archaeological area surrounded by the modern city of Karima, the cultivated fields, the Nubian desert. b) Archaeological evidences at Gebel Barkal. © Google Earth 2013

Moreover, the vicinity to the arid area of the Nubian desert, exposes the site to constant strong winds and sand storms, which periodically cover and uncover the ancient structures (see §5.2). Concerning the archaeological evidences, Gebel Barkal is characterized by two major necropolis constituted by two groups of Royal Pyramids in the N-W part of the site and in the central part of it. In the southern part, it presents well-known surface palaces and temples remains (Figure 7.4, b), partially visible and currently investigated thanks to the missions of international archaeological excavations. The unique relevant morphologic element is constituted by the *jebel*, the "Holy Mountain" rising for about 100 meters from the flat desert surface.

7.3.1 ALOS PALSAR data processing chain

The present research activity started with the analysis of 26.7° and 23.10° incidence angles ALOS PALSAR images. The first step of the workflow consisted in extracting and then analysing all the SAR image polarimetric descriptors (Figure 7.5).

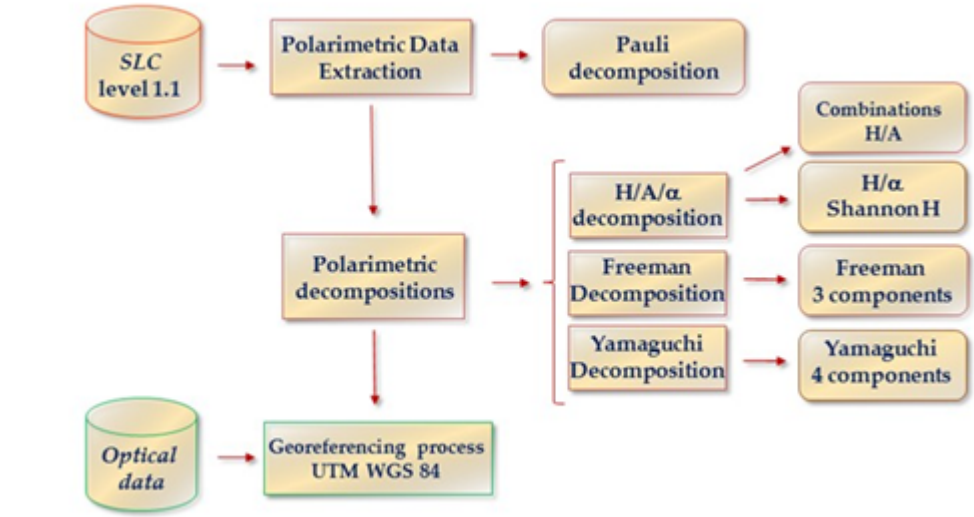

Figure 7.5: ALOS PALSAR processing chain

Images processing level 1.1, processed with PolSARpro software, presents range and azimuth compressed. At this level, the image in slant range is still a complex data, thus compromising the precise identification of the archaeological area. Due to the rectangular shape of pixel in the SLC data, pre-processing consists in a multi-look operation performed with a window of 5 pixels in row and 1 in column, thus transforming the product into a more familiar geometric visualization. A Pauli coherent decomposition (R: |HH-VV|; G: |HV|; B: |HH+VV|) is thus derived (Figure 7.6).

At this step of the processing chain, a first physical interpretation of the Pauli decomposition is possible from a qualitative point of view. As a following step, the T3 matrix, containing all the information concerning the interaction between waves and targets, is extracted, thus performing a removal of the random phase contained in the scattering matrix S (see §3.9). Subsequently, several polarimetric decompositions are applied, in order to observe the target backscatter and to understand which polarimetric decomposition showed better the ones related to the presence of archaeological structures.

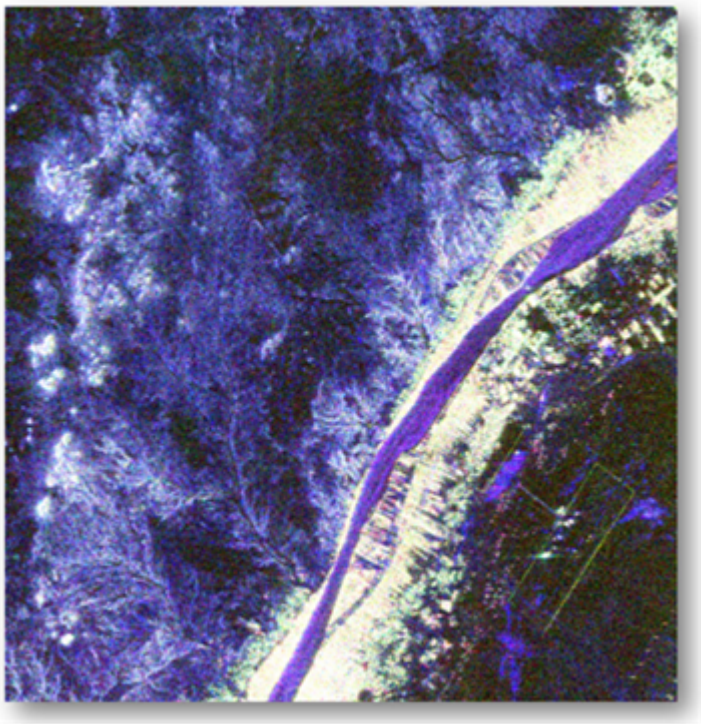

Figure 7.6: Pauli coherent decomposition RGB image

The resulting polarimetric descriptors are thus georeferenced (UTM WGS84) using the KOMPSAT-2 optical imagery as master image (Table 7.1). The geocoding processes between ALOS PALSAR and optical data has been performed by means of the selection of GCPs (Ground Control Points), paying attention to the creation of a homogeneous cloud of points over all the area of the archaeological site. Several difficulties were encountered, not only due to the lack of reference optical data, for which only one optical image was available, but also because the KOMPSAT-2 image presents important environmental and topographic changes in the area not easily traceable in SAR data and vice versa. In fact, in a period of 3 years (2006/2009), period covering the acquisitions of PALSAR and KOMPSAT-2, the realisation of highways and infrastructures close to the site boundaries changed the overall environment, with a consequent lack of correspondence of reference elements between optical and SAR data.

Geometric Model	Polynomial Order	Reference map Projection	Resampling Method	Pixel Spacing meters
Polynomial	1	UTM WGS84 Zone: 36N	Nearest Neighbour	20

Table 7.1: Georeferencing process details

Following this workflow, via comparison of the information, it is possible to derive an initial hint of the different type of scattering mechanisms occurred over the archaeological structures. By overlapping SAR Pauli RGB decompositions with optical imagery (Figure 7.7), the archaeological evidences are located and, together with them, some well-defined scattering mechanisms are noticed (see §7.3.2).

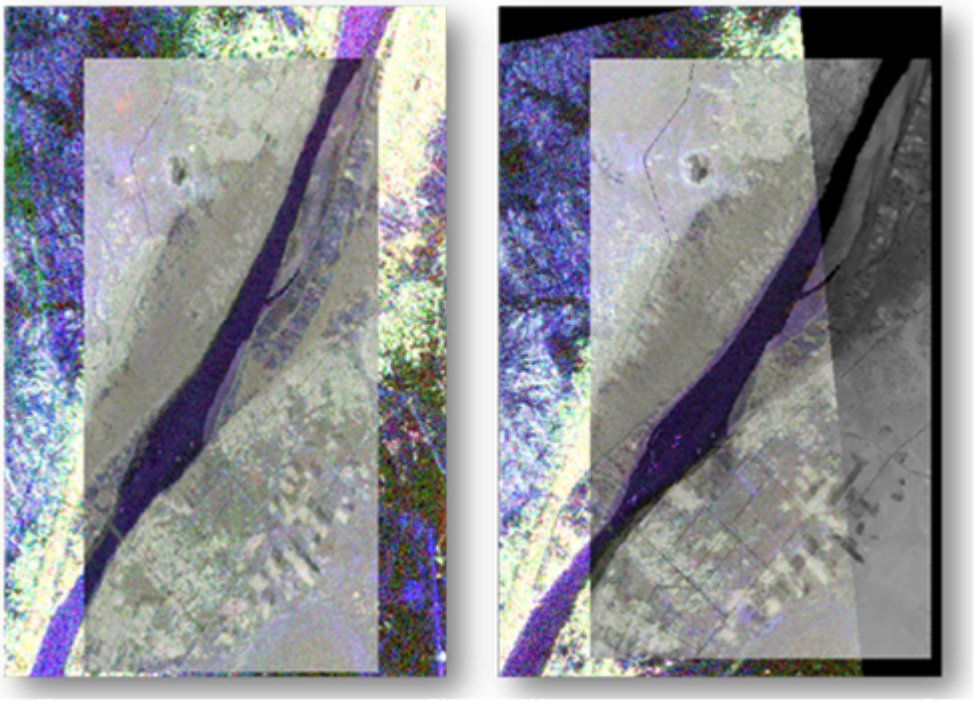

Figure 7.7 : ALOS PALSAR Pauli decomposition RGB image (2006, left ; 2009, right) overlaid to KOMPSAT-2 image (2008)

In order to deepen the analysis, the observation of occurred scattering mechanisms continues over other polarimetric decompositions thus providing additional information about the nature of the noticed backscatter.

7.3.2 ALOS PALSAR polarimetric descriptors and results

The processing chain performed with PolSARpro over the two available ALOS PALSAR acquisitions is dedicated to the identification of the polarimetric descriptors that seemed to be most sensitive to the detection of features of archaeological interest. The present PhD research is thus addressed to the exploitation of a specified selection of polarimetric parameters, which demonstrate significant output for an archaeological investigation.

Figure 7.8 : First step of the Processing chain: Pauli decomposition

The first descriptor observed from a qualitative point of view has been the Pauli decomposition descriptor (Figure 7.8). Pauli RGB image (Figure 7.9) visualises the sum of all the backscattering contributions coming from the illuminated targets. It provides a first knowledge about the three principal scattering mechanisms of single bounce, double bounce and volume scattering. In Figure 7.9, it is possible to notice the strong backscatter coming from three major areas at Gebel Barkal: the modern city of Karima in the NE portion of the site, the palm cultivation in the SE site area, the "Holy Mountain" in the central part and the topography surrounding the site. Close to the *jebel*, in the west portion of the archaeological area, the two Royal cemeteries are well identifiable in both SAR acquisitions.

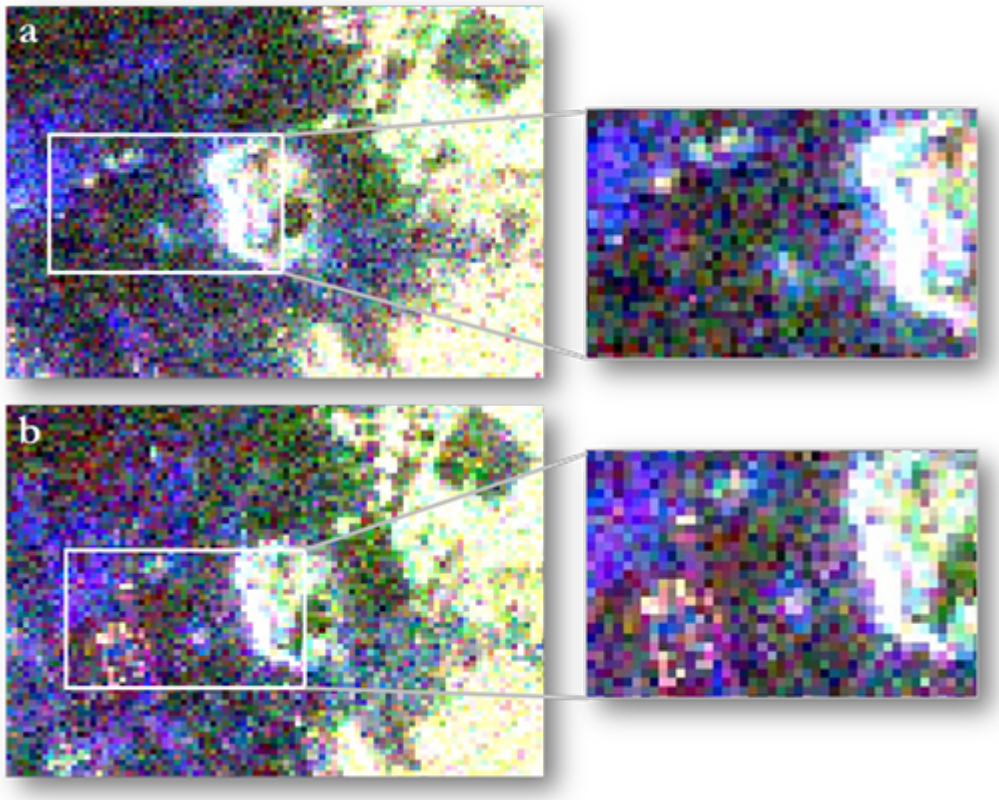

Figure 7.9 : August 2006 (a) and November 2009 (b) Pauli RGB decompositions. In the detail, the archaeological area of Royal cemeteries

By considering the three years distancing time between the two acquisitions, some changes that occurred in the area can be recognised. In fact, a modern infrastructure has been built very close to the second group of pyramids of the Royal cemetery (Figure 7.9, b).

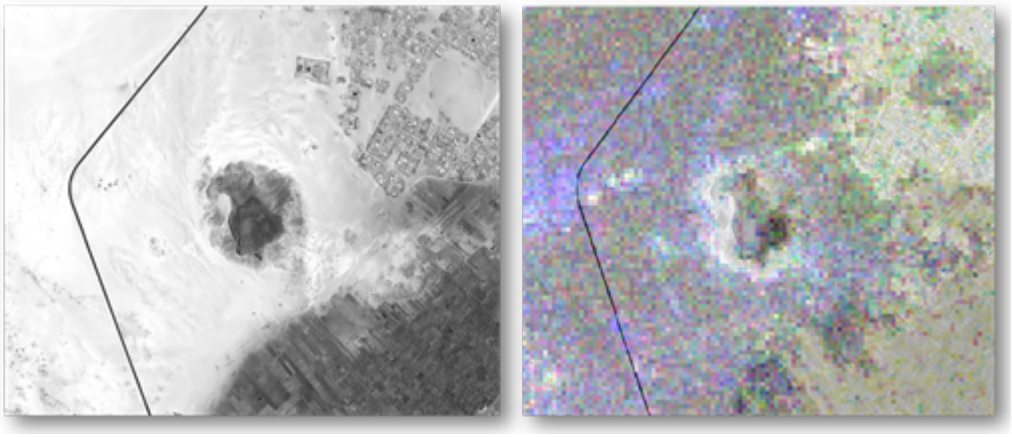

Figure 7.10 : Kompsat-2 panchromatic image (left) overlaid with ALOS PALSAR Pauli RGB decomposition (right)

Given the difficulty in recognize modern and ancient structures as well as topographic elements in complex data as SAR images are, a comparison with the KOMPSAT-2 acquisition is made, in order to enhance the correspondence between the most noticeable scattering mechanisms and the different kind of target illuminated. PALSAR data have thus been overlaid to the panchromatic band of KOMPSAT-2 image at 1 meter of spatial resolution (Figure 7.10).

By analysing SAR Pauli image and Kompsat-2 data, it can be noticed how the major contribution is given by the larger archaeological structures as well as by urban and agricultural areas. Unfortunately, due to the not enough high spatial resolution of PALSAR data, only the major structures have been identified ; for this reason, ALOS PALSAR investigation has been focused in the field of Pyramids in the west area of the site.

Looking to the detail of the image shown in Figure 7.11, we can easily distinguish the two groups of Royal pyramids (yellow squares), and, in the image acquired in 2009, the modern infrastructure close to the site (white arrow, right image). However, a third backscattering has been noticed close to the NW group of pyramids (Figure 7.11, red ellipse). The qualitative analysis performed by observing satellite optical data, reveals how any surface structure seemed to be

located in correspondence of the noticed backscattering, both in the KOMPSAT-2 image and on Google Earth acquisitions.

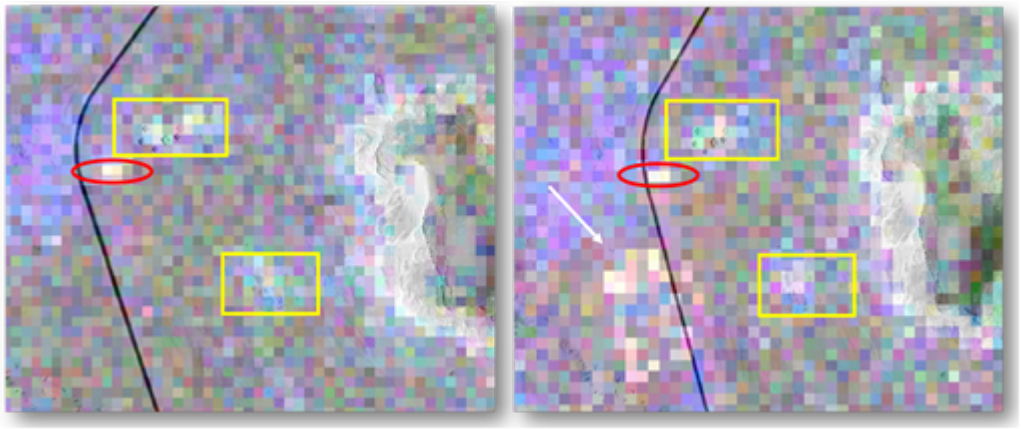

Figure 7.11 : ALOS PALSAR Pauli RGB images (2006, left ; 2009, right) overlaid to KOMPSAT-2 image

Moreover, the available cartography, dating back to 1995, does not seem to report archaeological evidences in that point, while the persistence of the backscattering after three years from the previous acquisition addresses the investigation to consider the climate archived information (see §6.4). In fact, supposing a target detection in that point due to the L-band wave penetration in the ground, the presence of precipitations in the days before the acquisition and in the same day could be decisive for the absorption/loss of the signal. Thanks to the consultation of the archives of Weather Online website (see §6.4), no precipitation phenomena were affecting Gebel Barkal area in both SAR acquisition dates (

Figure 6.13 and Figure 6.14). The absence of precipitations phenomena for the days of interest as well as the very low percentage of humidity registered confirm the dryness of the sand in the area.

Once this first qualitative analysis was completed, additional polarimetric descriptors (see §3.10.4) have been analysed in order to gain archaeological information and to validate the nature of the supposed scattering mechanisms noticed, both upon the already known structures and upon the general morphology surrounding them. In particular, the study is thus focused on the observation of the already noticed backscattering in the qualitative analysis, in order to observe the scattering behaviour in the same point in the other polarimetric descriptors performed. This approach provides additional information in discriminating scattering mechanisms coming from the different targets.

Figure 7.12 : SAR Polarimetric Decomposition: Yamaguchi 4 Components decomposition

Among the several polarimetric decompositions analysed, the Yamaguchi 4-component decomposition turned out to be the most meaningful one for the purpose of the present research (Figure 7.12). A sliding window of 3x3 was applied.

As mentioned in Chapter 3, Yamaguchi decomposition starts from the assumption that in nature reflection with symmetric conditions is not very common, as previously stated by Freeman decomposition (see §3.10.4). Due to the presence of urban and cultivated areas where symmetry conditions are not valid, Yamaguchi 4-component decomposition has been selected for the present research. This decomposition produces a RGB image where the red channel corresponds to the double bounce scattering, the green channel corresponds to volume scattering and the blue channel corresponds to single bounce scattering. This allows an interpretation of the physics behind the colour representation

(Figure 7.13) that can be linked to the most common classes of backscattering (urban areas, vegetated areas, surface).

By observing the RGB image of the three typology Yamaguchi decomposition is composed of, a more detailed scattering mechanisms discrimination has been noticed in Yamaguchi_G4U1 (Figure 7.13, bottom). In this decomposition, it can be noticed as part of the city of Karima is presenting a double bounce mechanism (yellow arrow), typical from buildings, while in Yamaguchi_Y4O (Figure 7.13, top) the backscattering coming from the city is entirely assimilated to a volume scattering, typical from vegetation, due to the orientation of the buildings. In fact, in this kind of decomposition, vegetated and urban areas are still presenting a similar contribution, which, however, is better represented compared to what it has been observed in the Freeman decomposition.

What can be noticed is that the cultivated area in the southern part of the Jebel presents a volume scattering (Figure 7.13, orange arrow) as well as the major part of the buildings in Karima in the NE part of the image. In addition, the two groups of Royal Pyramids (Figure 7.13, red arrow), as well as the Jebel itself, are represented as a combination of single bounce and volume scattering contribution. Following the same consideration, in the area close to the NW group of Pyramids the strong backscattering is shown as a double bounce mechanism in Yamaguchi_ Y4R and Yamaguchi_G4U1 (Figure 7.13, middle, bottom), generally more representative of urban areas, while it appears as a combination of single bounce and volume scattering in Yamaguchi_Y4O (Figure 7.13, top).

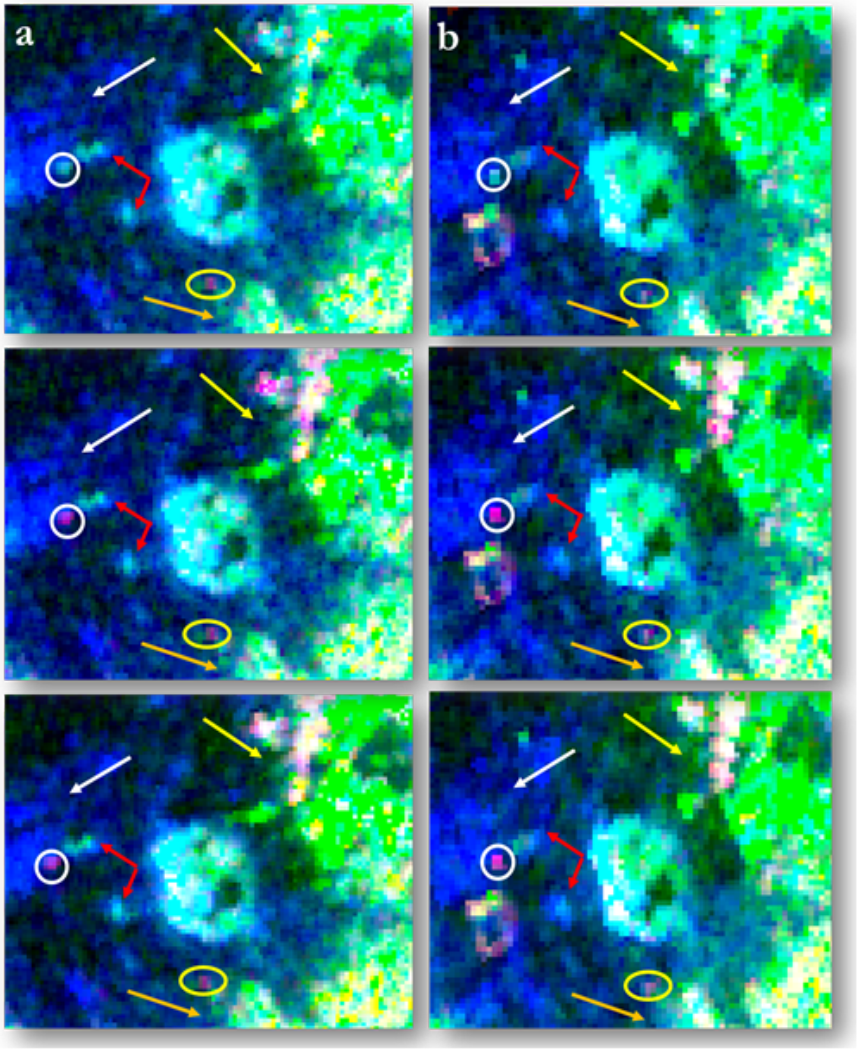

Figure 7.13 : PALSAR images acquired on August 2006 (a) and November 2009 (b). Yamaguchi Y4O (top) Yamaguchi Y4R (middle) and Yamaguchi G4U1 (bottom) RGB components

Comparing this target response with the one given by a well-known building in the area (Figure 7.13, yellow ellipse), which presents the same scattering mechanism in all the three components, i.e. a double bounce, a deeper analysis on the nature of the noticed strong backscattering is required. Moreover, an important consideration arises from this initial analysis of Yamaguchi decomposition: the scattering mechanism generated by the light morphology surrounding the archaeological area (Figure 7.13, white arrow) is recorded as a pure single bounce.

This consideration lead the study to take in account the effective different nature of the noticed target and the surrounding topography in SAR data, while optical

data do not present any apparent surface difference between the area of the target and the morphology.

In order to deepen the analysis of Yamaguchi_G4U1 decomposition, in which the archaeological and topographic features seemed to be better discriminated, the single channels related to different scattering mechanisms are observed. The recognition of the strong backscatter in the single channels is not as immediate as in the qualitative study carried out on the RGB images. For this reason, its identification has been achieved by means of the latitude and longitude coordinates of the area (18°32'15" N 31°49'14" E WGS84), so as to locate and verify as precise as possible the correspondence of the well-defined scattering mechanism between SAR data.

In Figure 7.14, Yamaguchi decomposition channels corresponding to the double bounce (top), single bounce (middle) and volume scattering mechanisms (bottom) for the two PALSAR acquisitions are shown. By identifying the latitude/longitude position of the backscattering noticed in the RGB images illustrated above, is possible to observe the amplitude values recorded in that point for each channel of the same polarimetric decomposition in the two PALSAR acquisitions (Table 7.2). As a result, the strong backscattering is detected with a high contribution of single bounce and a low contribution of double bounce mechanism, which is recorded only for this target, while it is not detected in volume scattering channel. In order to compare this response to both archaeological and urban features, what arises from a wider analysis is that the urban area of Karima (Figure 7.14, red arrows), as well as the palm plantations following the Nile river in the southern part of the site (green arrows) present the same major contribution, i.e. a volume scattering mechanism.

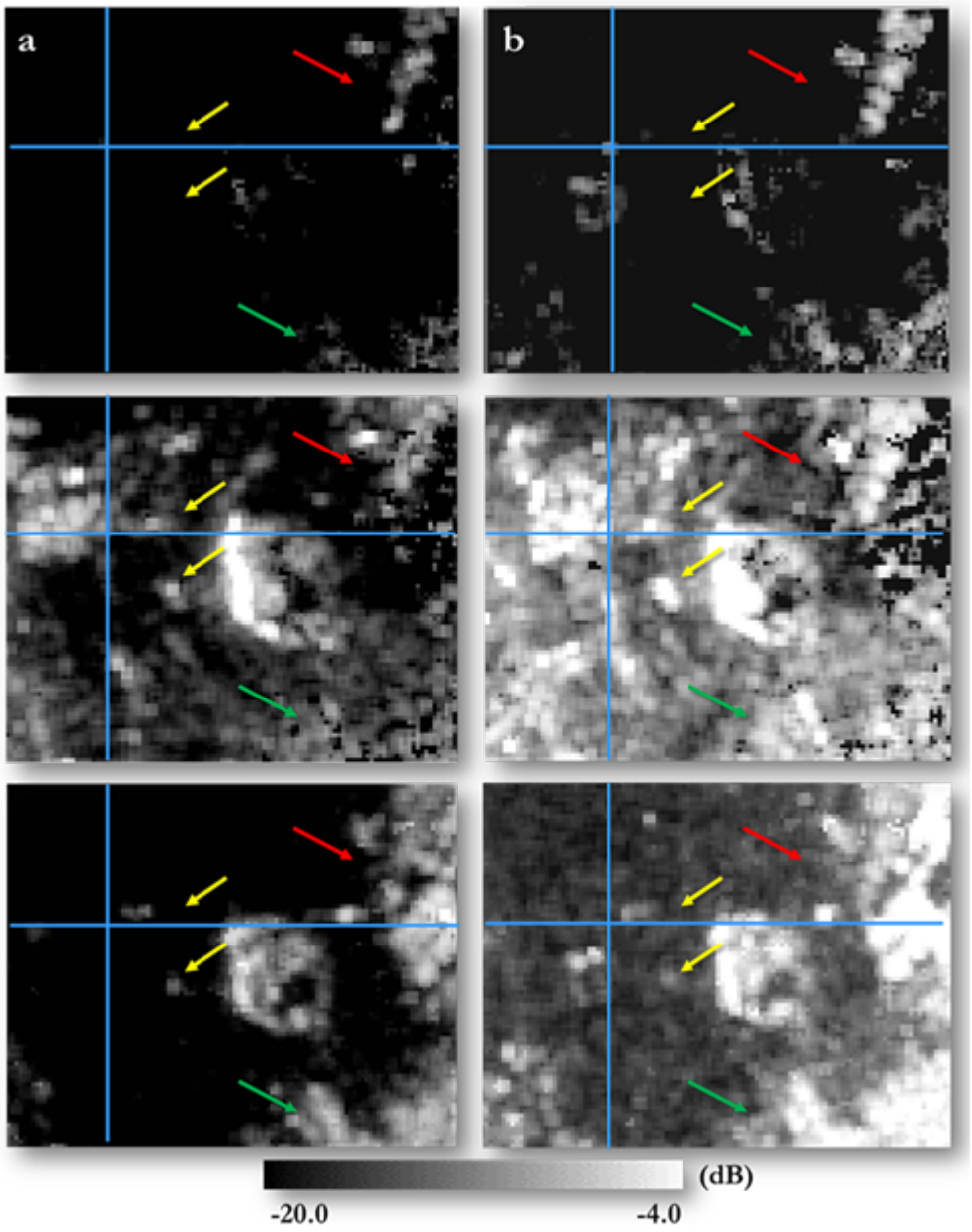

Figure 7.14 : Yamaguchi G4U1 decomposition single channels 2006 (a) and 2009 (b) acquisitions. Double Bounce (top); Single Bounce (middle); Volume scattering (bottom)

Acquisition date	□	Yamaguchi G4U1_Dbl	Yamaguchi G4U1_Odd	Yamaguchi G4U1_Vol
2006/08/14	26.70°	-16.99 dB	-10.97 dB	-20 dB
2009/11/05	23.10°	-13.01 dB	-6.77 dB	-16.99 dB

Table 7.2 : Yamaguchi 4 components decomposition single channels amplitude values

The reasons generating this kind of responses are linked to the orientation of buildings in the central part of the city, which is assimilated to a typical vegetation backscattering. In fact, if we consider the longitudinal SW/NE portion of the city in the northern part of the images, it is very well detected in the double bounce and single bounce channels as expected for buildings and their roofs (red arrows). Due to their orientation respect to the electromagnetic wave, the two groups of Royal Pyramids are partially illuminated in the volume scattering channel as well, while the major backscattering contribution they send back to the sensor is registered as a single bounce mechanism.

Hence, the scattering mechanism detected close to the NW group of pyramids and very well detected in the single bounce channel with a lower contribution in the double bounce, presents the same principal scattering mechanism coming from surface archaeological structures and from the light surrounding morphology, but is distinguished by a double bounce backscatter contribution that is not recorded neither for existing archaeological features nor for topographic elements. As known, low frequency L-band wavelength presents a deep penetration capability in very dry environments, as the case of Gebel Barkal is. The mentioned considerations done with ALOS PALSAR data have thus addressed the research to the assumption of a penetration of the incident wave in the ground, detecting a target not visible in KOMPSAT-2 and Google Earth acquisitions, as well as in the available cartography. Following this workflow and in order to verify or confute this hypothesis, the four RADARSAT-2 imagery acquired with a similar incidence angle of ALOS PALSAR data are studied.

7.3.3 RADARSAT-2 processing chain

The RADARSAT-2 processing chain, presented in Figure 7.15, has been performed on four higher spatial resolution polarimetric RADARSAT-2 images (□ = 27.06°), specifically acquired in 2012 and 2013 (April, November, January, July). When performing polarimetric decompositions, in order to preserve as much as possible spatial resolution, partially lost in ALOS PALSAR, and thanks to the more understandable visualisation of the single look complex product given by a nearly square shape of pixels (Figure 7.16), a different processing chain has been applied on RADARSAT-2 data.

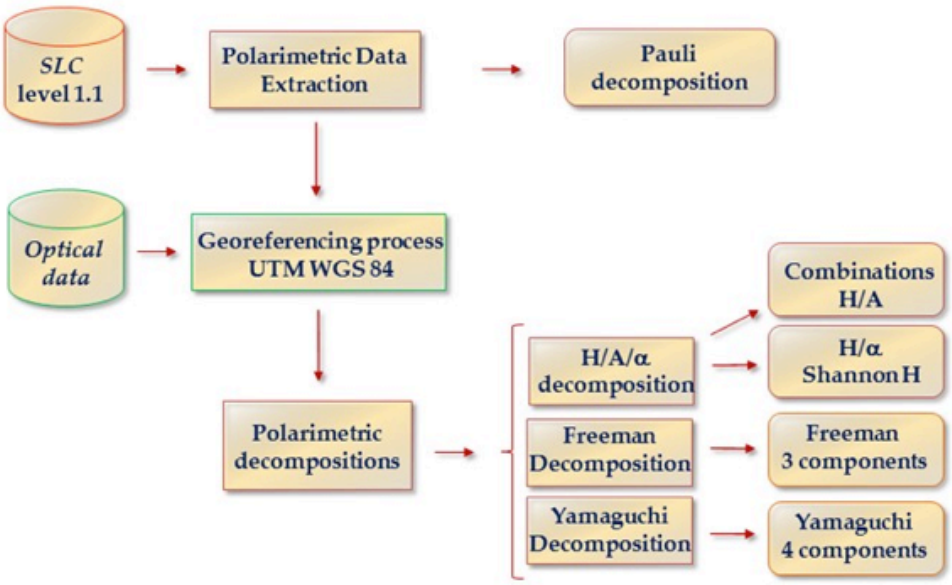

Figure 7.15 : RADARSAT-2 Processing chain

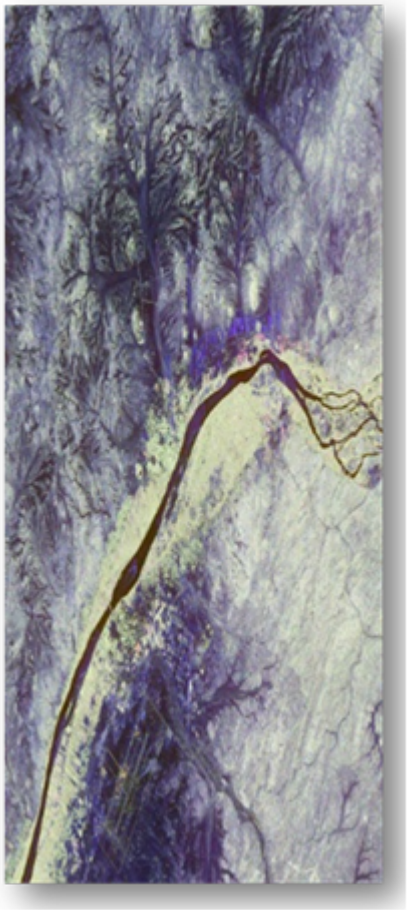

Figure 7.16 : RADARSAT-2 Single Look Complex Pauli RGB visualisation (2012/04/28)

After T3 matrix extraction, the T3 elements are directly georeferenced with optical data (Table 7.3). In the case of RADARSAT-2 data, the georeferencing process has been performed as one of the first steps of the processing chain by means of NEST software [54] that geocodes RADARSAT-2 T3 matrix in WGS84 datum (Figure 7.17).

The georeferenced T3 matrix is at this point imported again in PolSARpro, where it is processed to perform polarimetric decompositions, providing, as a result, already georeferenced polarimetric decompositions outputs.

Projection	DEM Resempling Method	Image Resempling Method	Pixel Spacing meters
UTM WGS84	Bilinear	Bilinear	10

Table 7.3 : Georeferencing process parameters (NEST)

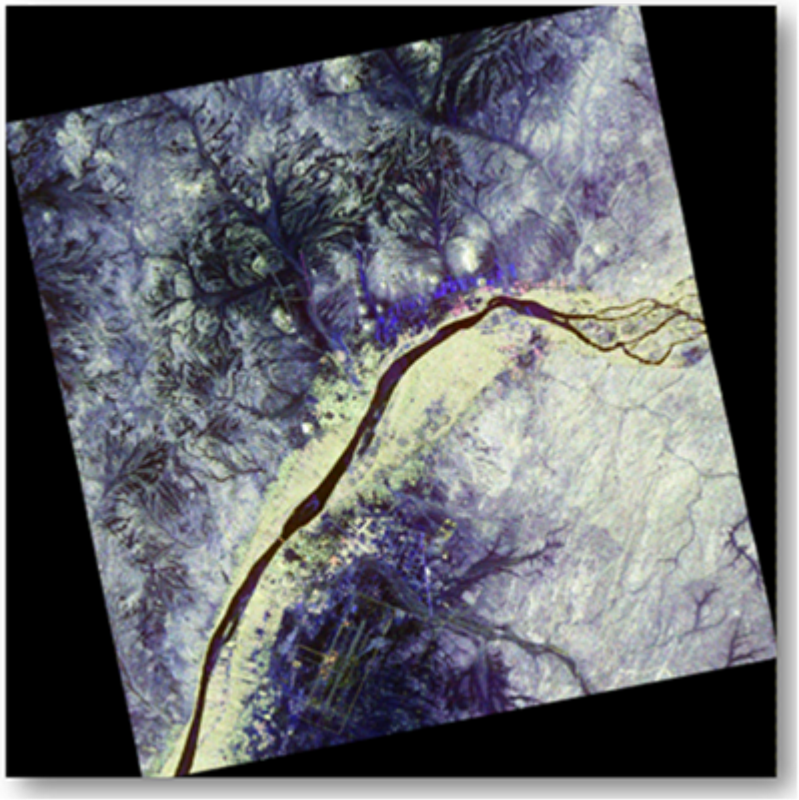

Figure 7.17 : Georeferencing process output (NEST) RADARSAT-2 polarimetric descriptors and results

The georeferenced polarimetric outputs have been then performed applying a sliding window of 3x3 (pixels are merged 3 by 3), in order to reduce the speckle effects and, at the same time, preserve as much as possible the spatial resolution.

In the frame of the multi-frequency analysis, the same polarimetric descriptors analysed in PALSAR images have been selected and examined for the four RADARSAT-2 27.6° incidence angle acquisitions. The qualitative analysis already carried out on ALOS PALSAR data was applied also to RADARSAT-2 data, to derive a first overview of the scattering mechanisms occurred in the area in 2012 and 2013 (Figure 7.18).

Figure 7.18 : First step of SAR processing chain: Pauli decomposition

In order to obtain an overall visualisation of the different type of scattering mechanisms occurred over the archaeological structures, over the surrounding morphology and over the vegetated and urban areas, RADARSAT-2 polarimetric Pauli RGB decomposition has been overlaid to the more recent Google Earth acquisition (November, 2012), for a first crossed qualitative analysis (Figure 7.19).

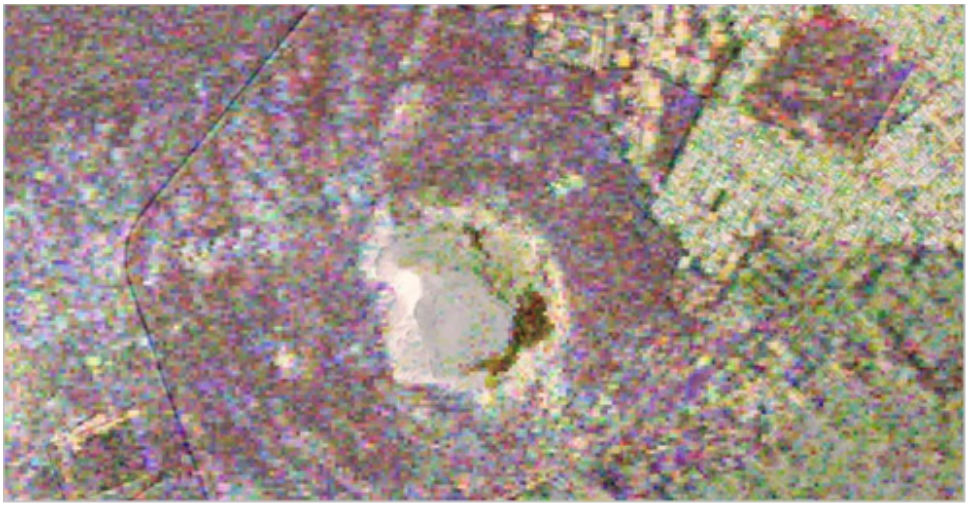

Figure 7.19 : Pauli RGB image acquired in April, 2012 overlaid to Google acquisition acquired in July, 2012

The scattering mechanisms distribution already observed in ALOS PALSAR data is thus compared to the ones noticed in RADARSAT-2 images at this initial phase of polarimetric descriptors analysis, then deepened by examining other polarimetric descriptors. By observing the four C-band Pauli RGB decomposition images (Figure 7.20), each of them overlaid to the most recent of the three Google Earth acquisitions, it has been noticed that the archaeological structures

and the morphology of the site are more easily recognizable thanks to the higher spatial resolution of RADARSAT-2.

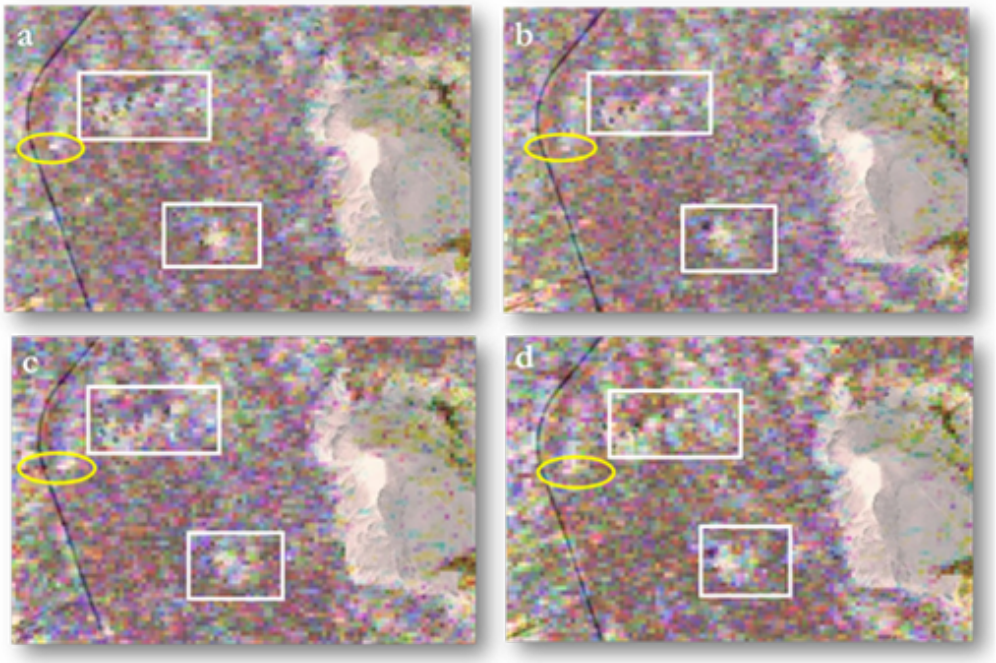

Figure 7.20 : Pauli RGB decomposition (a: April 2012 b: November 2012 c: January 2013 d: July 2013) overlaid to Google earth image (July 2012)

However, the higher spatial resolution posed a problem of less clear backscattering discrimination compared to what observed in ALOS PALSAR data, highlighting a more detailed distribution of backscattering in the urban area and in the surface morphology of the site to which C-band is more sensitive. Nevertheless, a well-localised backscattering has been detected in the area close to the NW group of Royal Pyramids (Figure 7.20, white squares), thus confirming, a first level analysis, the persistence of an important scattering mechanisms in the same area identified in ALOS PALSAR data (Figure 7.20, yellow ellipse).

Considering the absence of surface archaeological structures recorded on the cartography and in optical data, also in the case of RADARSAT-2 data analysis, the meteorological information about the days of the acquisitions are derived in order to know if any precipitation phenomenon was registered in the area. In fact, a C-band target detection in that point could be easily affected by light precipitations or by a contrast of humidity in the soil. Thanks to the archives of WeatherOnline website, in this case as well, the absence of precipitations and a very low percentage of humidity was registered in the days before and in the days

of the acquisitions, thus confirming, again, the dryness of the sand in the area (Figure 6.14).

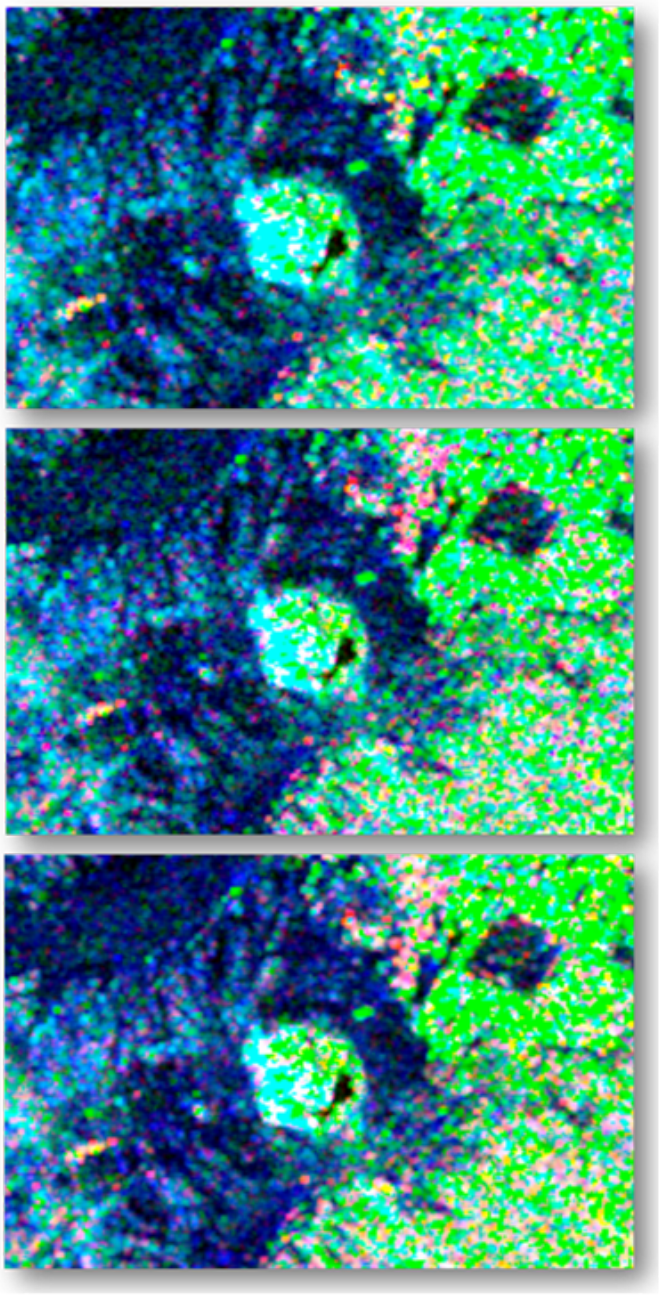

Figure 7.21 : Yamaguchi 4-component decomposition RGB image. Y4O (top) Y4R (middle), G4U1 (bottom) of RADARSAT-2 image (2012/04/28)

The RADARSAT-2 processing chain is performed following the same workflow defined for ALOS PALSAR data, in order to observe the backscattering behaviour of noticed targets in the output of the polarimetric descriptors performed and to compare it with the one noticed in ALOS PALSAR data.

As mentioned before, after analysing several polarimetric descriptors, the one that showed a significant amount of information for archaeological structures detection is the Yamaguchi 4-component decomposition, and, in particular, the Yamaguchi G4U1 decomposition (Figure 7.21).

At a first level analysis, the overall observation of the Yamaguchi decomposition RGB images lead to the similar conclusion derived for ALOS PALSAR data (Figure 7.21). In fact, both the palm cultivations in the southern part of the site and the urban area of Karima presented a strong volume scattering, due to the orientation of buildings in the central part of the city (Figure 7.21).

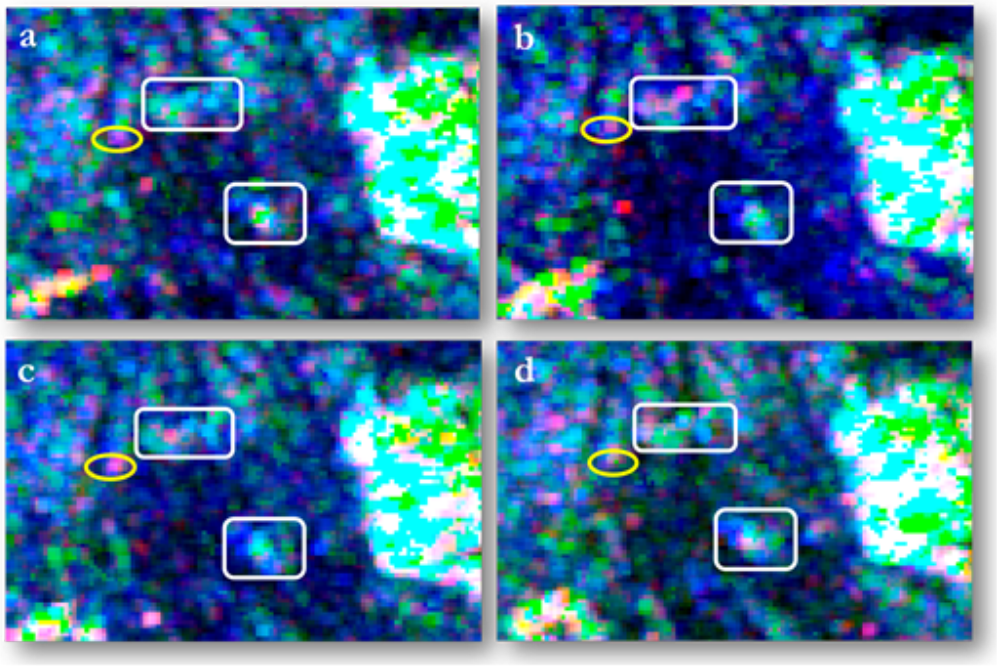

Figure 7.22 : Yamaguchi G4U1 decomposition RGB image (a : 2012/04/28, b : 2012/11/06, c : 2013/01/17, d : 2013/07/07)

Observations made for modern buildings of Karima are not valid concerning the Royal Pyramids backscattering (Figure 7.22, white squares), for which a contribution of all the scattering mechanisms is registered, with a higher percentage of single bounce mechanism. Indeed, being C-band more sensitive to surface characteristics, the sum of all the contributions can be due not only to the different walls inclination presented by the two Royal Cemeteries, but also to the reciprocal orientation of pyramids, which varies for each pyramids thus facing differently oriented walls to the incident wave. At a deeper analysis, it is possible to notice how the recorded single bounce backscattering from pyramids, is due,

indeed, to the inclination of pyramids wall, varying form 68° to 60° [40] respect to the incident 27° wave, which, as expected, results to detect more a single bounce backscatter (Figure 7.23).

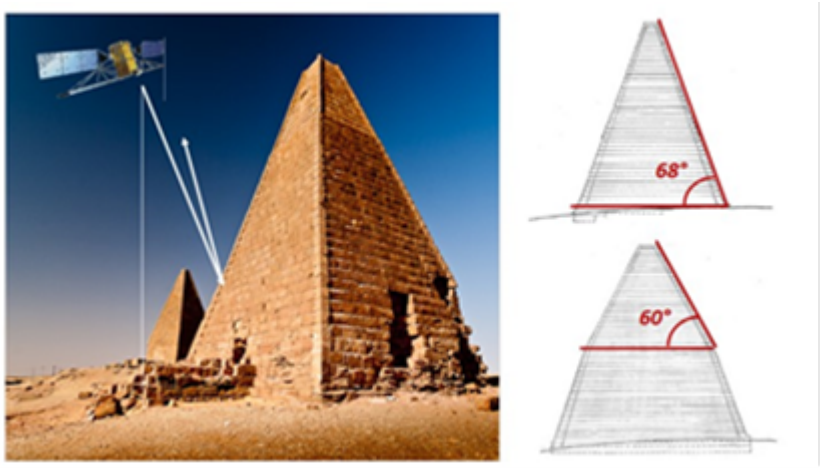

Figure 7.23 : 27° incident wave on the Pyramids

Moreover, the C-band sensitivity to surface characteristics generates also single bounce scattering mechanism with some double bounce contributions coming from the morphology of the site. Analysing the strong backscatter individuated in Pauli RGB and in Yamaguchi G4U1 decomposition RGB images, the nature of the scattering contributions are investigated in each channel of Yamaguchi G4U1 decomposition (Figure 7.24, Figure 7.25).

In particular, the single channels of the decomposition are analysed for each RADARSAT-2 acquisition to understand if the typology of the noticed backscattering, apparently recorded in Yamaguchi G4U1 RGB image as a double bounce, could also be due to other scattering contributions. The exact location of the backscattering is localised, once again, by using latitude and longitude coordinates, which matched with the reference latitude and longitude parameters of ALOS PALSAR data, thus confirming the coherence between data geocoded by means of different processes. In addition, the backscattering coming from the NW group of Pyramids (Figure 7.24 and Figure 7.25, red arrow) and the central Royal Cemetery (Figure 7.24 and Figure 7.25, yellow arrow) is analysed, as well as the scattering contribution coming from the surrounding morphology.

Once the strong backscattering is localised in all the four RADARSAT-2 acquisitions, the corresponding amplitude values of each Yamaguchi_G4U1 decomposition channel are observed.

As reported in Table 7.4, concerning the strong backscattering close to the NW group of Pyramids (Figure 7.24 and Figure 7.25, red arrow), a high value of single bounce scattering has been registered, with a low contribution of double bounce and a lower contribution of volume scattering.

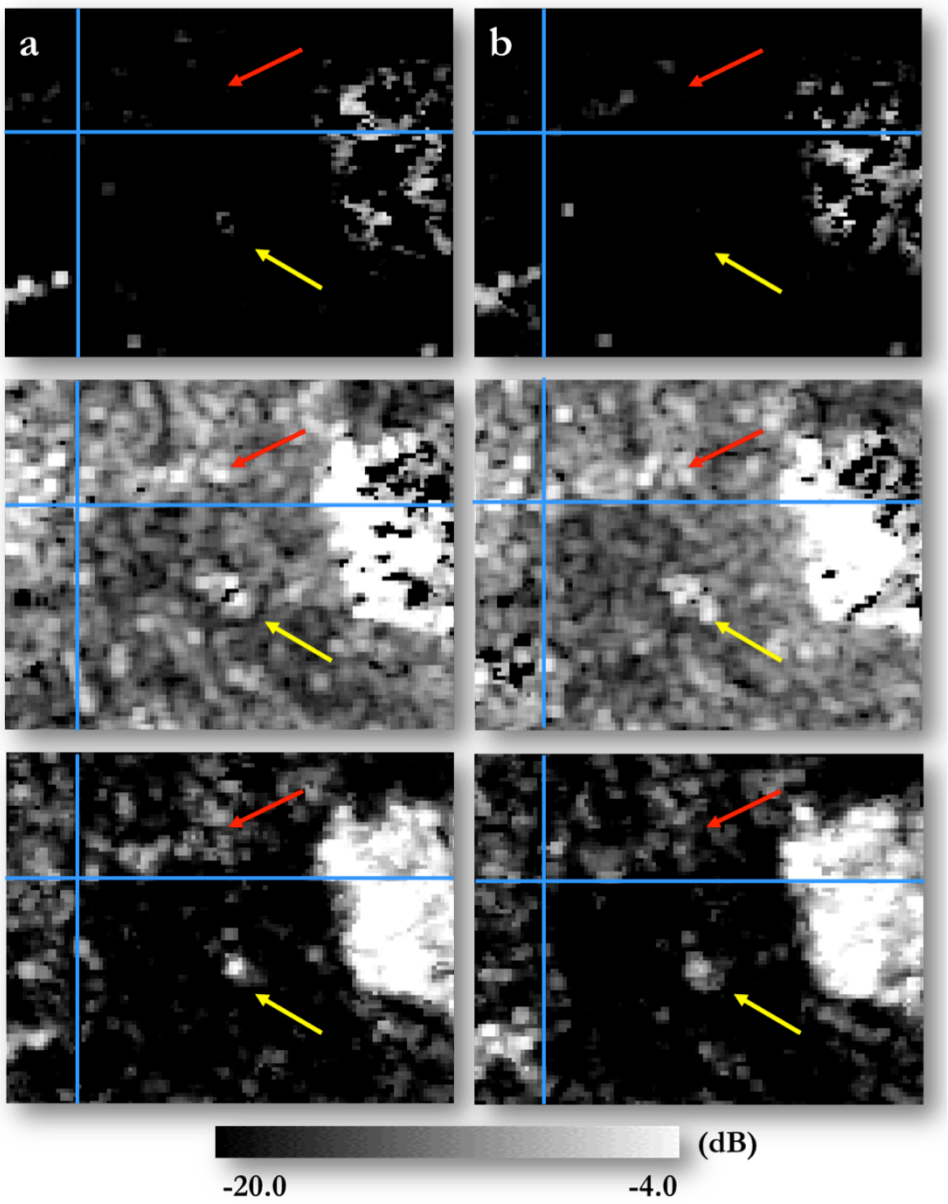

Figure 7.24 : Yamaguchi G4U1 decomposition: Double bounce (Top), Single bounce (Middle) and Volume scattering (Bottom) for each acquisition date: April 2012 (a), November 2012 (b)

By comparing these values to the ones recorded in ALOS PALSAR data, a strong response in single bounce mechanism is identified in both SAR data, as well as a low contribution of double bounce, which however, seemed not to be recorded for the morphology of the site in each RADARSAT-2 acquisitions.

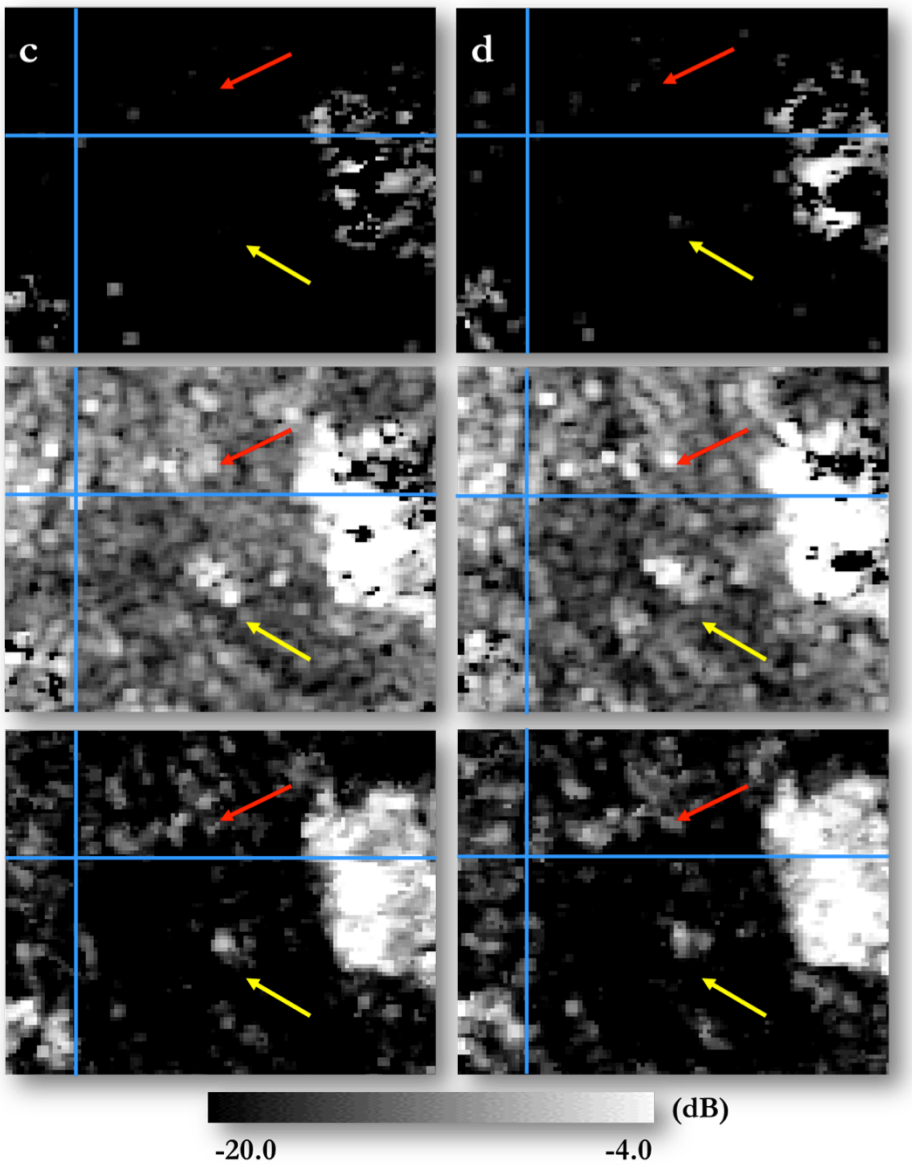

Figure 7.25 : Yamaguchi G4U1 decomposition: Double bounce (Top), Single bounce (Middle) and Volume scattering (Bottom) for each acquisition date: January 2013 (c), July 2013 (d)

Acquisition date	□	Yamaguchi G4U1_Dbl	Yamaguchi G4U1_Odd	Yamaguchi G4U1_Vol
2012/04/28	27.6°	-16.99 dB	-4.97 dB	-20 dB
2012/11/06	27.6°	-16.99 dB	-8.24 dB	-20 dB
2013/01/17	27.6°	-15.23 dB	-5.68 dB	-20 dB
2013/07/04	27.6°	-16.99 dB	-8.54 dB	-16.99 dB

Table 7.4 : Yamaguchi G4U1 decomposition single channels amplitude values

In fact, being C-band more sensitive to the surface topography, several surface scatterers have been detected also in the surrounding portion of the site in which L-band seemed not to record any backscatter. By comparing the recorded backscattering close to NW group of pyramids to the one of surface archaeological structures, it has been noticed that the pyramids amplitude values present the same percentage of scattering contributions, with an exception for volume scattering contribution that is higher for the central group of Pyramids (yellow arrow) due to their orientation.

7.4 Multi temporal ALOS PALSAR and RADARSAT-2 crossed analysis

Considering the acquisition time of multi-frequency dataset composed by ALOS PALSAR and RADARSAT-2 data, considering the different band the sensors present and the relative different frequencies, some considerations are proposed. The evidence of a target whose persistence in time can be appreciated over seven years (2006-2013) in the same area represents the first of them (Table 7.5).

ALOS PALSAR	RADARSAT-2
2006/08/14	2012/04/28
	2012/11/06
2009/11/05	2013/01/17
	2013/07/04

Table 7.5: Images acquisition dates

As stated before, in the cartographic documentation derived from UNESCO reports on the area, no surface archaeological evidence is registered in the point corresponding to the strong backscattering noticed in ALOS PALSAR data (Figure 7.26). It has to be reminded that the morphology of the site is composed by sand and sand-stone rocks, which have shown a backscattering similar to the one noticed close to NW group of Royal pyramids. This is particularly evident in RADARSAT-2 data, for which, from a qualitative analysis point of view, the strong backscattering is more highlighted in the acquisitions of April 2012 and January 2013 (Figure 7.27 and Figure 7.28, yellow ellipse).

Nevertheless, supposing this backscattering was due to the sandstone topography of the site, we could expect to have the same responses for all the morphological evidences in the area (Figure 7.26, Figure 7.27 and Figure 7.28, red arrow). This could be true when observing RADARSAT-2 imagery, whose higher spatial resolution allows to discriminate several strong backscattering due to the morphology of the site, as well as the scattering mechanism close to the pyramids (Figure 7.27 and Figure 7.28, red and white arrows). However, this is not confirmed in ALOS PALSAR data, in which we can still easily distinguish it but not the ones related to the morphological surface evidences (Figure 7.26, red arrow).

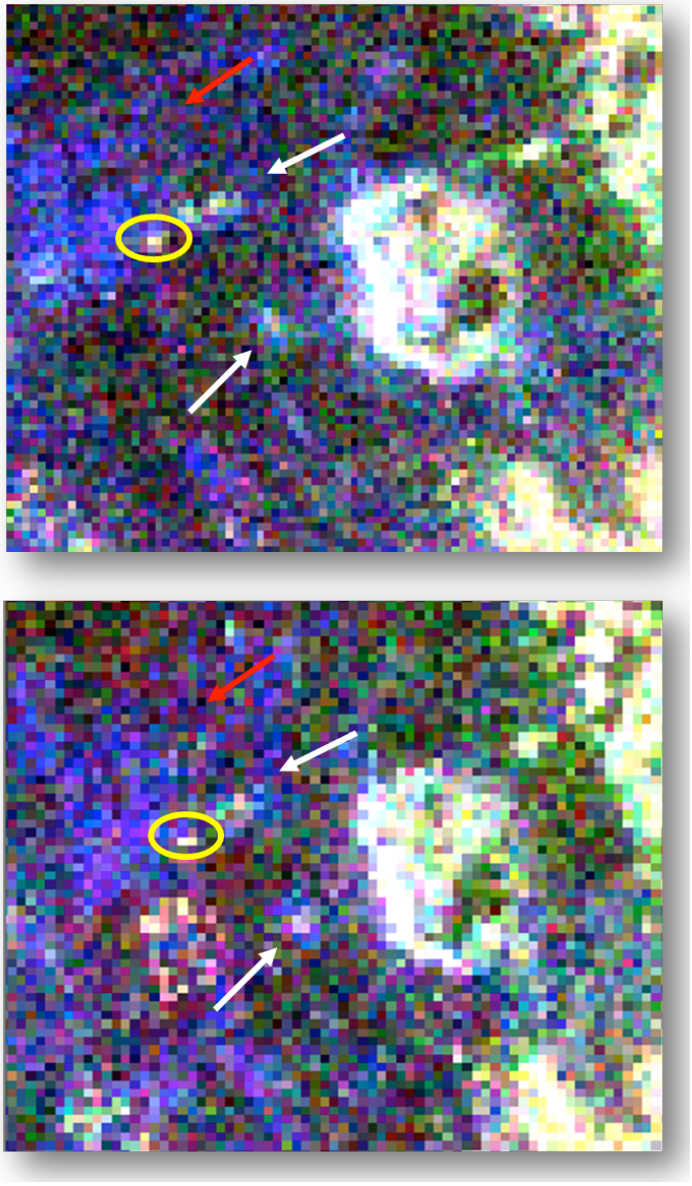

Figure 7.26 : ALOS PALSAR Pauli RGB images (2006, left ; 2009, right)

Moreover, it is important to consider, from a technical point of view, the typology of polarimetric acquisitions selected for this research, which is characterised by a different frequency and by a similar incidence angle configurations. In fact, being respectively a 26.20° / 23.10° (ALOS PALSAR) and 27.06° (RADARSAT-2) incidence angle, we can assume that ALOS PALSAR L-Band wave deeply penetrated sand detecting a target in the ground, as reported in both acquisitions (Figure 7.26, yellow ellipse) while RADARSAT-2 C-band lightly penetrated sand, demonstrating a higher sensitivity to the general morphology of the site.

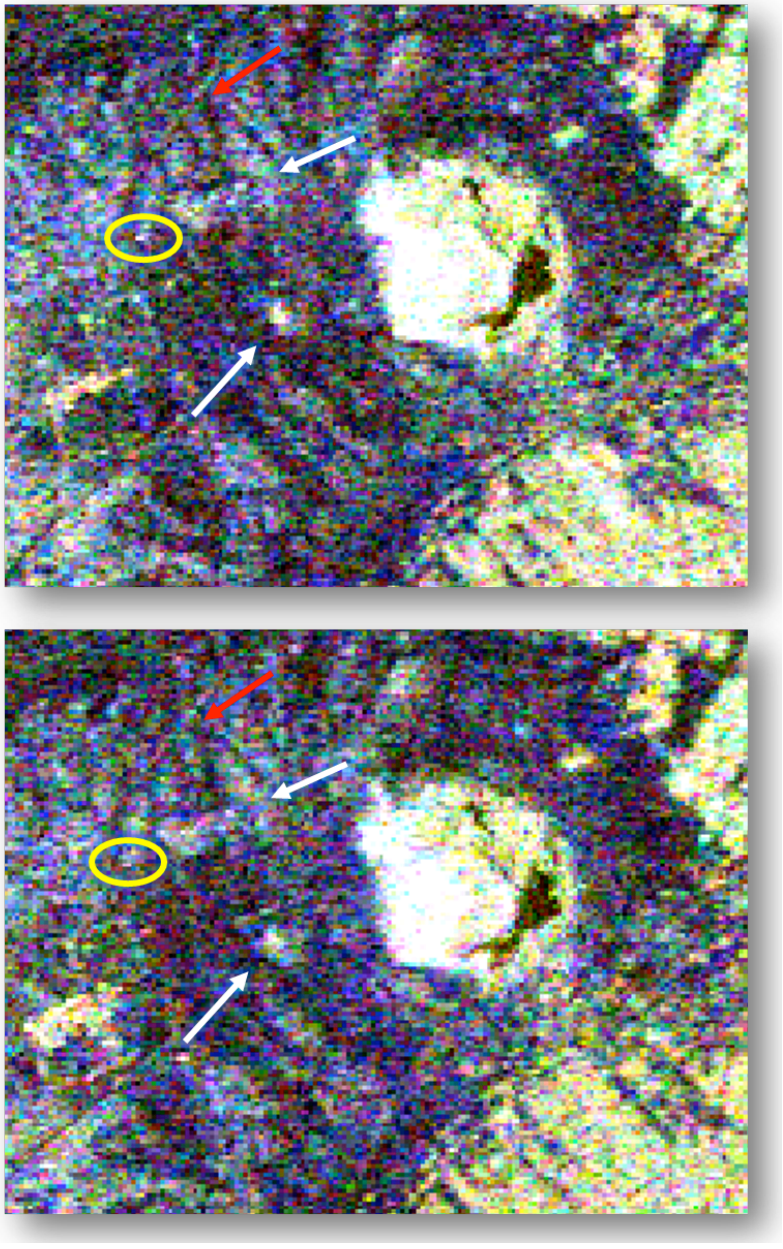

Figure 7.27 : RADARSAT-2 Pauli RGB images (2012/04/28, top ; 2012/11/06, bottom)

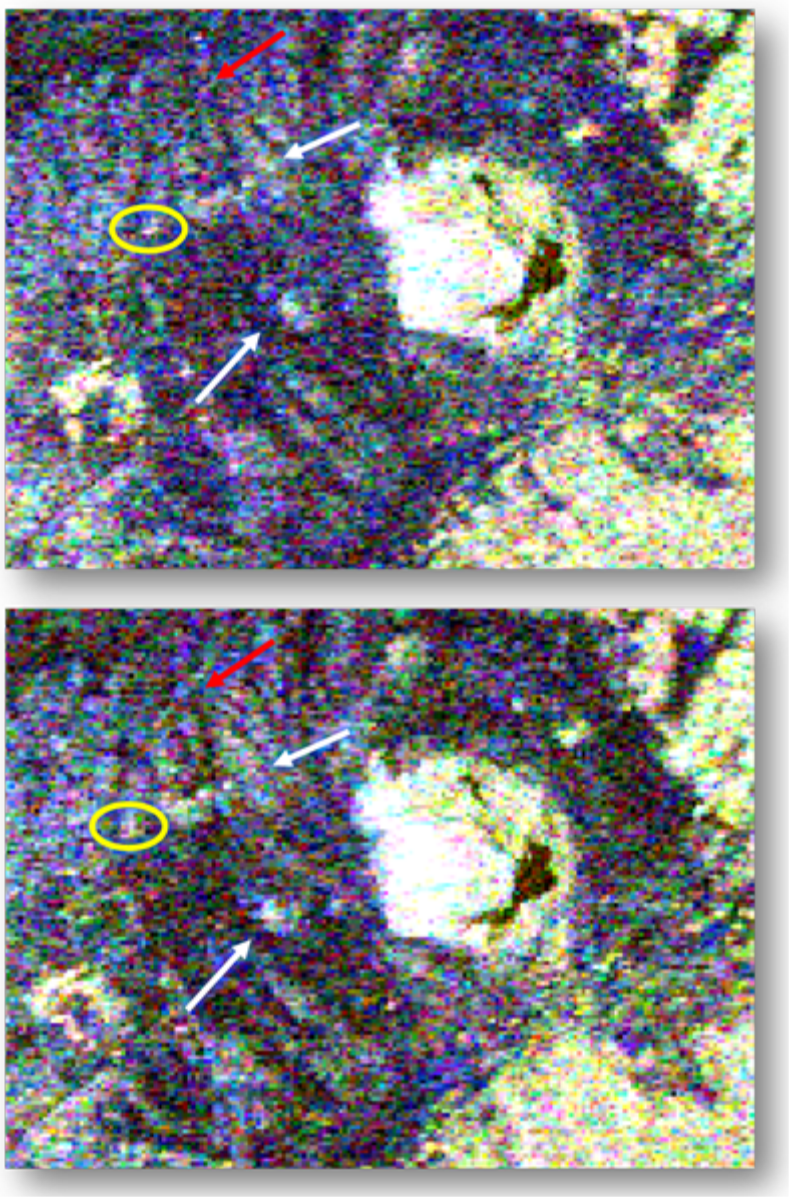

Figure 7.28 : RADARSAT-2 Pauli RGB images (2013/01/17, top ; 2013/0707, bottom)

Indeed, considering the absence of meteorological events that could affect wave interaction with targets in each acquisition date, it is important to point out that using higher frequency RADARSAT-2 C-band, it is also possible to discriminate this point target, despite of its lower penetration capability and thanks to the narrow observation incidence angle (Figure 7.27 and Figure 7.28, yellow ellipse).

In order to confirm this hypothesis, one of the future development of the present research could be to study the geological sediments of the ground in Gebel Barkal, so that it could be possible to provide an estimation of L-band and C-

band effective penetration capability and depth in this kind of environment. This proposal can be developed in the frame of the Gebel Barkal project realised in collaboration with the University of Turin and the University of Venice (see §9).

7.5 A validation method

As any scientific experimental approach requires, the traditional and still most reliable validation method for archaeology is represented by ground truth surveys. Unfortunately, this is not always feasible due to local political constraints or to specific permissions that should be conceded only by local institutions, and many of the World Heritage sites still needed to be monitored and protected all over the world. The case of Gebel Barkal archaeological area is an exceptional one. Since antiquity it has been considered as a sacred place to be preserved, where many international and local institutions, as well as Universities, had the opportunity to work onsite for excavations and topographic surveys (see §5.1.2).

In order to complete the present research and to validate the results obtained, thanks to the above mentioned collaborations (University of Turin, University of Venice, see §7.1), a ground truth campaign was carried out in the frame of the last expedition of November-December 2013 by Prof. E. Ciampini. A layout showing the area of the anomaly was provided to archaeologists, as the designated zone is not pertinent to the Italian archaeological excavations concession (Figure 7.29).

Figure 7.29 : Layout performed in the GIS project with the representation of excavations areas and the anomaly

Last excavations in the area were directed by the Spanish Fundacio Clos of Barcelona (see §5.1.2), and they were not assigned to other Institutions during the last years.

The layout used by archaeologists illustrates the area of the anomaly in a red square close to the NW group of pyramids, indicated by a red arrow. In the red square close to the Gebel is indicated the area of Italian excavations, while in the blue square the concession given to other international Institutions. Based on the layout, Prof. E. Ciampini performed a surface recognition by taking some photographs and analysing the presence of archaeological finds in the surface stratum. Unfortunately, due to the special permissions ruling the digging concessions and to the local authority regulation, only a general survey of the area was carried out. In fact, it has not been possible to perform a closer surface investigation, although some photographs of the area give an overall idea of the kind of morphology and topography of the site (Figure 7.30).

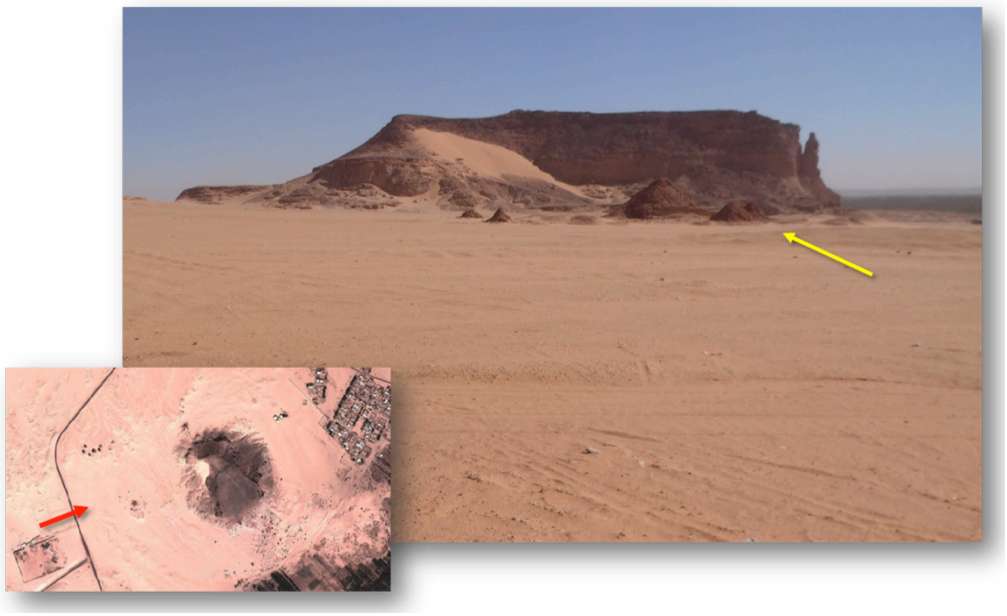

Figure 7.30 : Gebel Barkal site, central Royal Cemetery and Jebel Mountain. Courtesy of E. Ciampini (Dec, 2013)

In Figure 7.30, showing a picture taken from the western part of the area (red arrow), it is possible to notice the general topography of the site, which extends flat to the central group of Pyramids (yellow arrow), just before the Jebel Mountain.

Although the general morphology of the site is characterised mostly by the Jebel itself, in the NW part of the archaeological area, some light topographic features can be recognised (Figure 7.31).

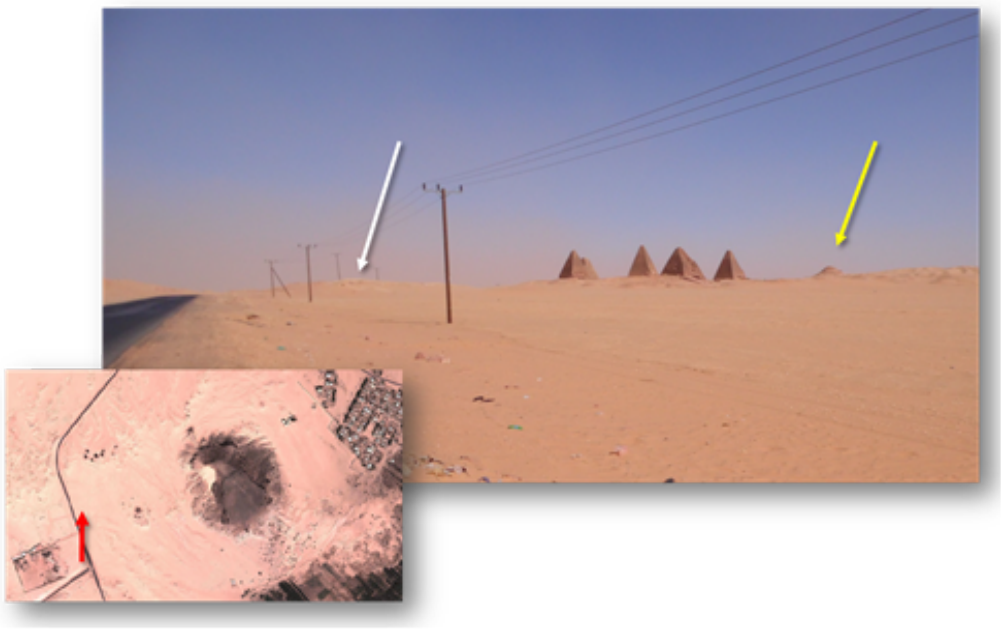

Figure 7.31 : Gebel Barkal investigated area. Courtesy of E. Ciampini (Dec, 2013)

The picture taken from the Southern part of the investigated area (red arrow) shows a wide view of the Royal Cemetery and of the area in which the anomaly detected by SAR polarimetric data has been noticed (white arrow). Unfortunately, not disposing of a closer view and more detailed pictures, it is complicated to define if some surface archaeological findings can be related to the presence of an archaeological feature in the ground. Moreover, looking at the photograph, it is immediately evident how the morphology could have caused a backscattering in that point. Nevertheless, what is important to remind is that the very soft building material of Gebel Barkal pyramids (see §5.2.1) is heavily exposed to the severity of the local environment, thus originating mounds of stones and sand that result in topographic reliefs (Figure 7.31, yellow arrow).

In order to deepen the photographic analysis here presented, a second and more specific ground truth campaign will be performed in the frame of the excavation mission at Gebel Barkal scheduled for November 2014. Even if it will be not possible to perform a real excavation in the same occasion, it will be proposed in the frame of future missions at Gebel Barkal site.

7.6 Conclusion

The methodology presented in this chapter is the result of a wider study carried out in the frame of this research. It could not be considered as definitive or complete. Nonetheless, it points out how SAR polarimetric data can be managed for archaeological purposes. It has to be considered the complexity of SAR data with respect to optical imagery in this field. The most important difficulties linked to SAR data interpretation and analysis for non-experts, are linked to the visualization of some scatterers responses in SAR data that could be misunderstood with some others. This is the reason why for the present research, an *a priori* knowledge of SAR imagery has been developed. In fact, while the visual aspect is better enhanced in optical data with respect to SAR ones, the physical aspect constitutes the added value polarimetric SAR data provided due to the penetration of the electromagnetic wave in the ground.

Of the two approaches carried out in this PhD research, the multi-frequency polarimetric study has been presented in this chapter.

The study has been focused on the detection of surface and subsurface archaeological structures, comparing ALOS PALSAR L-band, with a central frequency of 1.27 GHz, with RADARSAT-2 C-band sensor, whose central frequency is 5.405 GHz. It has been demonstrated how a persistent backscattering (2006-2013) not related to surface archaeological features can be traceable in different polarimetric data presenting the same incidence angle configuration but different frequency (ALOS PALSAR – 26° and RADARSAT-2 – 27°). The nature of the backscattering has been investigated by means of several polarimetric decompositions, among which Yamaguchi G4U1 decomposition turned out to be the most significant polarimetric descriptor analysed. The single channels of the decomposition, for all the available images, reported a combination of single and double bounce scattering mechanisms for the strong backscattering noticed, combination that has not been recorded for the surrounding morphology of the area. As no surface evidence has been recorded in optical and cartographic data, a penetration of ALOS PALSAR L-band in the dry environment of Gebel Barkal has been thus supposed, thanks to the absence of meteorological precipitation that could have affected the interaction of the wave with the soil. In addition, a

lighter C-band penetration in the ground has been supposed as well, despite of its lower penetration capability but thanks to the steeper incidence angle of the analysed images.

The SAR polarimetric analysis over Gebel Barkal continues, at the present stage of the research, with a multi-incidence angle approach, described in Chapter 8.

This page intentionally left blank

Chapter 8

Polarimetric SAR multi-incidence angle analysis

In the following chapter, a discussion about the multi-incidence angle analysis performed over the area of Gebel Barkal is presented. This kind of analysis wants to integrate the already shown multi-frequency approach selected for this research, where integration means applicability of a different analysis for the investigation of the previously obtained results and evaluation of the potential of diverse incidence angle configurations for the detection of surface and subsurface archaeological features. Therefore, the multi-incidence angle analysis here presented is conceived as a support-analysis as well as an autonomous study for the already mentioned archaeological purposes.

After the description of the processing chain applied and of the obtained results, the conclusive part of the chapter focuses on the usefulness of the two incidence angle configurations selected and introduces to the data integration performed in the GIS Gebel Barkal archaeological project, illustrated in Chapter 9.

8.1 RADARSAT-2 multi-incidence angle configuration

Although the initial approach followed in this research was a multi-frequency analysis performed over the same area by means of two different polarimetric sensors (different frequency but similar incidence angle configuration), the study of a multi-incidence angle analysis is secondly carried out. The objective of such

analysis is the comparison of the results obtained in the approach previously investigated and the ones obtained with a multi-incidence angle analysis. In particular, the study has been focused on the examination of the already noticed backscattering and on the investigation of new ones, as well as on the scattering behaviour of surface archaeological evidences.

As aforementioned, the 45.41° configuration mode is more sensitive to double bounce scattering mechanism, while the 26.7° is more sensitive to single bounce (see §7.1). This *a priori* knowledge addressed the research to deepen the analysis to understand the different kind of information we can derive from a multi-incidence angle investigation for the detection of surface and subsurface archaeological features, according to the different typology of each feature.

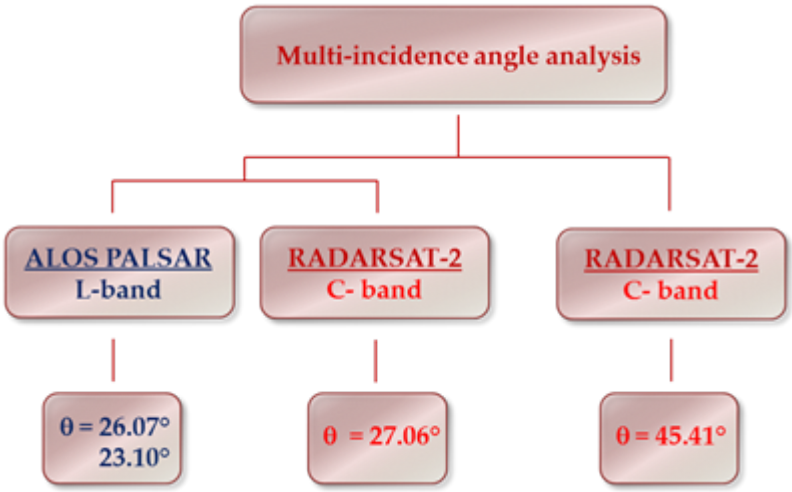

Figure 8.1 : RADARSAT-2 Multi-incidence angle analysis

For this kind of analysis, the 27.06° RADARSAT-2 acquisitions, observed from a multi-frequency point of view with ALOS PALSAR data, are compared with four RADARSAT-2 imagery acquired with a 45.41° incidence angle configuration (Figure 8.1).

The processing chain performed over the 45.41° RADARSAT-2 acquisitions is the same applied in the case of the multi-frequency analysis above described: after the extraction of the T3 matrix, data are directly geocoded in order to preserve the higher spatial resolution as possible. Once the T3 matrix is geocoded, all the polarimetric decompositions are derived (Figure 8.2), as done for the 26° configuration (see §7.3.3).

RADARSAT-2 45° images have been scheduled and provided in the same acquisition cycle of the 27.06° acquisitions, thus following the same seasonal selection criterion for the acquisition dates: 1st May 2012, 11 November 2012, 20 January 2013, and 7 July 2013.

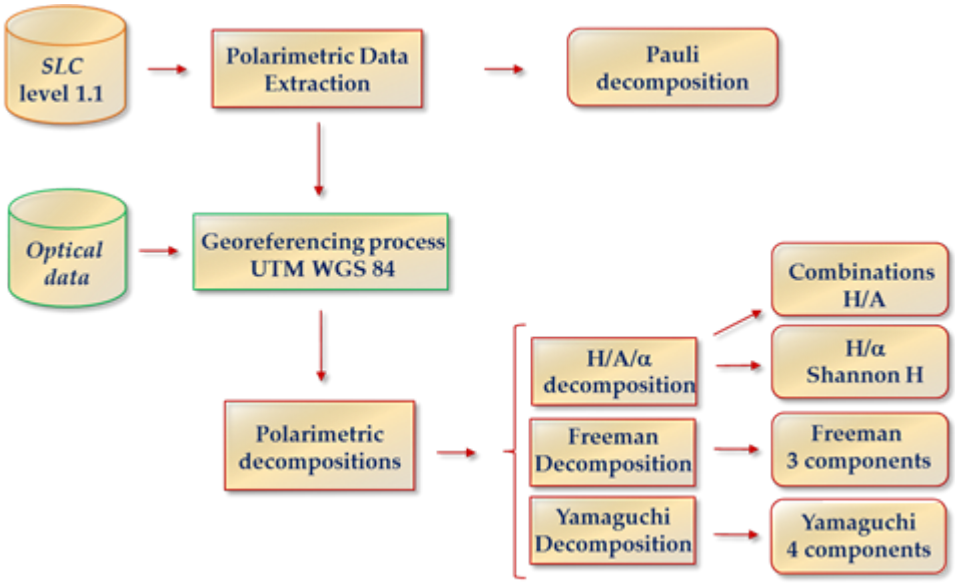

Figure 8.2 : RADARSAT-2 45° processing chain

8.1.1 RADARSAT-2 45.41° polarimetric descriptors and results

Starting from a qualitative analysis, the Pauli decomposition is the first polarimetric descriptor investigated, providing a first level indication about the overall scattering mechanisms occurred (Figure 8.3).

Figure 8.3 : First step of SAR processing chain: Pauli decomposition

Pauli RGB images of each acquisition are thus overlaid to the KOMPSAT-2 image as well as to the more recent Google Earth acquisition, in order to analyse the changes occurred in time and the backscattering that could be related to archaeological structures (Figure 8.4).

As initial analysis, via comparison of data, the 45° configuration mode presents, from a visual point of view, a more detailed definition of scattering mechanisms compared to the 27.06° configuration (see §7.3.4, Figure 7.19).

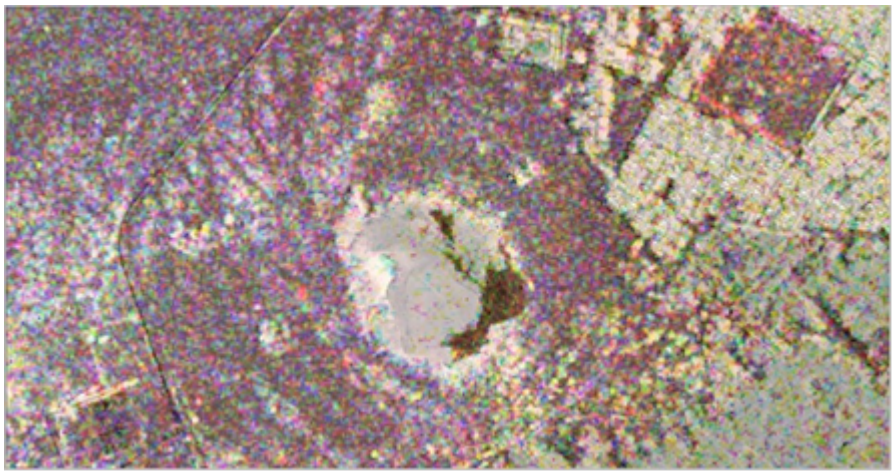

Figure 8.4 : RADARSAT-2 45° Pauli RGB image (2012/05/01) overlaid to Google Earth acquisition (2012/11/07).

It is possible to notice, as shown in the example reported in Figure 8.4, how some strong double bounce backscattering are particularly highlighted in some portions of the image: the NE perimeter of the Islamic Cemetery, the "spot" double bounce in the western part of the archaeological site, and the well-defined backscattering coming from the modern city of Karima (NE), from the modern infrastructures to the very western part of the image, and from the palm cultivation belt (SE).

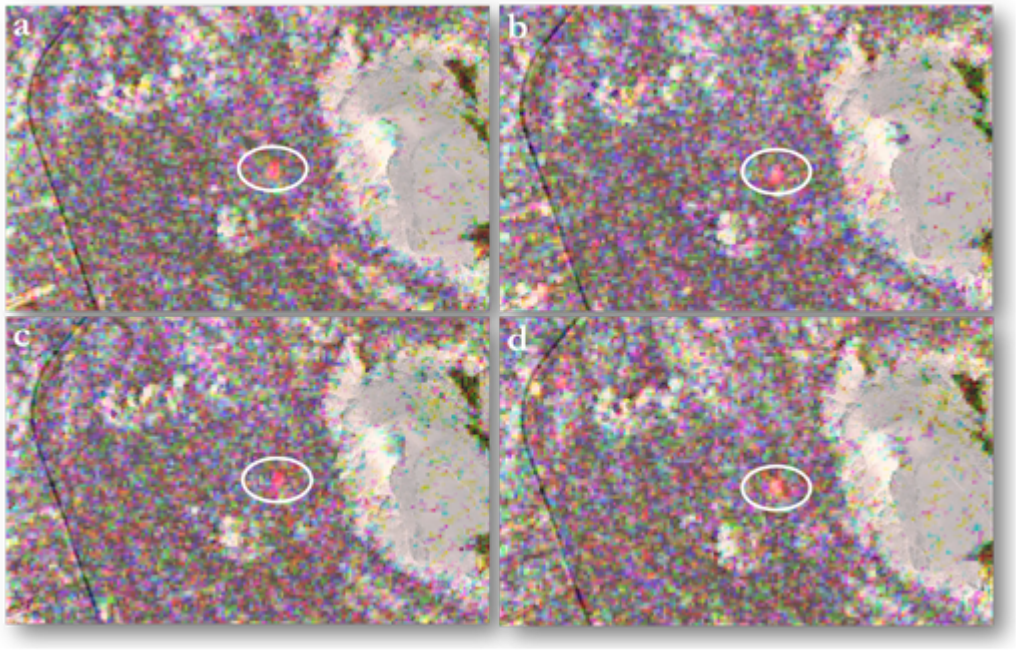

Figure 8.5 : 45° RADARSAT-2 Pauli RGB images (a : May, 2012 b : November, 2012 c : January, 2013 d : July, 2013) overlaid to Google acquisition (November 2013)

Focusing on the archaeological area analysed in the present research and represented in each RADARSAT-2 acquisition, it is noticed how the strong backscattering identified close to the NW group of pyramids in the multi-frequency analysis did not present a so evident contribution in 45° incidence angles acquisitions. On the contrary, a strong double bounce contribution is detected between the central group of Royal Pyramids and the Jebel Barkal Mountain (Figure 8.5). The analysis is thus addressed to the observation of further polarimetric descriptors, selected because of their significant contribution to the detection of anomalies.

In the case of the multi-incidence angle study, a meaningful descriptor is Shannon Entropy (see §3.10.3), which provides information about the degree of randomness of backscattering present in the area (Figure 8.6).

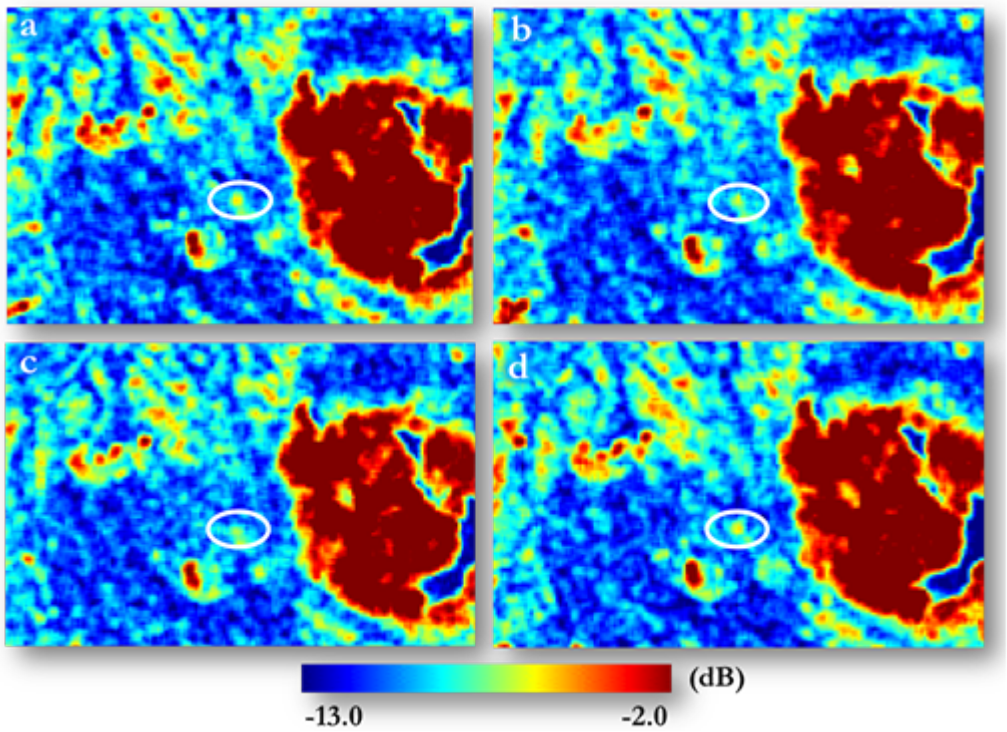

Figure 8.6 : Entropy Shannon polarimetric descriptor. a : 2012/05/01 ; b : 2012/11/11 ; c : 2013/01/20 ; d : 2013/07/07

Acquisition date	**2012/05/01**	**2012/11/11**	**2013/01/20**	**2013/07/07**
Shannon Entropy	-6.47 dB	-7.22 dB	-8.11 dB	-6.21 dB

Table 8.1 : Shannon Entropy amplitude values

According, in fact, to the values recorded in each RADARSAT-2 acquisition, it is possible to understand if the noticed and persistent double bounce scattering (Figure 8.6, white circles) was due to the sum of several backscattering contributions or it has to be ascribed to a specific one. The amplitude values (Table 8.1), recorded for the noticed anomaly in each acquisition date in Shannon Entropy descriptor, can be defined representative of a medium degree of entropy, (colour coded image in Figure 8.6), which is characteristic of the contemporary presence of more than only one scattering contribution.

In order to discriminate the nature of the identified backscattering, the attention focused on other polarimetric decompositions, and in particular, on the already mentioned Yamaguchi 4-Component Decomposition (Figure 8.7), which, also for the multi-incidence angle analysis, is considered one of the most relevant descriptors from an archaeological and topographic point of view.

The qualitative analysis carried out on the Yamaguchi 4-component decomposition highlights a different visualisation of the overall scattering mechanism representation compared to the one examined in the 26° configuration. The 45° configuration mode appears to enhance all the double bounce contribution, the major part of which are related to buildings and structures not so well recognisable in the 26° incidence angle acquisitions (see §7.3.4, Figure 7.21).

Analysing the different backscattering coming from the different targets, the urban area and the palm cultivations in the southern portion of the images present a similar backscattering contribution, i.e. a volume scattering, due to the orientation of buildings, which are assimilated, hence, to a typical vegetation response.

The northern part of the city, differently oriented, presents a double bounce contribution both in Yamaguchi Y4R and in Yamaguchi G4U1 decompositions. The observations made for the urban area are, in the 45° configuration mode, valid also for the Royal Pyramids, for which all the scattering contributions are registered, according to their reciprocal orientation and to the relation between pyramids' wall inclination (from 60° to 68°) and its interaction with the 45° incident wave (Figure 8.8).

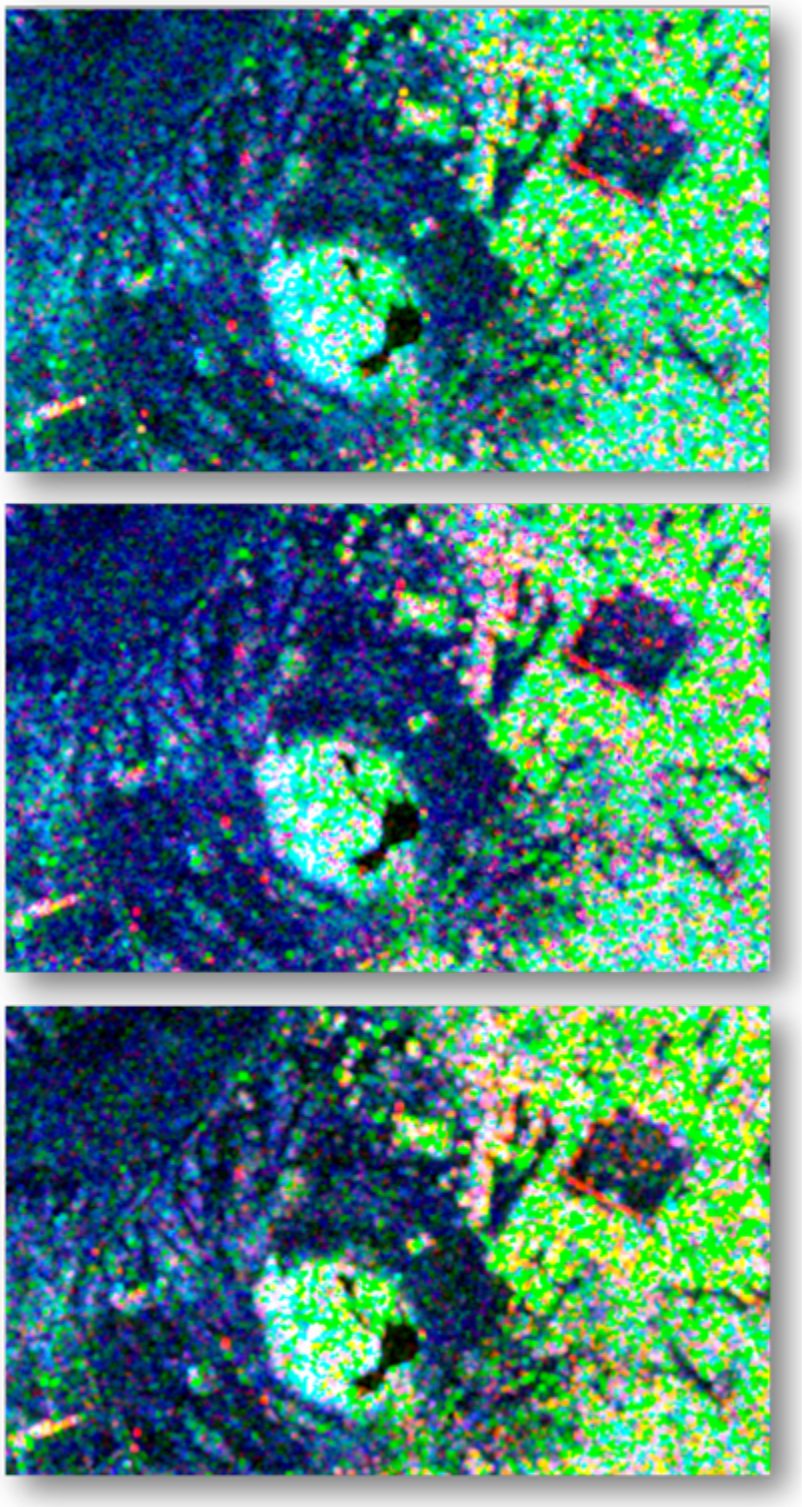

Figure 8.7 : Yamaguchi Y4O (top), Yamaguchi Y4R (middle), Yamaguchi G4U1 (bottom) decomposition images (2012/05/01)

.

Figure 8.8 : 45° incidence wave on the pyramids' wall

Contrary to the analysis performed in the multi-frequency study, for which the Yamaguchi GU41 has been selected among the three different Yamaguchi decompositions, in the 45° incidence angle images Yamaguchi Y4R decomposition turned out to be the most representative of the major backscattering noticed (Figure 8.9).

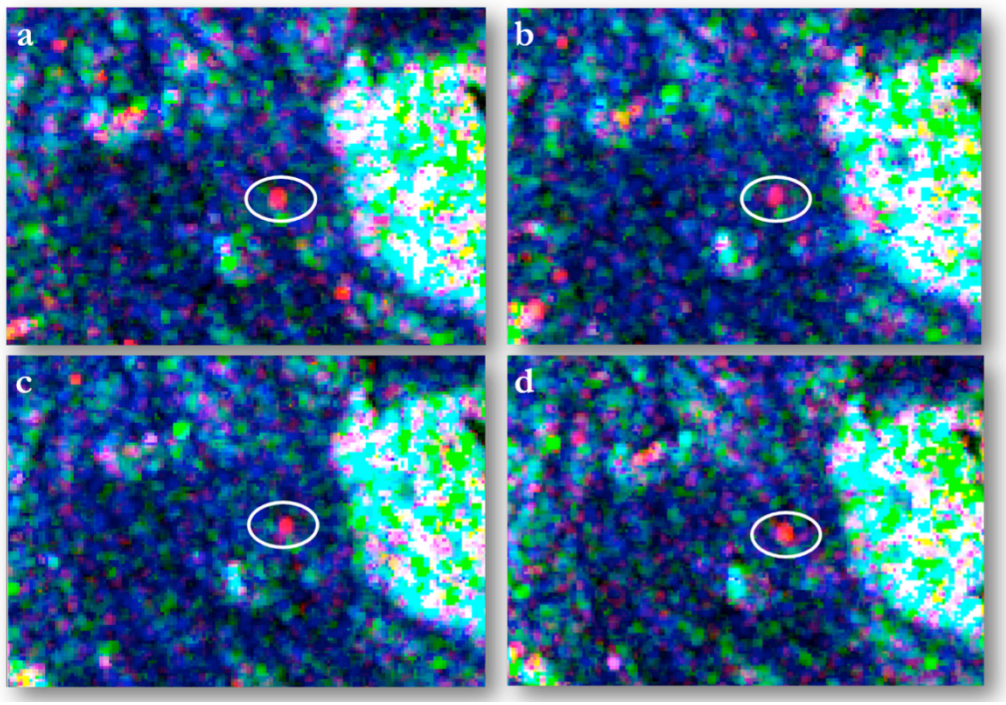

Figure 8.9 : Yamaguchi Y4R decomposition RGB image (a : 2012/05/01 ; b : 2012/11/11 ; c : 2013/01/20 ; d : 2013/07/07

The selection of Yamaguchi Y4R decomposition is related to the very well defined double bounce scattering mechanism of the urban area as well as of the archaeological structures it presents, to which the polarimetric descriptor is more sensitive, providing a better detection of the structures compared to the other Yamaguchi descriptors. From a qualitative point of view, the strong backscattering confirmed the hypothesis already proposed for the previous polarimetric descriptors: a strong double bounce scattering occurred in the area between the central group pf Royal Pyramids and the Jebel Mountain, in each RADARSAT-2 acquisition. Although several distributed double bounce backscattering can be identified in all the archaeological area, as already noticed in Pauli decomposition RGB images, the attention is focused on this well-defined response, for any structure or morphological element is supposed to have generated it, as well as on pyramids' backscattering, in order to understand the wave behaviour when illuminating this particular typology of structures.
Once the Yamaguchi decomposition is selected, the single channel related to double bounce, single bounce and volume scattering are analysed, to observe the amplitude values they present and to define, hence, the typology of scattering mechanisms occurred (Figure 8.10 and Figure 8.11).

As starting point, the backscattering of the general morphology as well as the one of pyramids (Figure 8.10 and Figure 8.11, red and yellow arrows) are observed. Concerning the NW group of pyramids, it is possible to notice how, according to their orientation, the backscattering varied between a double bounce and a single bounce contribution. On the contrary, the central Royal Cemetery presents a more enhanced single bounce and volume scattering contributions, with no contribution of double bounce. Considering the sensitivity of C-band to surface morphology, it is worth to notice how the backscattering related to the topography of the site is represented by a prevalence of single bounce response, thus providing the same contribution noticed in the 26° incidence angle images.
The localisation of the noticed backscattering is operated once more by means of the latitude and longitude coordinates (31° 49' 30" E 18° 32' 12" WGS84) in all the polarimetric descriptors (Figure 8.10 and Figure 8.11, blue cross). Once the localisation is performed, the amplitude values recorded in each Yamaguchi Y4R decomposition are analysed (Table 8.2).

According to the amplitude values recorded, a significant double bounce scattering mechanism is individuated for the presented anomaly, with low single bounce and volume scattering contributions in each 45° acquisition, with an exception for the image acquired in November 2012, which presents a light single bounce backscattering.

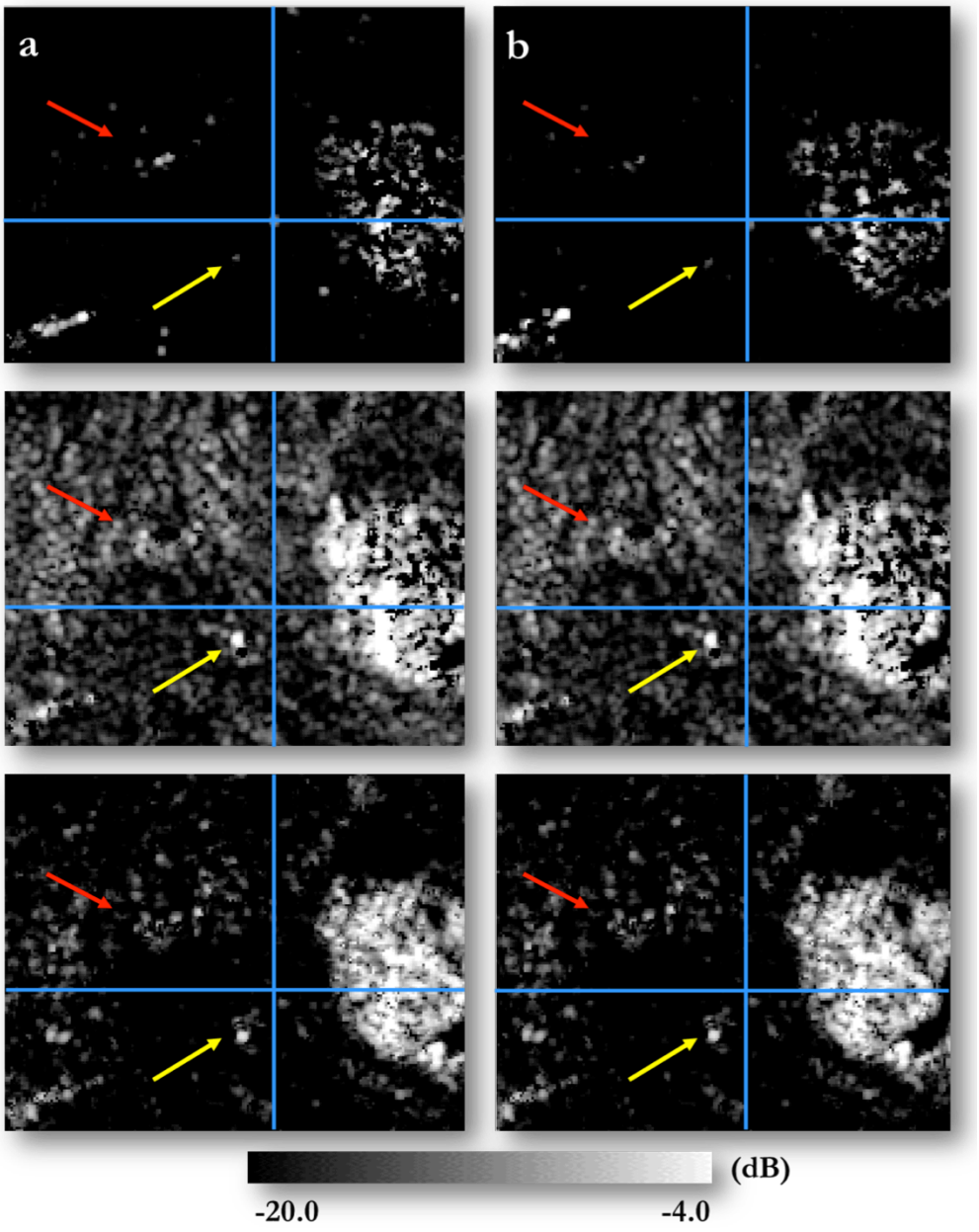

Figure 8.10 : Yamaguchi Y4R decomposition Double Bounce (top), Single Bounce (middle), Volume Scattering (bottom) for each acquisition date : a) May, 2012 ; b) November 2012

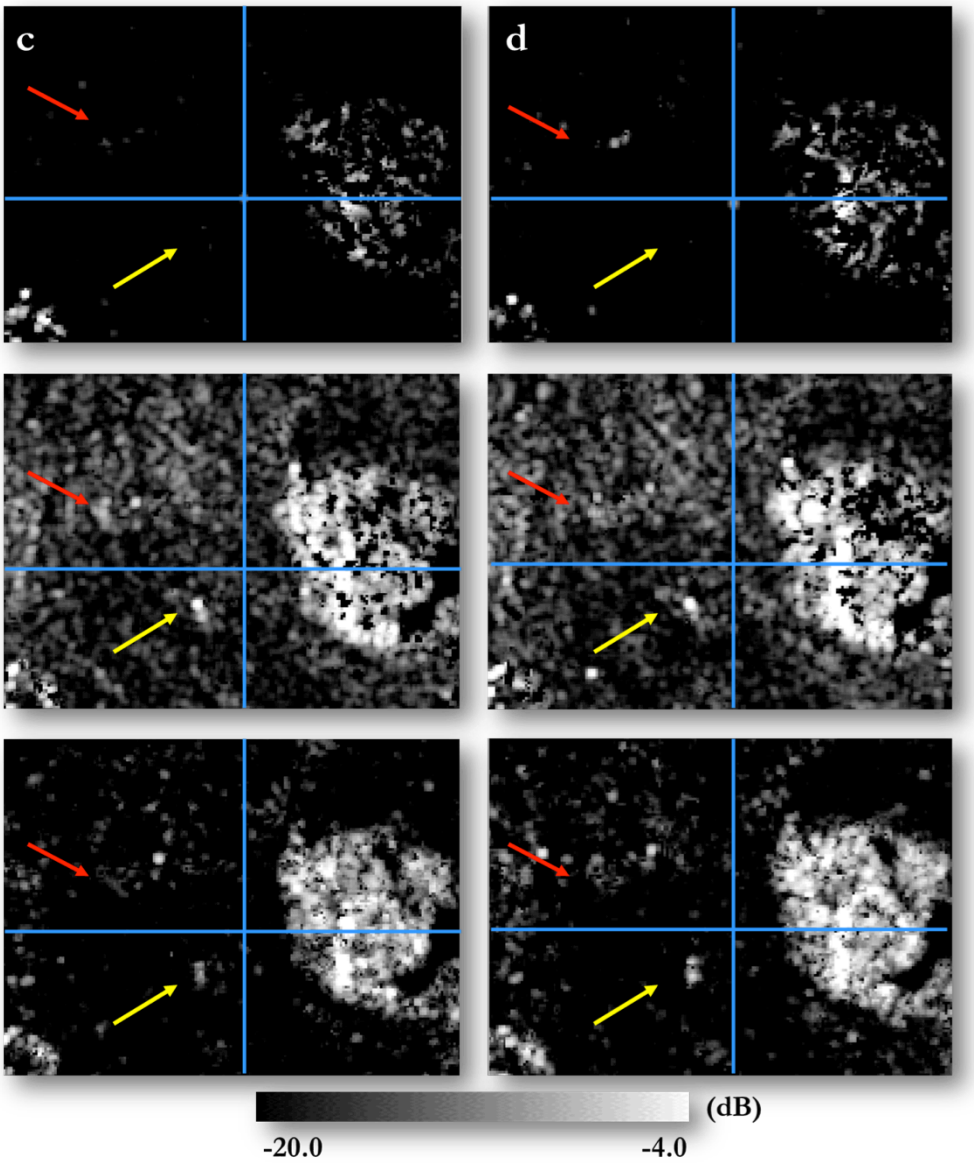

Figure 8.11 : Yamaguchi Y4R decomposition Double Bounce (top), Single Bounce (middle), Volume Scattering (bottom) for each acquisition date: c) January, 2013; d) July 2013

Acquisition date	□	Yamaguchi Y4R_Dbl	Yamaguchi Y4R_Odd	Yamaguchi Y4R_Vol
2012/05/01	45.41°	-10.45 dB	-20 dB	-20 dB
2012/11/11	45.41°	-12.22 dB	-16.99 dB	-20 dB
2013/01/20	45.41°	-12.22 dB	-20 dB	-20 dB
2013/07/07	45.41°	-10.45 dB	-20 dB	-20 dB

Table 8.2 : Yamaguchi Y4R decomposition single channels amplitude values

Therefore, the consideration arisen can be the following: the target illuminated by the 45° incident wave reflected a very clear double bounce signal, typical of standing vertical features. By overlapping the performed polarimetric descriptors to the available optical images, no correspondence to structures or evident features are noticed.

On closer inspection, by observing the optical dataset, some light morphology is observed. In order to understand if it could be related to the noticed backscattering, a deeper analysis of the area is carried out by performing an enhancing filter (Equalization Filter) on the KOMPSAT-2 image, then overlaid to polarimetric descriptors (Figure 8.12, a).

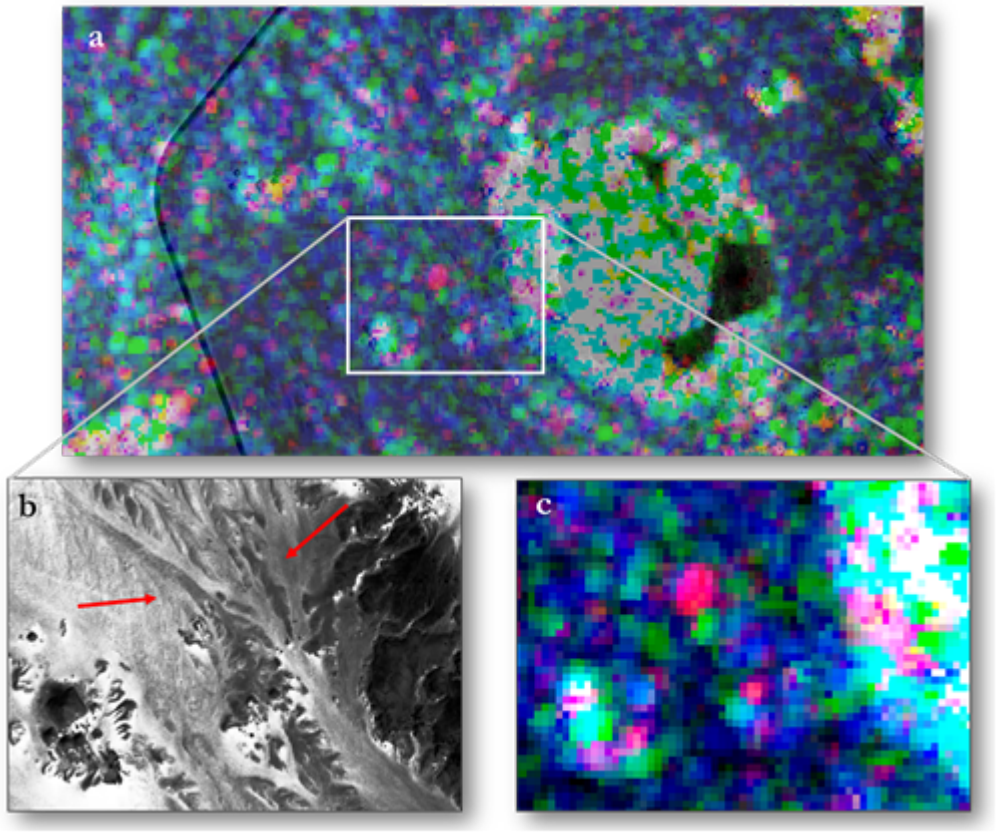

Figure 8.12 : Yamaguchi Y4R RGB image (c, 2012/11/11) overlaid to KOMPSAT-2 panchromatic band (b, 2008/05/16)

After performing an enhancement of the topography in the investigated area, the appreciation of reliefs as well as sand dunes is clearer. Alternated double bounce, single bounce and volume scattering are represented in polarimetric descriptors (Figure 8.12, c). In the correspondent portion of the KOMPSAT-2 acquisition, a

heterogeneous combination of reliefs, sand dunes, and pyramids remains characterizes the area (Figure 8.12, b).

The individuation of the target causing such a noticeable backscattering is rather problematic. Nevertheless, it is noticed how it could be referred to a surface variation of height, orientation and morphology of the reliefs located between the Jebel Barkal and the Royal Cemetery (Figure 8.12, b, red arrows), mostly taking into account the interesting presence of the anomaly in all the acquisitions analysed. In addition, considering the typology of response the Royal Cemetery presented, it is noticed how various scattering mechanisms contributions are detected, for which the interaction of the incident wave with the sand dunes and the small pyramids surrounding the principal one causes a non-univocal backscattering comparable to the ones noticed along the reliefs above illustrated.

8.2 RADARSAT-2 27 deg and 45 deg crossed analysis

The multi-incidence angle analysis here described shows the different capability of the two configurations selected for RADARSAT-2 acquisitions. The polarimetric sensor works in C-band, whose sensitivity to surface characteristics is well known, contrary to L-band penetration capabilities analysed in the multi-frequency study (see §7.1).

C-band	**□ = 27.6°**	**□ = 45.41°**
Acquisition date	2012/04/28	2012/05/01
	2012/11/06	2012/11/11
	2013/01/17	2013/01/20
	2013/07/04	2013/07/07
Topography sensitivity	✓	✓
Single bounce sensitivity	✓	x
Double bounce sensitivity	x	✓
Penetration capability	light	x
Precipitation phenomena	x	x

Table 8.3 : 27 deg and 45 deg acquisitions

The selection of the acquisition date for the 45° incidence angle images is scheduled on the basis of the 27° configuration (Table 8.3). In this way, both the configurations are relevant to the same cycle of acquisition, providing different incidence angle images acquired in the same season (time distance between 27° and 45° configuration: up to 4 days). Moreover, the observation of the meteorological conditions for each 27° incidence angle acquisition is valid also for the 45° configuration, for which any precipitation phenomenon was recorded.

The two configuration selected, 27° and 45° incidence angle, allowed the identification of different scattering mechanisms, due to the interaction of the incident wave with different targets. For the 27° configuration it has be shown how a steeper incident wave enhances the single bounce mechanism coming from the walls of the pyramids as well as from the topography of the site. Moreover, it helped in the identification of the backscattering noticed in ALOS PALSAR data, presenting the same incidence angle configuration (see §7.3.2). The 45° configuration allowed the detection of double bounce contributions occurred in the area that are not noticed in the 27° configuration. Urban elements, as the perimeter of a modern cemetery and city buildings are better identifiable in the 45° configuration, as well as different morphological features surrounding the archaeological area. However, the anomalies noticed in the 45° configuration in all the acquisition dates pose a problem of univocal correspondence to surface features, due to the lack of adequate cartography or aerial photographs that could provide contour lines and reliefs' position. Considering the sensitivity of C-band to surface topography and considering the wider incidence angle (45°) of the incident wave, this kind of response is related to the different orientation the light topography in that point.

These considerations will be then deepened in the frame of the next excavation missions at Gebel Barkal, when the topographic restitution of lacking areas will be carried out, and when a survey, also in this portion of the area, will be performed.

8.3 Conclusion

With the aim to observe the kind of scattering mechanisms and their relations with structures and morphology compared to the multi-frequency approach, a

multi-incidence angle analysis has been performed, comparing RADARSAT-2 27° configuration with RADARSAT-2 45° incidence angle acquisitions.

It has been shown how the strong contribution noticed in the polarimetric multi-frequency study, both in ALOS PALSAR lower frequency data (□ = 26°) and in RADARSAT-2 higher frequency data (□ = 27°) has not been detected in 45° higher frequency RADARSAT-2 data, while different typology of backscattering have been noticed and linked to the morphology of the site. A more spread general double bounce mechanism has been detected in the images, which configuration (45°) is considered to be more sensitive to double bounce mechanism, on the contrary of 27° configuration, more sensitive to single bounce scattering mechanism. In particular, a strong double bounce backscattering has been detected, analysing different kind of polarimetric decompositions (Yamaguchi Y4R decomposition), between the central group of Pyramids and the Jebel Mountain. Being C-band, and in particular the 45° configuration, more sensitive to surface topography than L-band is, the nature of this backscattering has been linked to a change in the morphology, noticed thanks to enhancing operations performed over optical data.

The multi-frequency (see §7) and the multi-incidence analysis of both ALOS PALSAR and RADARSAT-2 data demonstrated their usefulness in the study of the archaeological area of Gebel Barkal, then integrated with the results of ground truth campaign performed in the frame of the excavation mission of November – December 2013. Due to archaeological concession restrictions, the ground truth survey will be deepened in the future excavation missions. It gave, however, hints for reflections related to the results obtained in polarimetric SAR analysis. The combination of the high penetration capability in very dry environments (L-band, ALOS PALSAR) and the medium spatial resolution (C-band, RADARSAT-2) provided by the two polarimetric sensors have been exploited as a powerful tool for surface and subsurface features recognition.

All the results presented in this and in the previous chapter, have been integrated in a dedicated GIS project for Gebel Barkal area that will be presented in the following chapter, showing how to manage different data, coming from different sources, for the archaeological investigation.

This page intentionally left blank

Chapter 9

GIS: a potential application

This last chapter illustrates the importance of managing data coming from different sources in a unique tool for archaeological purposes. This possibility is given by the Geographic Information System (GIS), whose basic principles are illustrated in the first paragraph of this chapter.

At this point of the presented work, the research focuses on its conclusive step: the potential application of such a powerful tool, as GIS is, in the archaeological domain (Figure 9.1). After the presentation of data used and results obtained in the research, SAR polarimetric multi-frequency and multi-incidence analysis are, in this conclusive phase, integrated with optical data and correlated together in order to retrieve a synoptic observation of data and information.

With the aim to present one of the potential application of GIS in archaeology, a Royal Pyramids rendering completing the already realised Three-Dimensional reconstruction of other archaeological structures and an interactive representation of the data merged in a dedicated project on Gebel Barkal site are shown. The project is realised in collaboration with the University of Turin, Italy (see §9.2).

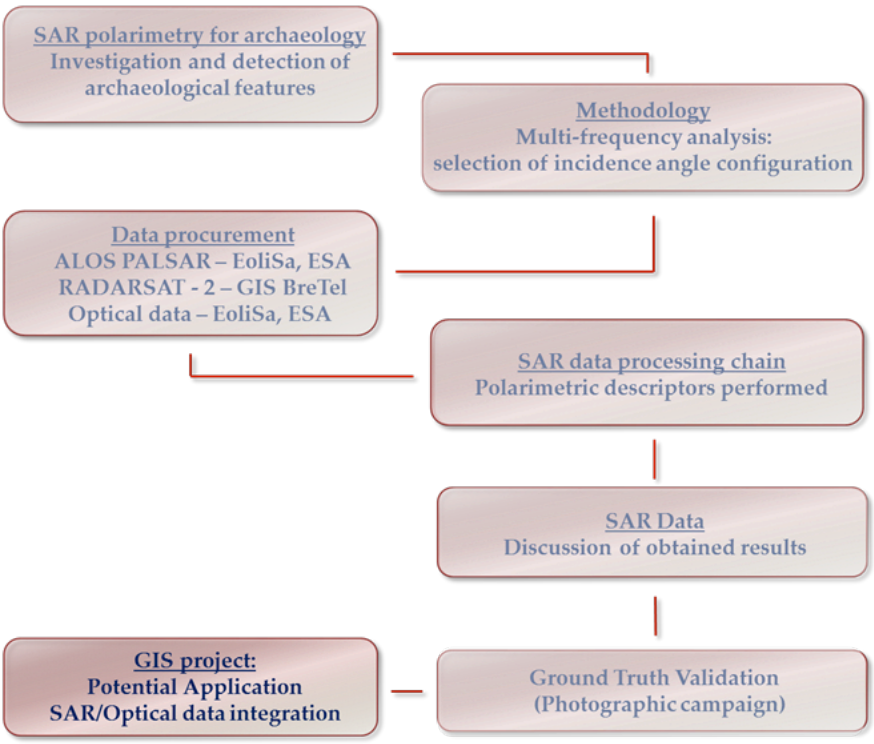

Figure 9.1 : Research workflow

9.1 The Geographic Information System (GIS): from the geographic data to the geographic information

Many definitions of GIS have been suggested over time. A GIS system could be defined as a structure constituted by a powerful set of instruments and technologies committed to acquire, store, manage, transform, analyse and visualize georeferenced spatially indexed data [55] (Figure 9.2).

Beyond this general definition, a Geographic Information System is defined, in detail, by [56]:

- a *Geographic* component : each georeferenced information, referred to as a particular portion of Earth's surface identified by a coordinate system, is equipped with a so-called geospatial information, represented from a cartographic point of view by maps, aerial, satellite images and so on, in which each pixel has a position in a chosen reference frame (for example WGS84) ;
- an *Information* collection : the integration of different data, coming from different sources, in a digital system, where data are geographically

registered on a common geographic base, allows the extraction of a higher amount of information [57] characterised by specific attributes ;

- a *System* organisation, which includes hardware, software, data and procedures.

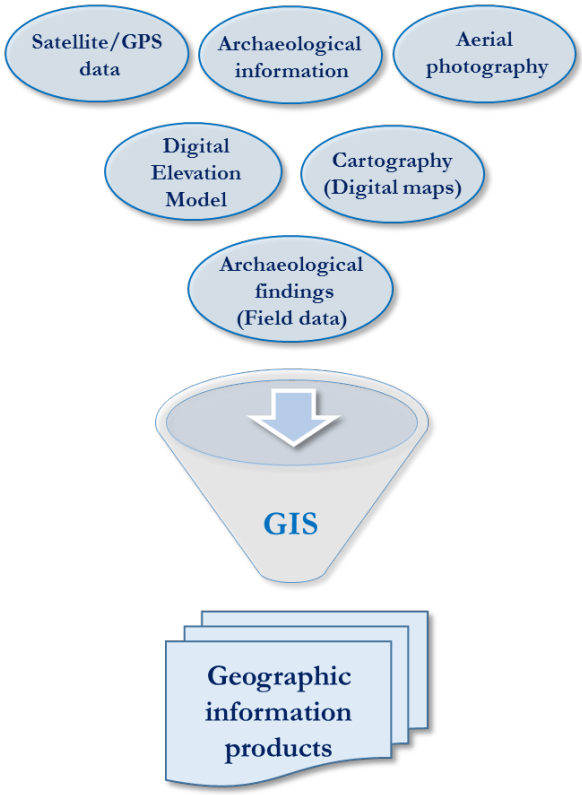

Figure 9.2 : Example of data management in a GIS

The problem solving capacity of GIS environments is at the origin of its diffusion in the '90s, when different application fields started to use it systematically. The noticeable spreading of information that comes from the use of GIS is at the basis of the interest archaeology demonstrates in this tool. If archaeologists think to the possibility to include cartography as a digital format in a GIS, they think also to the importance of disposing of tools able to transform cartography in a virtual representation of landscapes, by means of the tridimensional reconstruction of real scenarios. GIS environments, in fact, are capable of organizing all the input data collected in a GIS from "static information tools" to "interactive geographic information", correlating data and highlighting their reciprocal relationships [58].

The interactive benefit GIS provides is reachable thanks to several tools able to link spatial information with the related archived attributes through the creation

of layers. A *layer* is defined as the exemplification of objects belonging to the real world with all their geometry, position and properties that constitute a geographic database. It is possible, in fact, to identify and compare data in which is needed to know the link between *raster* (ex. SAR and optical images and digitalised cartography) and *vector* (ex. cartography vectorialisation, for the creation of thematic maps) layers. The comprehension of their reciprocal relationships can be achieved by *overlay* operations among layers. This operation allows to put in geographical communication all the raster and vector data referred to the same area but containing different thematic informations, as shown in next paragraphs.
Is therefore clear how a Geographic Information System could be widely used in many application fields, not least in the archaeological one, in which geography, findings' maps, topography, photographs, excavation documentation are managed, traditionally, independently.

9.2 A Geographic Information System for Gebel Barkal: State of Art

Why a GIS could be useful for archaeology? Only recently, archaeologists have started to recognise the great potential of Geographic Information System. The archaeological community finds the answer to this question, when facing with the possibility to manage multiple layers of information displayed in a single map, as archaeological maps coming from different sources, or with the possibility to record excavations findings in a unique database. These are only some of the several advantages a GIS system provides to the archaeological research. It is well known, in fact, that archaeologists often suffer from the lack of data collection systems and updated maps that can be useful to manage, from a geographic point of view, the information coming from the field and, possibly, to address future excavation missions.

In occasion of the 2013 EGU (European Geoscience Union) Assembly in Wien (April, 2013), Professor Luigi Perotti (University of Turin, Geositlab) showed his interest in the Gebel Barkal SAR polarimetric research presented, due to a work he previously conducted in Gebel Barkal area. It was, thus, decided in that occasion, to give prominence to a more complete project including his data and

the ones presented in this research. Since the end of July 2013, data coming from his work and from the present one have started to converge in a unique GIS project for Gebel Barkal (see §9.3).

In 2005 and 2006, Professor L. Perotti, carried out a GNSS (Global Navigation Satellite System) survey to define a local reference frame in the archaeological area of Gebel Barkal. The main purpose of his work was to update and improve the already existing maps of the excavations and to realise a high-spatial resolution reference cartography, by means of a Quickbird image (spatial resolution in the panchromatic band: 60 cm) acquired in 2003, which could be used by the archaeologists working in the area. Moreover, he also wanted to carry out a precise observation of the archaeological evidences on the area, for which aim he performed several image processing techniques operating over the four available bands of Quickbird image as histogram stretching, density slicing, filtering and image pan-sharpening [45]. The horizontal accuracy obtained for the Quickbird orthoimage made it comparable to a 1:5000 scale map. The orthoimage was effectively used to guarantee congruence between all of the ground surveys and in the meantime, to make them easier to be read and interpreted by archaeologists.

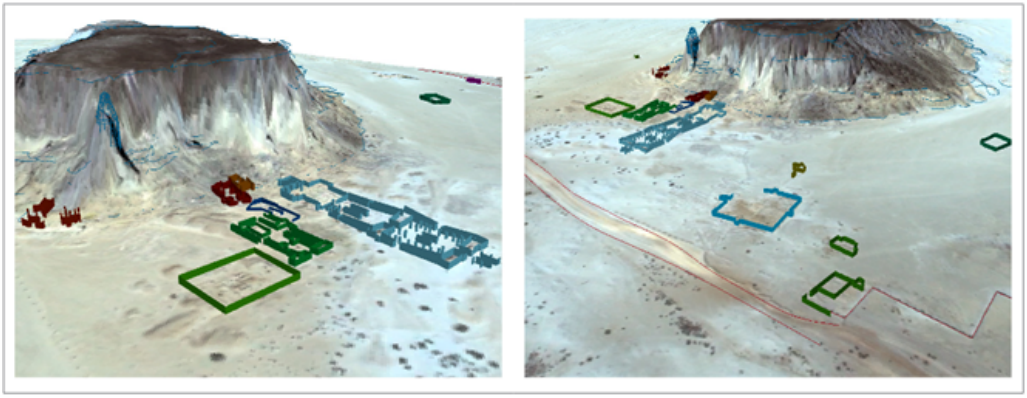

Figure 9.3 : 3D representation of archaeological temples and palaces of Gebel Barkal in GIS environment. Courtesy of L. Perotti

The orthoprojected satellite image was finally used as basis for all of the field surveys performed in Gebel Barkal area, including buildings, temples and main topographic features. Hence, a first global data integration was thus possible inside a GIS. The conclusive part of his work was the Three-Dimensional site modelling, draping the orthoimage on a DSM to generate a 3D model of the archaeological evidences excavated on site, as shown in Figure 9.3.

9.3 Contribution of the present research to the already existing GIS: creation of an optical multi-temporal dataset

As soon as the Gebel Barkal project started to grow, the archaeologists excavating in past years and in the current missions at Gebel Barkal were contacted. A meeting with Professor A. Roccati (Egyptologist first at the University of Rome, then at the University of Turin, Italy), previous supervisor of excavations, was fixed in the end of July 2013, and a meeting with the present supervisor Professor E. Ciampini (University of Venice, Italy) was fixed in September 2013. Their precious information about the actual state of conservation of the site and the planned future excavations helped in the definition of the project's purpose, which will continue in next years for the collection of all kind of data relative to the archaeological area of Gebel Barkal.

First step of data integration in the project has been the realisation of an optical multi-temporal dataset. As aforementioned, the only available archaeological map over Gebel Barkal area presents incongruences in structures proportions and topography (see §6.2), mostly evident after the georeferencing process (Figure 9.4).

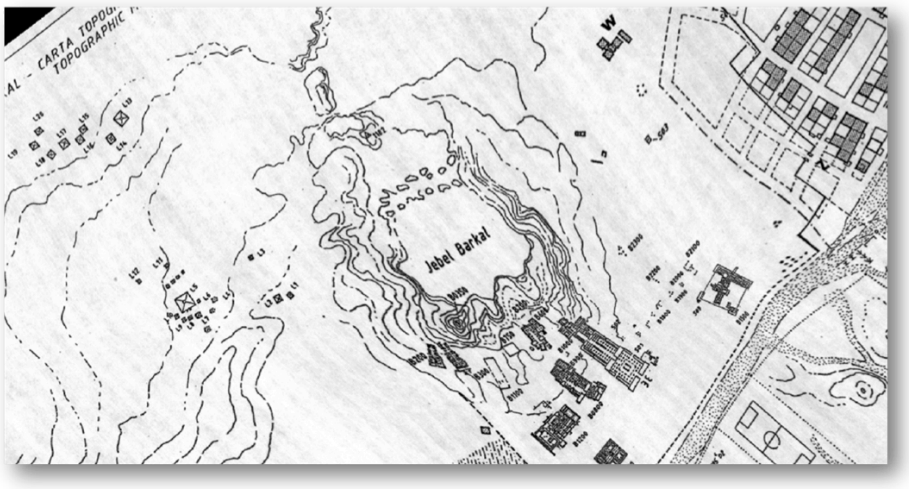

Figure 9.4 : Georeferenced archaeological map (1995) resulted from a forced georeferencing process

Archaeological structures, the general topography, as well as the Gebel, and the urban borders of the area present not real proportions and dimensions, posing a

problem of correspondence between the cartography and the collected data. Therefore, the lack of high-resolution satellite optical image that could provide information about changes occurred in time in the area, as well as about topography, constitutes a critical aspect.

Thanks to the work realised by Prof. L. Perotti, the Quickbird orthoimage has been included in the project as reference basis, in order to supply a valid cartographic documentation (Figure 9.5, upper image). The only one KOMPSAT-2 image acquired on 16 May 2008 available on the ESA EoliSa archive (see §6.2), has then been included in the project (Figure 9.5, lower image).

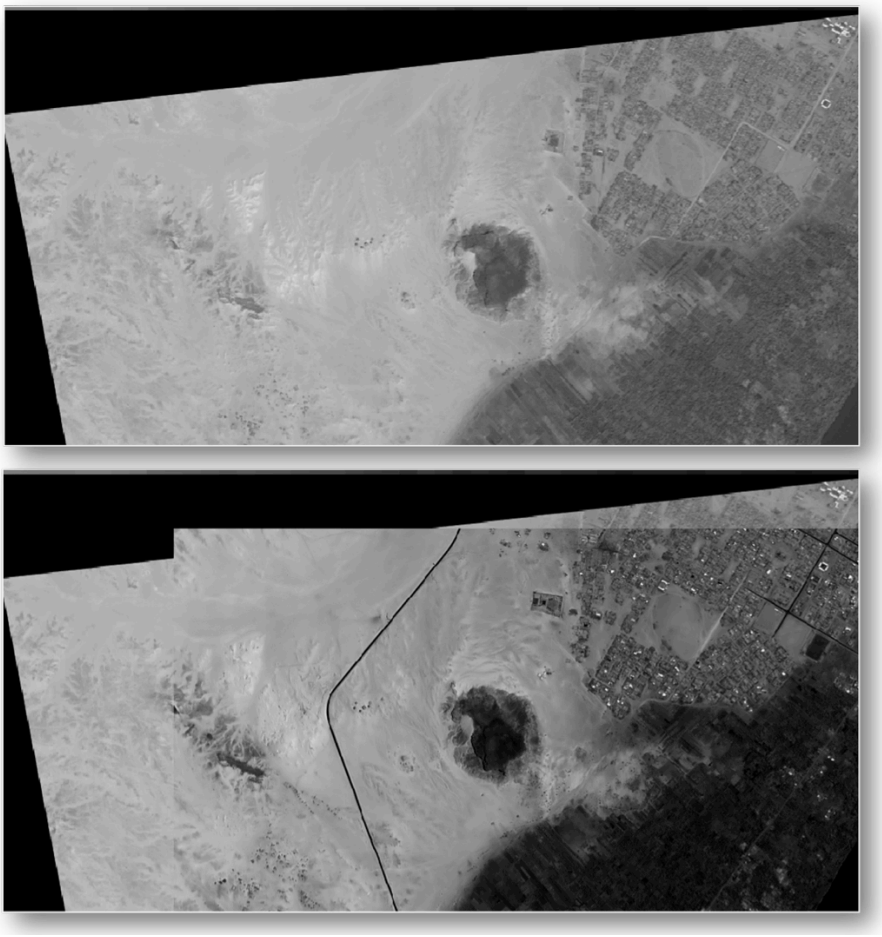

Figure 9.5 : High-Resolution Quickbird orthoimage over Gebel Barkal, after Perotti (top) and KOMPSAT-2 image overlaid in the project (bottom)

In addition to KOMPSAT-2 and QuickBird images, three Google Earth acquisitions, derivated from the chronological archive and obtained at the higher spatial resolution as possible, complete the multi-temporal optical dataset (Figure 9.6). Google Earth acquisitions provide general information about the

topographic changes occurred in the last eight years (2004 – 2012) in the surroundings of the archaeological area.

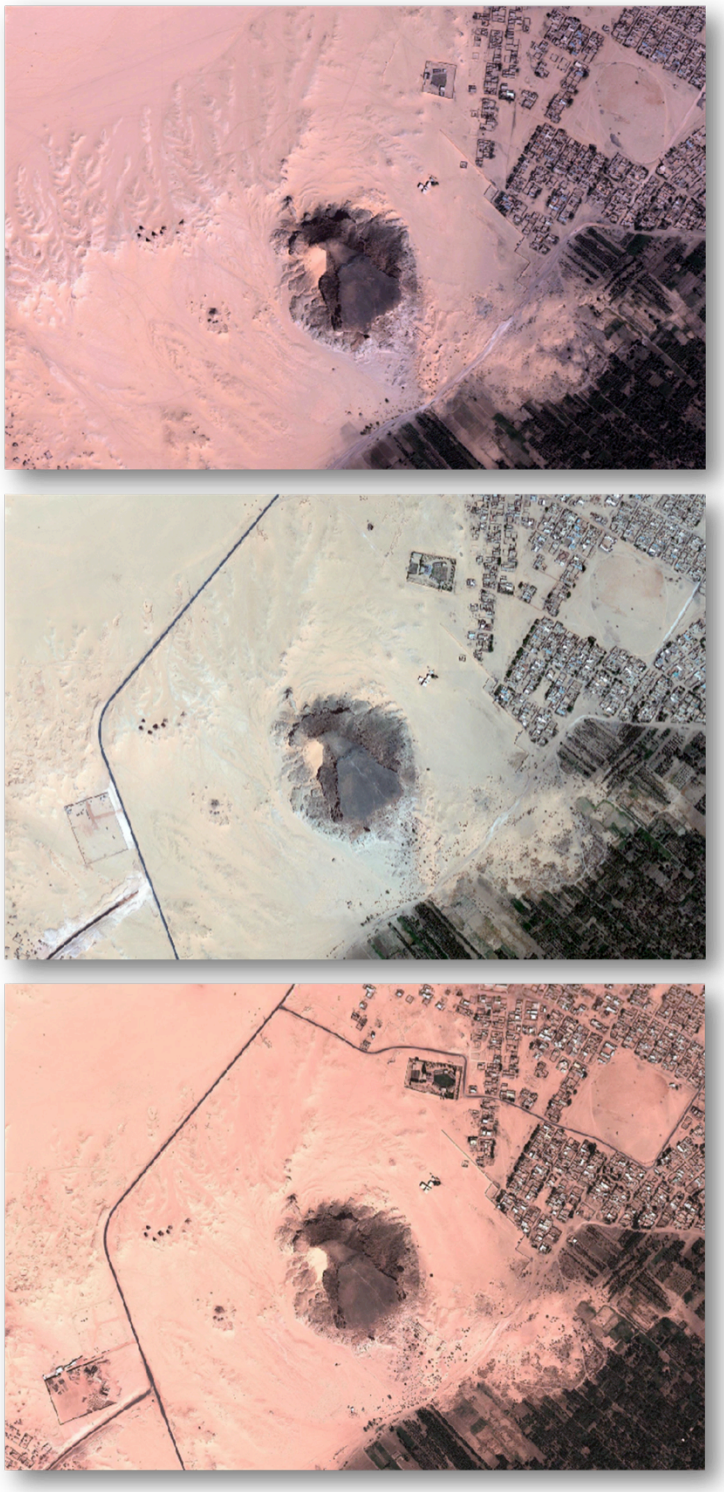

Figure 9.6 : Google Earth' acquisitions. 2004/01/03 (top) ; 2009/10/14 (middle) ; 2012/11/07 (bottom)

Looking at the images illustrated in Figure 9.6, it is possible to notice the realisation of a street axis and connected infrastructures as well as the expansion of the built up area both in the NE and in the SO part of the area. Nevertheless, no relevant changes related to the archaeological structures are recorded.

Principal aim of the dedicated GIS project for the archaeological area of Gebel Barkal, is to realise an updated database, used to unify, in the same environment, all the existing satellite optical data coming from the work of Prof. L. Perotti and from other sources, as well as SAR polarimetric data analysed in the present research. All the data imported in the GIS, have been georeferenced according to the QuickBird orthoimage reference system (UTM WGS84 datum). Where an image presents a different coordinates system, it has been re-projected in UTM WGS84 to obtain the precise matching among images. This procedure allows "the vertical" geographic identification of a given point through data (Figure 9.7).

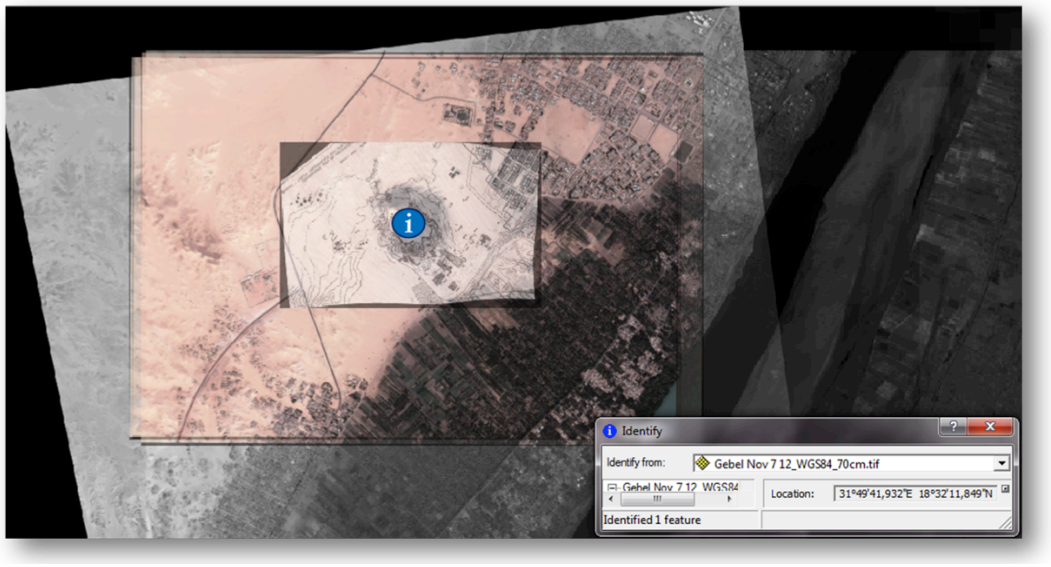

Figure 9.7 : Geographic link through optical data

From a visual point of view, the gathered information provided a help in the localisation of archaeological structures, their interactions with topography and urban area in time and, most important, they allow a simultaneous observation of all the anomalies noticed in the remote sensing analysis.

The creation of the project constitutes the starting point of a wider archaeological research, which will include the whole archaeological documentation not yet published, as well as the documentation still to be developed (photographs,

findings' maps, cartography, technical drawings etc.), and will constitute the reference basis for the future excavation missions to be held by the University of Venice in 2014.

9.4 Integration of SAR polarimetric data in the GIS project

Once the optical multi temporal dataset is created, all the data analysed in the research are integrated in the GIS project. After performing a further geographic correction, Google Earth images reach the precise geographic matching with the Quickbird ortophoto, so that they can be then used as the more recent reference images for the synoptic observation of processed SAR polarimetric data.

The first SAR polarimetric data added in the project are the polarimetric descriptors of the two ALOS PALSAR acquisitions. What a GIS offers, at this point, is the immediate visualisation of data presenting different acquisition time, so to enhance the representation of changes recorded in each presented image (Figure 9.8), through the data transparency tool.

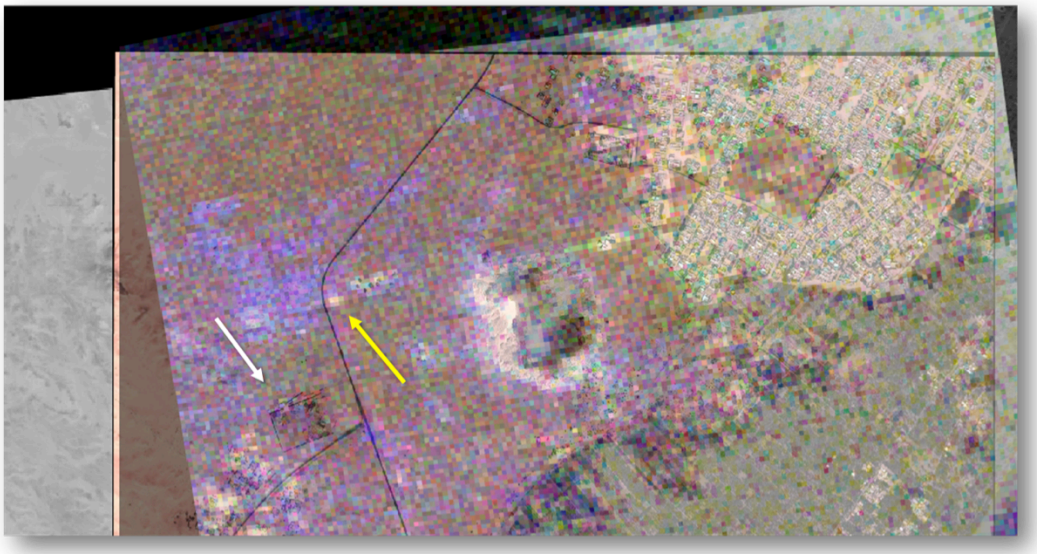

Figure 9.8 : ALOS PALSAR Pauli RGB image (2006/08/14) visualised over Google Earth acquisition (2012/11/07)

As illustrated in Figure 8.9, it can be seen how modern infrastructures (white arrow) and streets, built in last years and visible in Google Earth acquisitions, are not yet built in the 2006 ALOS PALSAR image. On the contrary, as highlighted by the yellow arrow, it is possible to notice how the strong backscattering

detected in the multi-frequency analysis is well localised in the SAR image and thus localised through data. When adding the second ALOS PALSAR image, acquired three years later (May, 2009), it is clear how a better correspondence of modern structures in the different data can be recognised, even if still not definitive (Figure 9.9, white arrow). In fact, the construction of infrastructures is at an intermediate level compared to the final stage represented in 2012 Google Earth image, when the infrastructure is destroyed and a further structure is built. However, what can be noticed is the persistence of the detected strong anomaly on both SAR images (Pauli decomposition RGB image acquired on August, 2006, Figure 9.8; Yamaguchi G4U1 decomposition RGB image acquired on May, 2009, Figure 9.9), anomaly not corresponding to any evident feature on optical data, previously and subsequently acquired (Figure 9.9, yellow arrow).

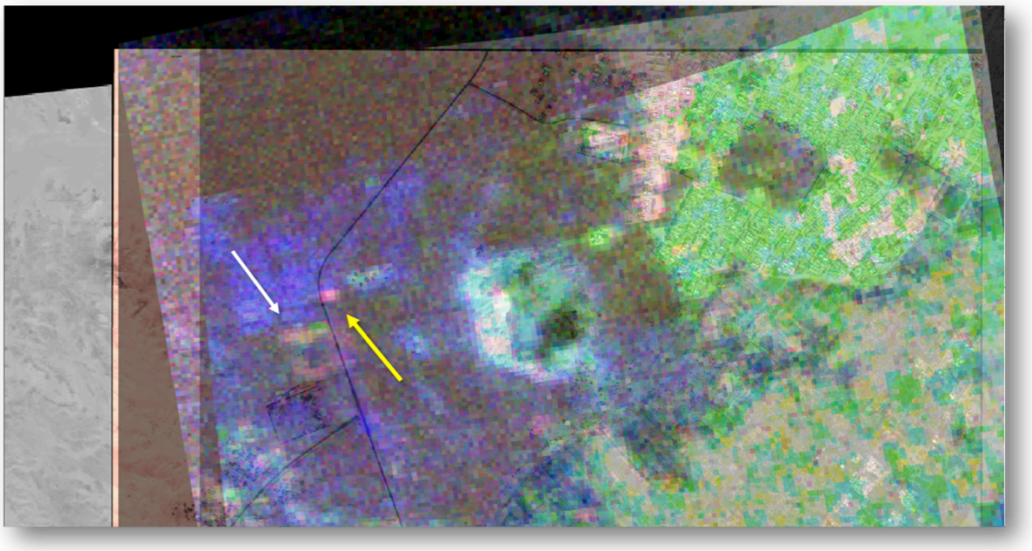

Figure 9.9 : ALOS PALSAR Yamaguchi_G4U1 RGB image (2009/05/11) overlaid to ALOS PALSAR Pauli RGB image (2006/08/14), to Google Earth image (2012/11/07) and to Quickbird ortophoto (2003/09/03)

This visual data analysis permits to perform an initial monitoring of the archaeological area, which allows to individuate the subsequent steps of investigation. In fact, the possibility of managing different data at the same time, switching from one to another layer according to the need of information requested, represents the benefit of a GIS project.

The integration between optical images and ALOS PALSAR data shows how changes can be traceable in time when disposing of a given distance in time acquisition (2003/2009). In the case of very close or a coincident time acquisition,

what can be interesting is the study of features backscattering on SAR data corresponding to features recognisable on optical data. As already mentioned, RADARSAT-2 data used for the present research have been specifically acquired with two different configurations: 27° and 45° incidence angle. Acquisitions of RADARSAT-2 data started in April 2012 and ended in July 2013, with an interval of two up to six months (see §6.3).

Apart from a simple synoptic visualisation of a given polarimetric descriptor with optical data as in the ALOS PALSAR example above reported, the visual analysis of integrated data can be performed at different levels. The multi-frequency data integration is completed by the RADASAT-2 27° incidence angle acquisitions, for which the most significant polarimetric descriptors have been inserted in the project (Figure 9.10).

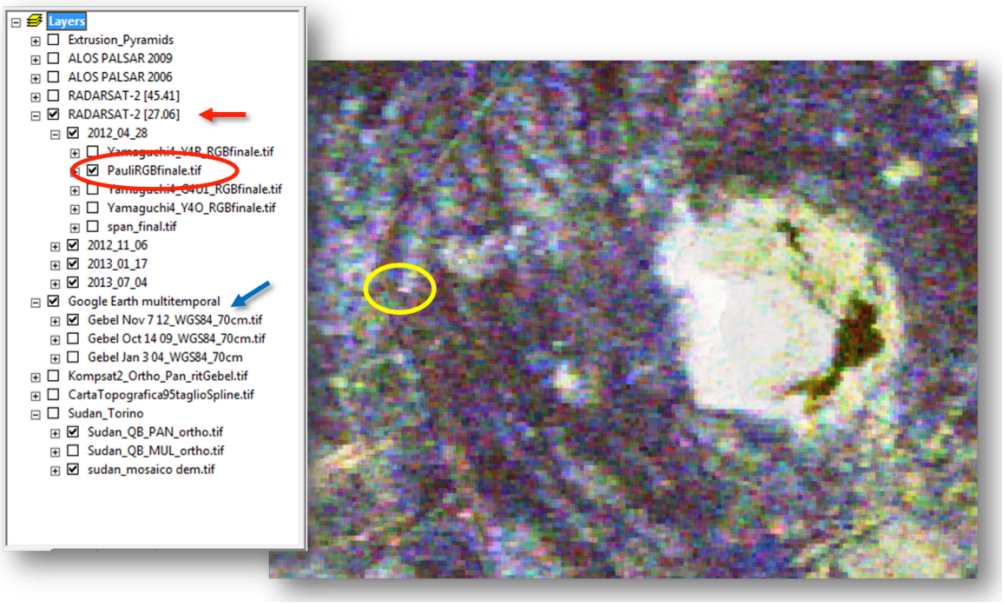

Figure 9.10 : List of data layers (left) and overlaid of RADARSAT-2 27° incidence angle Pauli RGB images with Google Earth acquisition (2012/11/07, right)

The integration of the 27° incidence angle images starts with the superimposition of the Pauli decomposition RGB images (Figure 9.10, red ellipse) relevant to all the acquisition dates (April and November, 2012 ; January and July, 2013 ; Figure 9.10, red arrow) over the Google Earth image acquired in the same year (November, 2012 ; Figure 9.10, blue arrow). It is thus possible to observe, thanks to a certain degree of transparency applied to the displayed layers, the sum of scattering mechanisms represented in the RGB visualisation and occurred in the

archaeological area. The known archaeological evidences are recognised and observed through data, as well as, once again, the strong backscatter noticed in the research analysis (yellow ellipse). With the same procedure, the Yamaguchi G4U1 decomposition RGB images analysed in the research (see §7.3.2, Figure 7.13) are imported in the project, as well as the single channels relative to each scattering mechanism contribution (Figure 9.11).

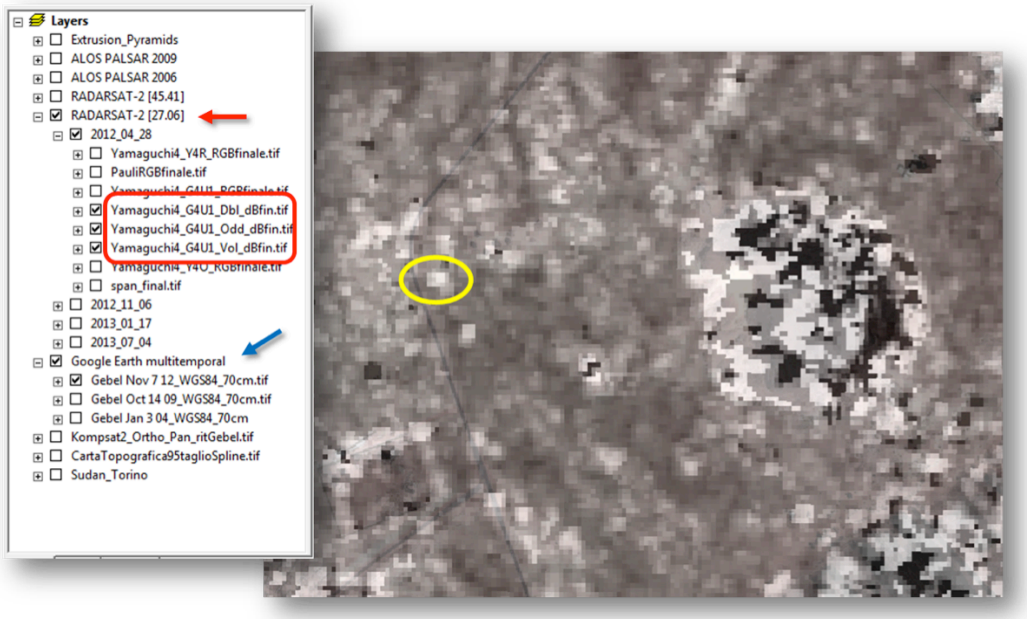

Figure 9.11 : List of data layers (left) and RADARSAT-2 27° Yamaguchi G4U1 Double bounce, Single bounce and Volume scattering (2012/04/28) overlaid to Google Earth acquisition (2012/11/07, right)

The integration of the multi-incidence angle data analysis (see §8.1) is realized following the workflow above presented. Thanks to the geographic communication of data in the project, the RADARSAT-2 45° configuration images are inserted to verify the presence continuity of the already noticed anomalies. In parallel, the new detected anomalies are studied in all the polarimetric descriptors performed (Figure 9.12).

As shown in Figure 9.12, the strong backscattering noticed in the multi-frequency analysis, identified by the latitude/longitude values, is not visible in the 45° acquisitions, while a different backscattering is localised between the central group of Royal Pyramids and the Jebel Mountain in the Pauli decomposition RGB images (Figure 9.12, top, yellow circle). All the polarimetric descriptors analysed are reported in the project to visualise the localisation of the anomaly, as shown in the Shannon Entropy descriptor in Figure 9.12 (bottom).

One of the principal and most useful outputs a GIS is able to provide is the thematic map. This kind of documentation is meaningful for archaeologists who need to represent a given characteristic in a symbolic and focused way. A visualisation similar to a thematic map can be considered the output of many image-processing operations that can be visualised in the GIS environment, according to the kind of information required.

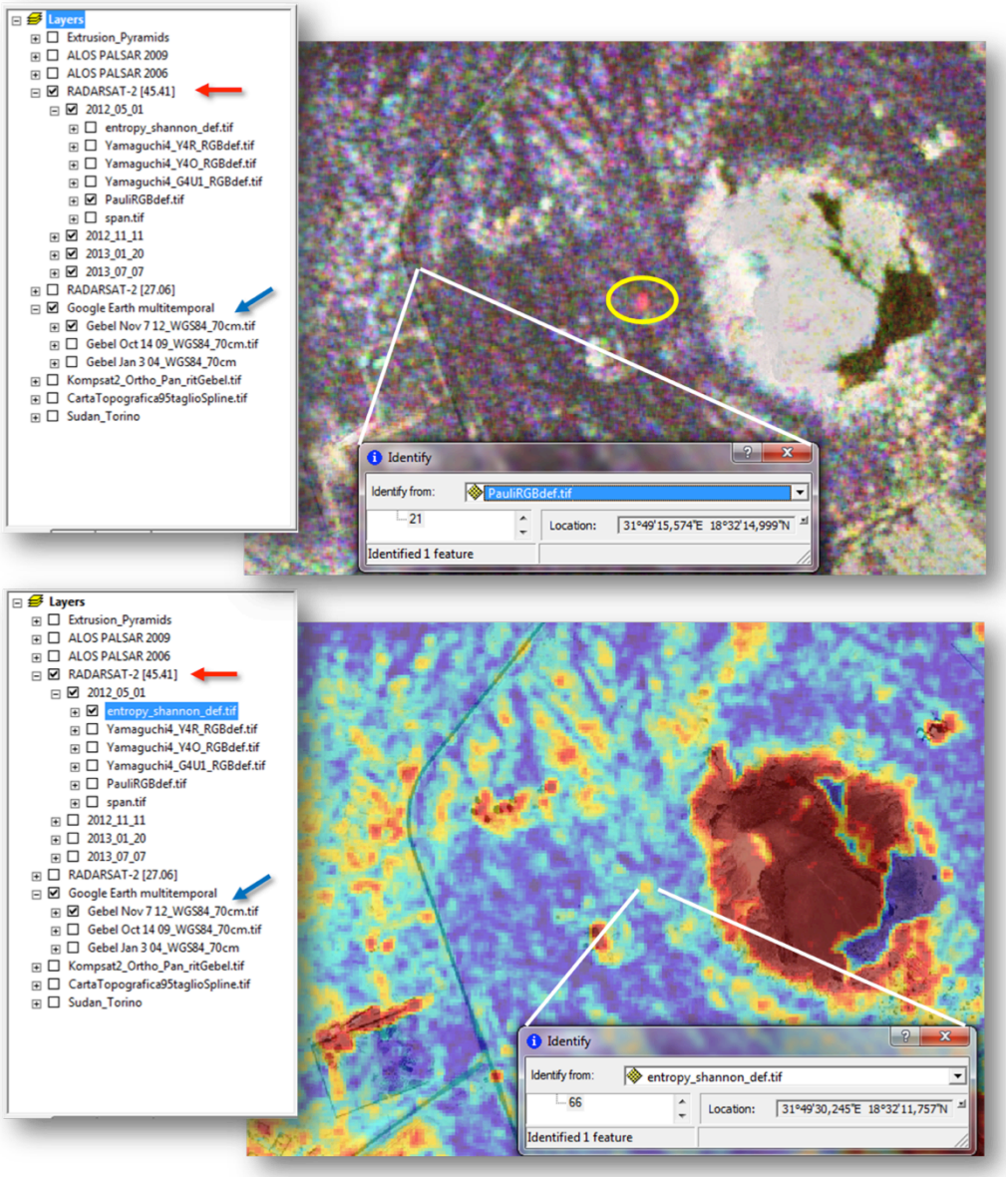

Figure 9.12 : RADARSAT-2 45° Pauli decomposition RGB images overlaid to Google Earth acquisition (2012/11/07, top) ; Shannon Entropy descriptor (2012/05/01) overlaid to Google Earth acquisition (2012/11/07, bottom)

As an example, the same Shannon Entropy descriptor illustrated in Figure 9.12 (bottom) is here represented after performing a classification operation. The

output image in Figure 9.13 shows uniquely all the Entropy values considered relevant (greater than a given value) representing the distribution of the Entropy value recorded for the anomaly in the entire image, superimposed to the DEM and to the optical dataset. Focusing on the Royal Cemeteries area, it is possible to notice how the colour representation, hence the recorded Entropy range value of the detected anomaly (blue circle), corresponds to the one of the NW group of Pyramids (green arrow), to the central group of pyramids (brown arrows), and to the topographic reliefs (blue arrows).

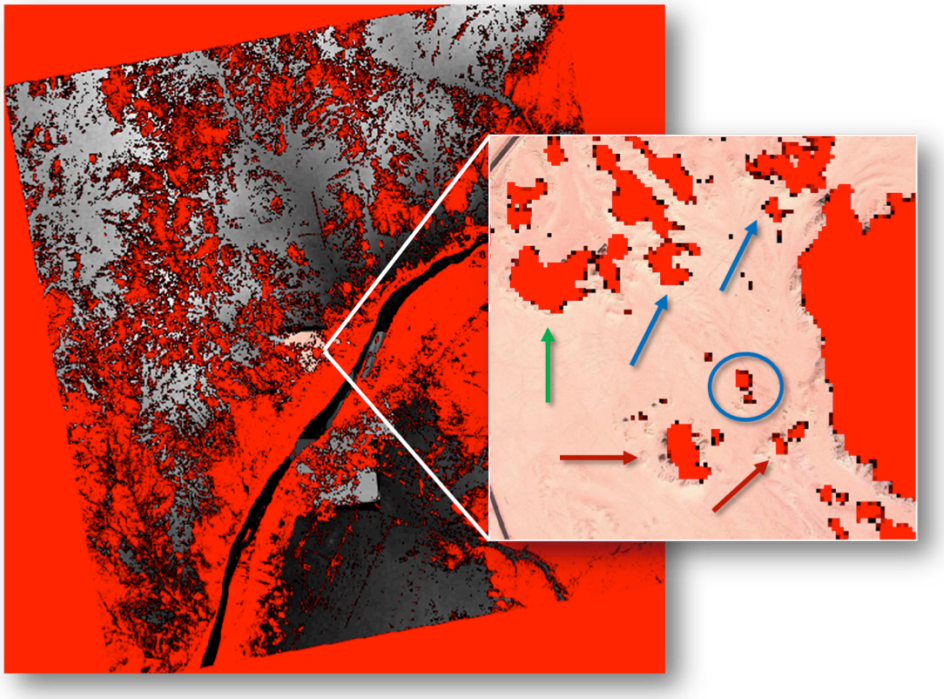

Figure 9.13 : Classification performed on Shannon Entropy descriptor overlaid to Google Earth acquisition (2012/11/07)

The usefulness of such representations is linked to visualisation purposes that point out how to put in communication different kind of data, in this case optical and SAR polarimetric data, focusing on specific information, that are then displayed in thematic outputs (maps, images, classes etc.). Conspicuous benefit coming from this kind of vectorialised maps and classified images are, thus, provided by the GIS project, in which thematic outputs constitute the starting point of the spreading of a complex knowledge (SAR polarimetric data) visualised in a conceptual language familiar to the archaeological community.

9.5 Archaeological interactive information

As shown, the amount of information data provide, thanks to their simultaneous visualization, constitutes the great potential of a dynamic container that can be consulted at different levels. The possibility of observing an overall view of an archaeological site, as well as details linked to specific aspects, facilitates the communication between archaeology and technology. This is truer especially when a 3D structures extrusion of ancient structures is added to the already remarkable amount of available information.

The last operation performed in the frame of the present research, is dedicated to the realization of a 3D rendering of the Royal Cemeteries structures. The digitalisation here proposed wants to provide an immediate idea of the overall environment and of structure's interaction with it. A deeper and more detailed rendering of the Pyramids, for which a specific digitalization is required, is scheduled for the future phases of the project.

First step of the rendering is the realisation of Pyramids, created by means of polygonal lines equipped with the height information for each point and with corresponding latitude/longitude values (Figure 9.14).

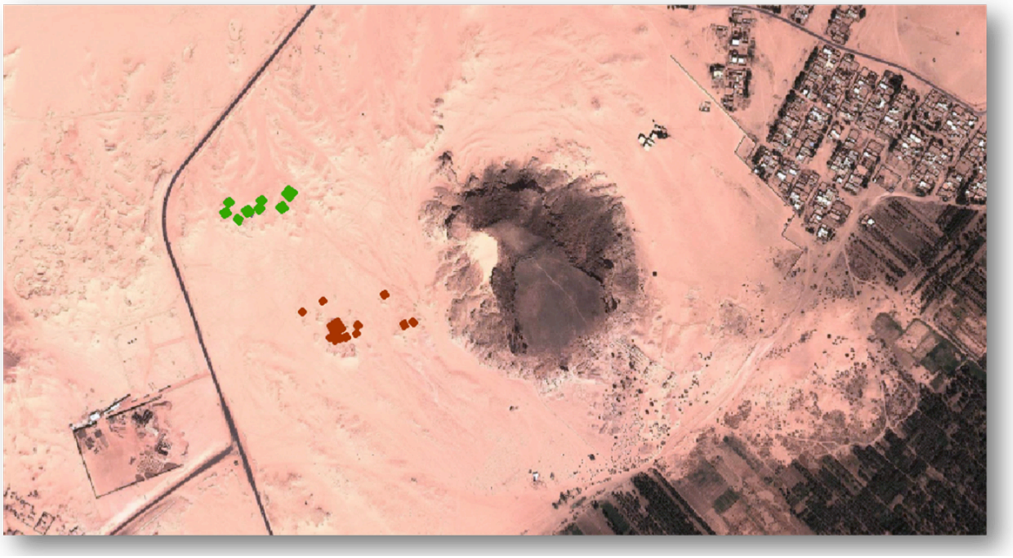

Figure 9.14 : Polygons showing the Royal Cemeteries pyramids (NW group, green; Central group, brown)

Based on the Digital Elevation Model (DEM), realized at 10 meters of resolution and furnished by Prof. L. Perotti, the most recent of the Google Earth acquisition

(November, 2012), as well the rendering realized over pyramids, are imported in the 3D environment and are draped over the DEM (Figure 9.15).

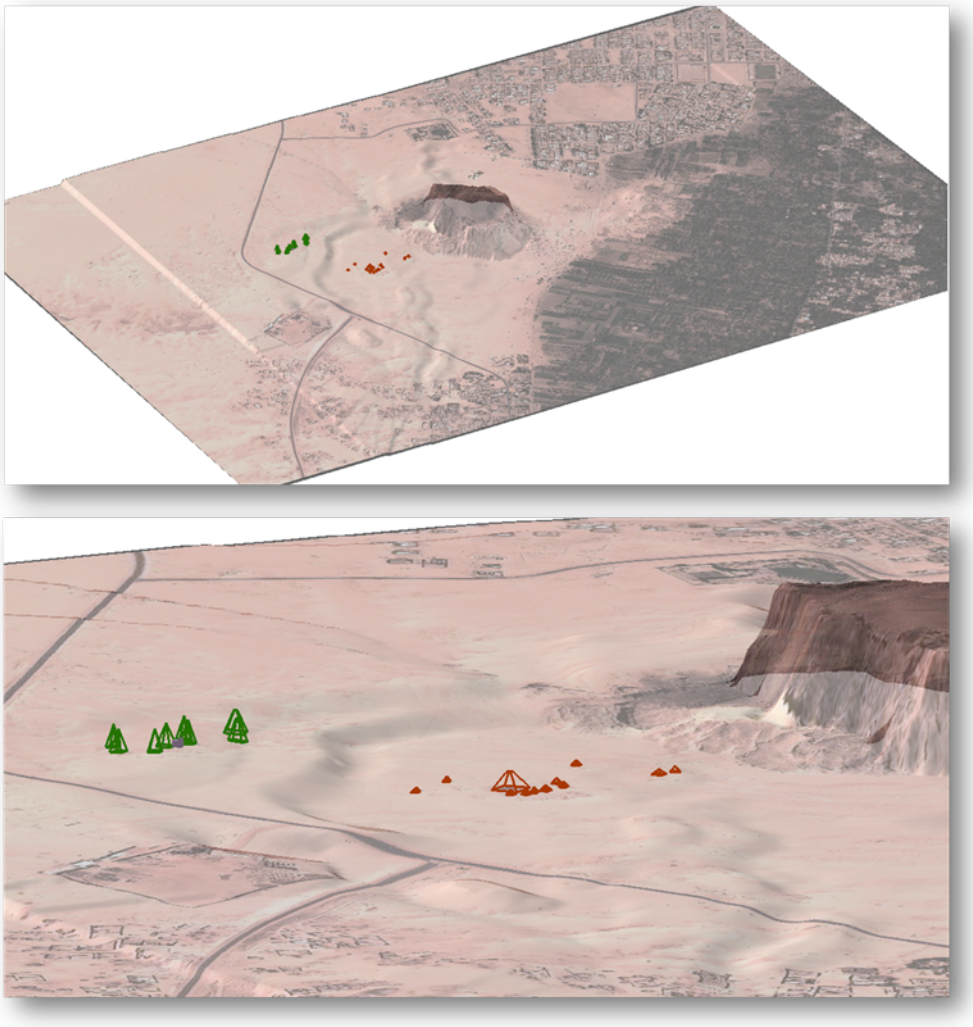

Figure 9.15 : Integration of DEM (Digital Elevation Model), Google Earth acquisition (2012/11/07) and 3D rendering of pyramids

This first integrated visualization provides an initial appreciation of the whole topography, together with the difference in building typology of pyramids and their reciprocal positions.

As following step, SAR polarimetric data are inserted in the 3D environment. As aforementioned, SAR polarimetric analysis constitutes complex data that require a specific knowledge. This complexity still prevents archaeologists to deepen the remote sensing investigation towards satellite radar data. The integration of SAR polarimetric data in the GIS project creates, at this point, a useful bridge between a very well-known source of information as optical images and a more complex,

and unknown, one. Thanks to this integration, the relationships between noticed anomalies and archaeological structures becomes more understandable also for non-experts, and emphasizes the communicative potential of such a multidisciplinary approach.

The perfect geographic communication among satellite data coming from different sources is possible after performing some operations on the images, which are, at this level, ready to be simultaneously presented as a whole : optical data, 3D structures reconstruction and the results obtained from the SAR polarimetric data analysis presented in previous chapters (Figure 9.16).

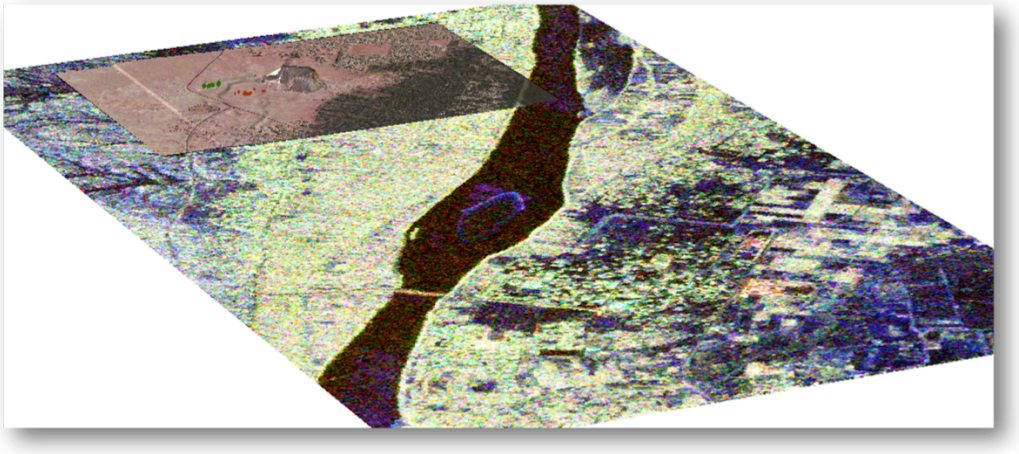

Figure 9.16 : RADARSAT-2 Pauli RGB image displayed in the 3D environment

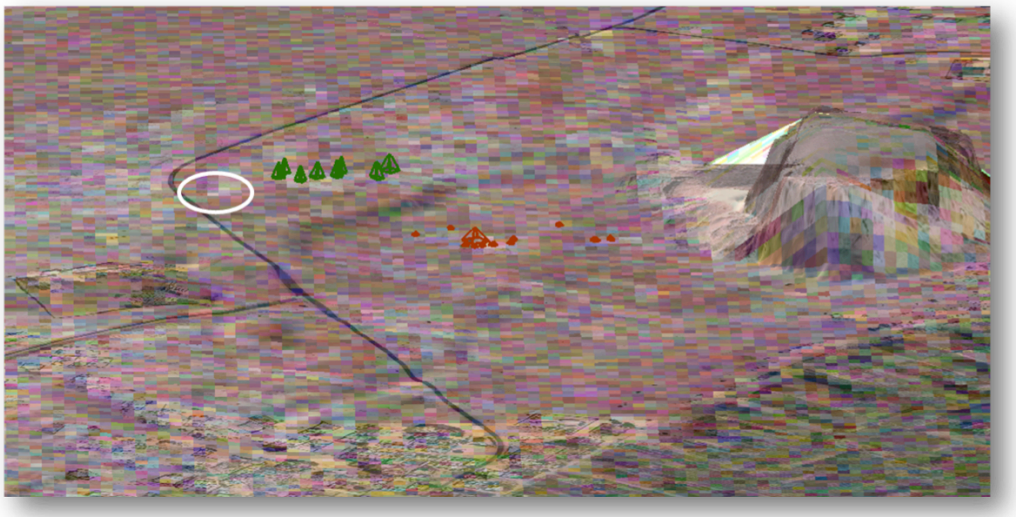

Figure 9.17 : RADARSAT-2 27° incidence angle Pauli decomposition RGB image overlaid to Google Earth acquisition (2012/11/07)

Looking to the detail of such integration, as illustrated in Figure 9.17 by one of the RADARSAT-2 27° configuration acquisition, the correspondence between

known surface archaeological structures and their backscattering can be noticed, as well as the presence of the noticed anomaly (white circle) in the multi-frequency analysis can be easily localized in the area.

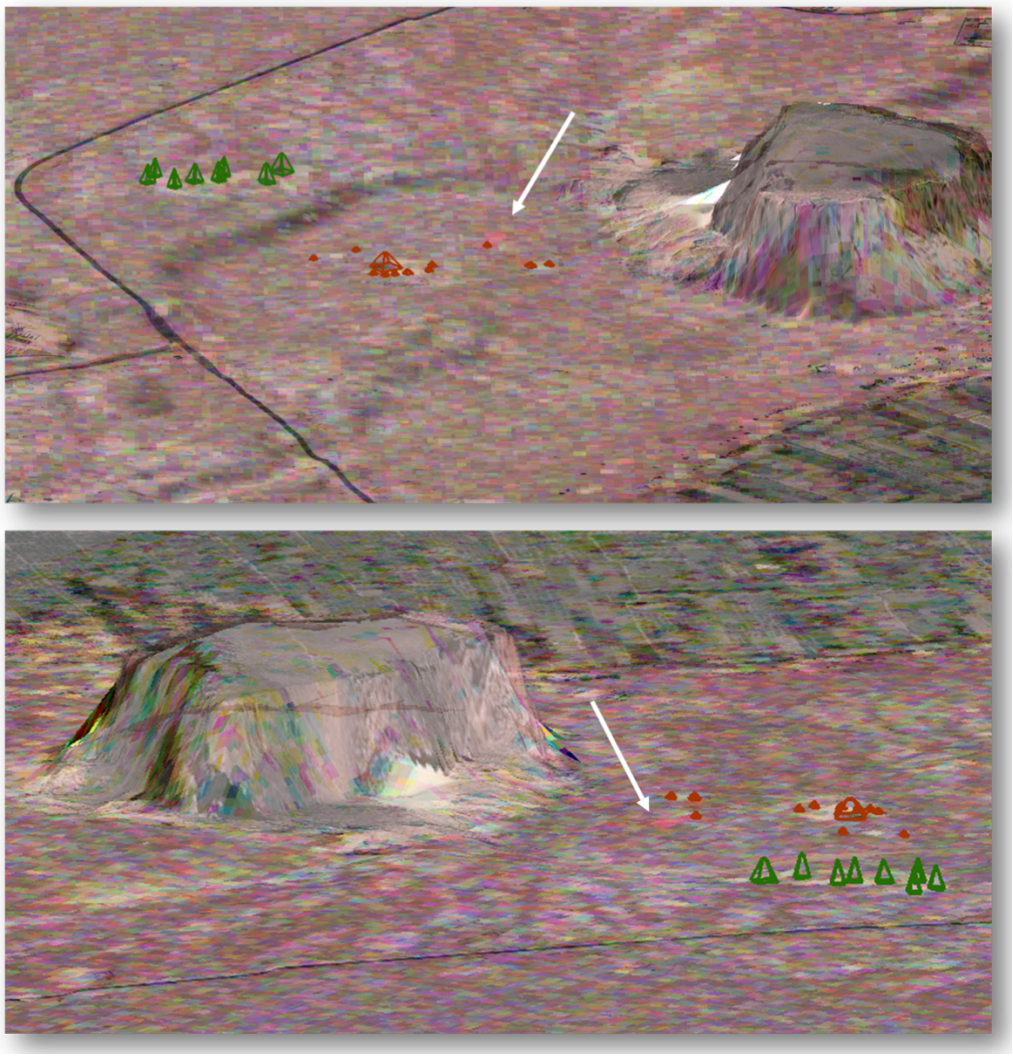

Figure 9.18 : RADARSAT-2 45° incidence angle Pauli decomposition RGB image overlaid to Google Earth acquisition (2012/11/07). View from SW (top), view from NW (bottom)

The interactive aspect of this representation consists in the possibility to look at the structures and at the general topography of the site from different point of view. In Figure 9.18, one of the RADARSAT-2 45° configuration Pauli decomposition RGB image is represented. Once again, the anomaly noticed in the multi-incidence angle analysis between the central group of Royal Pyramids and the Jebel Mountain can be recognised (white arrow). Changing the perspective, the visualisation of the surrounding environment of the area completes the

information derivable from such a representation, for example observing the development of the palms cultivation belt in the southern and eastern part of the area, behind the Jebel Mountain (Figure 9.18, bottom).

9.6 Conclusion

This conclusive chapter provided an overview about the very recent use of Geographic Information System in archaeology, about its usefulness and the amount of information that, thanks to it, can be linked together.

Starting from a previous work carried out by Professor L. Perotti over Gebel Barkal site, SAR polarimetric data analysed in this research converged in a common GIS project. Archaeologists supervising excavations *in situ* (Professor A. Roccati, Professor E. Ciampini) showed their interest in the application of SAR polarimetric technique for the study of Gebel Barkal area and in the development of a GIS project in which collecting and managing excavation's documentation, optical and SAR polarimetric satellite data.

As first step, an optical multi-temporal dataset has been created, then integrated with multi-frequency and multi-incidence angle data analysis, showing how to use different image outputs according to the kind of information needed. Data integration was then completed by a stylised 3D rendering of the two groups of Royal Pyramids, to be updated in future phases of the project, rendering that completed the already 3D rendering of temples and palaces realized by Professor L. Perotti. The interactive communication between data and information has been shown, with the purpose to illustrate how to visualise a complex information as the one represented by SAR polarimetric data, once it is related to more spread and immediate data like optical images, to which the remote sensing archaeological research is used.

Managing data of different nature in a unique layer has demonstrated how data can be visualized in an immediate way, giving priority to the layer of interest, represented by a SAR polarimetric descriptor, an optical image or the combination of them. This procedure allowed to carry out a constant monitoring and study of some specific and persistent backscattering, due to unknown features as well as to surface archaeological features like the two Royal Cemeteries.

Moreover, the observation of anomalies detected according to the specific images configurations analysed, and then integrated in the project, originated the planning of work indications that can be included in the future excavation missions at Gebel Barkal.

This page intentionally left blank

Chapter 10

Conclusions and Outlooks

10.1 Research scientific context and original contribution

Starting from a wide overview of remote sensing for archaeology state of art, this PhD research inserts its contribution in the recent scenario, in growing expansion, of new technologies applied to the traditional archaeology. It has been discussed how aerial photography and photointerpretation knowledge deeply influenced the way of looking at archaeological ruins, becoming the principal scientific investigation tool then converged to the analysis of very high spatial resolution optical satellite images.

As already mentioned in the dissertation, the use of SAR satellite data for the archaeological investigation is still unexplored. This is not only due to technical factors characterising SAR data, as the not enough spatial resolution requested for archaeological structures appreciation, but principally to data processing aspects not immediate solution (immediately solvable?):

- General complexity of data analysis and interpretation
- Need of a specific technical knowledge for archaeologists
- Inexistence of an automatic procedure designated to the recognition and extraction of archaeological features
- Lack of visual communication between the well-known aerial photographs or optical data and SAR satellite data.

This work demonstrated how to exploit a complex but significant technique as SAR polarimetry is, identifying the most suitable case study in the UNESCO archaeological site of Gebel Barkal (Sudan).
In particular, this work has been principally addressed to the application of two typology of analysis:

- a polarimetric multi-frequency analysis ;
- a polarimetric multi-incidence angle analysis.

The multi-frequency analysis between the two SAR polarimetric sensors of ALOS PALSAR (L-band), whose central frequency is 1.25 GHz, and of RADARSAT-2 (C-band) with a central frequency of 5.405 GHz, has been carried out on data presenting a similar incidence angle configuration, respectively 23.10° / 26.7° and 27.6°. Disposing of a good historic polarimetric dataset, from a multi-temporal point of view considerations, the persistence in time (2006/2013) of the target detected in SAR polarimetric images has been confirmed, while any kind of surface archaeological feature appeared to be present in cartography and optical images available. The climate information relative to the acquisition dates did not report any precipitation phenomena, thus not affecting the wave interaction with soil.

In order to deepen the available information about the nature of the target, primarily individuated by means of a qualitative analysis, several polarimetric descriptors have been investigated. The selection of the most meaningful ones for this particular kind of application drove the analysis towards the Yamaguchi 4 components decomposition, and in the detail, to the Yamaguchi G4U1 descriptor. It has been shown how, observing the related RGB decompositions and the amplitude values of the single channels representative of single bounce, double bounce and volume scattering contribution, it has been possible to distinguish the nature of the backscattering, apparently similar to the general morphology of Gebel Barkal site. Additional information on the interaction of the electromagnetic wave with structures have been derived, taking into account the inclination wall of Royal Pyramids and their reciprocal orientation respect to the incident wave. The single bounce mechanism' prevalence recorded for archaeological structures, as well as for the general topography of the site, has

been detected for the strong backscattering as well, distinguished, however, by a light double bounce contribution. What resulted to be very interesting, is the different contribution that ALOS PALSAR 26° acquisitions and RADARSAT-2 27° acquisitions gave to the observation of the archaeological area. Being in fact C-band more sensitive to surface characteristics and thanks to the higher spatial resolution provided, a more detailed visualisation of the overall occurred scattering mechanisms and a not well defined distinction of the detected backscattering has been observed. However, supposing the backscattering was due to the sand-stone topography of the site, we could have expected the same responses for all the morphological evidences in the area not only in RADARSAT-2 data but also in ALOS PALSAR acquisitions, where the backscattering is, on the contrary, very well recognisable.
The typology of polarimetric acquisition selected, characterised by a different frequency but a similar incidence angle configurations, leads the study to assume that ALOS PALSAR L-band deeply penetrated sand detecting a target in the ground, while RADARSAT-2 C-band lightly penetrated sand, detecting the same target, despite its lower penetration capability but thanks to the steeper observation incidence angle.

When approaching satellite remote sensing analysis for archaeological purposes, the most frequent question concerns the possibility to consider remote sensing as a new tool for the archaeological investigation. In order to answer to this question, for which probably we should need more than one answer, the PhD research here described, as any scientific experimental approach requires, pointed at the most reliable validation method for archaeology: ground truth.
Thanks to the collaboration with the University Ca' Foscari of Venice (Italy), a survey in situ carried out by Prof. E. Ciampini, supervisor of the Italian mission at Gebel Barkal, has been performed in the frame of the November-December 2013 expedition. Unfortunately, due to permissions ruling the concession on site, only a photographic campaign has been allowed. However, it gave precious information about the results obtained in the multi-frequency analysis and it will be completed in the frame of the future excavations at Gebel Barkal scheduled for November 2014.

Contextually, a polarimetric multi-incidence angle analysis has been performed as well, by analysing the two configuration of the flexible RADARSAT-2 sensor: 27.6° and 45.41°. The same cycle of acquisition allowed to analyse the different backscattering responses in the same date, for which the relative climate information did not report any precipitation phenomena. The strong backscattering noticed in the multi-frequency analysis has not been detected in the multi-incidence angle investigation. On the contrary, thanks to the higher sensitivity of 45° incidence angle configuration to double bounce scattering, a strong backscattering has been detected in the central part of the archaeological area. The contemporary presence of more than one scattering mechanism for this anomaly has been confirmed with the analysis of Shannon Entropy descriptor. In addition, Yamaguchi 4 components decomposition has been performed, for which the Yamaguchi Y4R descriptor turned out to be the more significant parameter. Several considerations have been proposed, both on the interaction of the 45° incidence wave with the inclination of pyramids' walls and on the amplitude values recorded in each Yamaguchi Y4R single bounce, double bounce and volume scattering channel. The clear double bounce reflection, typical of standing vertical features not traceable on optical data, has been thus analysed by performing an enhancing filter on the KOMPSAT-2 image. The orientation changes in surface topography observed has been, thus, related to the noticed backscattering, for which a ground truth survey will be performed in future excavations at Gebel Barkal.

The conclusive step of the research is represented by the realisation of a dedicated GIS project realised in collaboration with the University of Turin (Italy). The project wants to provide first a tool that can put in communication all the different data Archaeology uses today and, secondly, a tool able to visualise at different levels of complexity the archaeological information deriving both from the field and from the remote sensing analysis. It has been demonstrated how the Geographic Information System can be considered the "bridge" connecting technology and archaeology. Satellite optical and SAR images are gathered together thanks to the geographic link trough data, thematic map and classified images communicate according to the specific need requested. From a visual point of view, the project is equipped, and will be developed in this sense, with a

3D rendering of pyramids, operation that contextualises the site in its environment and that can be displayed as a synoptic observation of SAR polarimetric detected anomalies.

The present research offered its original and challenging contribution to the scientific non-invasive archaeological investigation, which represents, today, a very intense and wider application field. The scientific potential of the illustrated analysis fits perfectly with the current delicate needs of cultural heritage: such analysis have demonstrated how they can provide a multi-temporal and multi-data Cultural Heritage monitoring, which can be applied not only for documentation purposes, but which can be addressed especially to those areas exposed to threats of different nature that require a constant and prompt intervention plans.
This new and recent boundary to which the archaeological research extends, does not want to substitute the current method of investigation, based on aerial photointerpretation, cartography, high-resolution optical data, survey in situ. It aims, more specifically, to define an integrative and innovative non-invasive method to the mentioned ones, which completes an increasingly multidisciplinary field of research as Archaeology is today.

10.2 Future perspectives and outlooks

As aforementioned, the SAR polarimetric archaeological application described in this dissertation is based on only one possible combination of multi-frequency and multi-incidence polarimetric analysis, performed respectively with L-band ALOS PALSAR (1.27 GHz) and C-band RADASAT-2 (5.405 GHz) sensors, and with RADARSAT-2 27° and 41.45° incidence angle acquisitions, thanks to the flexibility of the sensor.
Wider multi-frequency and multi-incidence analysis will be possible with the launch of the SAR polarimetric sensor ALOS-2, which will provide a flexible incidence angle configuration selection, a higher spatial resolution (10 m in the full-pol mode) compared to ALOS PALSAR, at the same wavelength (L-band), thus granting the same penetration capabilities in the ground. The full-polarimetric characteristic will be provided also by the argentine SAR L-band SAOCOM sensor (10 m of spatial resolution). Unfortunately, the first P-band satellite of the BIOMASS mission, characterised by a deeper ground penetration

capability, will not acquire at the suitable spatial resolution requested for archaeological structure detection (ideally lower than 10 m). However, the aimed multi-frequency approach will be expanded also to the X-band wavelength, already available with TerraSAR-X and COSMOSky-Med sensors. These last sensors provide a very high sensitivity to surface topography and a very high spatial resolution (up to 1 m) for archaeological investigation. A further and interesting study the two sensors can support, beyond the multi-frequency point of view, might be the evaluation of the different kind of information derivable from dual – polarimetric (see experimental compact or hybrid-polarimetric) acquisitions compared to full - polarimetric acquisitions, with different and similar incidence angle observation mode.

As shown, the potential applications of polarimetric satellite SAR data for archaeological purposes can be developed in various directions, privileging specific sensors' characteristics that can define the individuation of the most suitable combination that can be considered interesting from an archaeological point of view.

Publications

Conference Proceedings

1. Patruno J, Dore N, Crespi M, Piro S, Sarti F, Remote sensing techniques in archaeology. From Space to Ground investigation through the microwave spectrum: SAR and GPR detection, in 31th EARSeL Symposium, 30 May / 2nd June 2011, Prague (Czech Republic) ISBN: 9788001048689

2. Patruno J, Dore N, Crespi M, Piro S, Zamuner D (2011). Integration of SAR data, optical satellite images and GPR investigations for archaeological site detection.. In: Proceedings of 9th International Conference on Archaeological Prospection, Izmir, Turchia, 19 - 24 September 2011 ISBN: 978-605-396-155-0

3. Patruno J, Dore N, Crespi M, Pottier E, A multi-sensor polarimetric analysis over archaeological sites, in proceedings Geoscience and Remote Sensing Symposium (IGARSS) 2012 IEEE International, 22-27 July 2012 , Munich, (Germany) E-ISBN 978-1-4673-1158-8

4. Dore N, Patruno J, Pottier E, A new research in Polarimetric SAR technique for archaeological purposes. Samarra (Iraq) and Djebel Barkal (Sudan) sites, in proceedings of the 3rd EARSeL Workshop in Advances in Remote Sensing for Archaeology and Cultural Heritage Management (Ghent, Belgium, 19-22 September 2012)

5. Patruno J, Dore N, Pottier E, Comparison of Polarimetric SAR sensors for archaeological purposes, in proceedings of the 3rd EARSeL Workshop in Advances in Remote Sensing for Archaeology and Cultural Heritage Management (Ghent, Belgium, 19-22 September 2012)

6. Pottier E, Dore N, Patruno J (2012). On the use of fully-polarimetric ALOS-PALSAR and Radarsat-2 datasets for monitoring the wetland dynamics and for detecting archaeological sites. In: 2012 3rd International Polarimetric SAR Workshop in Niigata (POLSAR-WS). Niigata (Japan), 23- 26 August 2012

7. Dore N, Patruno J, Pottier E, Crespi M, A RADARSAT-2 polarimetric multi-incidence angle analysis over archaeological sites. The ancient UNESCO city of Samarra (Iraq), PolInSAR 2013, 6th International Workshop on Science and Applications of SAR Polarimetry and Polarimetric Interferometry, 28 January-1st February 2013, Frascati (Italy)

8. Patruno J, Dore N, Pottier E, Crespi M, A multi-frequency polarimetric SAR sensors analysis over the archaeological area of Djebel Barkal (Sudan), PolInSAR 2013, 6th International Workshop on Science and Applications of SAR Polarimetry and Polarimetric Interferometry, 28 January-1st February 2013, Frascati (Italy)

9. Patruno J, Dore N, Pottier E, Crespi M, Multi-frequency polarimetric ALOS PALSAR and RADARSAT-2 analysis over the archaeological area of Djebel Barkal (Sudan), European General Union 2013, 7-12 April 2013, Vienna (Austria)

10. Dore N, Patruno J, Pottier E, Crespi M, RADARSAT-2 multi-incidence angle polarimetric analysis over the UNESCO site of Samarra (Iraq), European General Union 2013, 7-12 April 2013, Vienna (Austria)

11. Dore N, Patruno J, Pottier E, Crespi M, A multi-temporal and a multi-incidence angle polarimetric analysis over Samarra UNESCO site in danger, 4th EARSeL Workshop on Cultural and Natural Heritage, 6-7 June 2013, Matera (Italy)

12. Patruno J, Dore N, Pottier E, Crespi M, SAR polarimetry for archaeology. Multi-frequency analysis over the UNESCO site of Gebel Barkal, Sudan, 4th EARSeL Workshop on Cultural and Natural Heritage, 6-7 June 2013, Matera (Italy)

Reviews

1. Patruno J, Dore N, Jaia A.M., Galdieri G, Sarti F (2013). Risultati preliminari dell'osservazione di immagini ALOS PALSAR per l'indagine di tracce archeologiche sepolte. ARCHEOLOGIA AEREA, vol. 6, p. 79-88, ISSN: 2035-7540

2. Dore N., Patruno J (2012). Le nuove frontiere dell'archeologia Dalla fotografia aerea al telerilevamento satellitare SAR. ARCHEOMATICA, Volume: 2; Issue: 4, ISSN: 2037-2485

3. Patruno J, Dore N, Pottier E, Crespi M (2013), Polarimetric Multi-frequency and Multi-incidence SAR Sensors Analysis for Archaeological Purposes, in Archaeological prospection, 20, DOI: 10.1002/arp.1448

4. Dore N, Patruno J, Pottier E, Crespi M, New Research in Polarimetric SAR Technique for Archaeological Purposes using ALOS PALSAR Data, in Archaeological Prospection, 20, DOI: 10.1002/arp.1446

Tutorials and activities

1. Lectures for the 2nd level master "*Architettura per l'Archeologia, Archeologia per l'Architettura*", organized by "Sapienza" University, Faculty of Architecture and of Letters and Philosophy, 9 June 2011

2. Organization and lectures for the First Remote Sensing and Cultural Heritage course *Radar remote sensing application for the study and observation of archaeological sites* (17/09/2012–18/09/2012, Ghent, Belgium) realised in collaboration with EARSeL (European Association of Remote Sensing Laboratories), Ghent University (Belgium), UNESCO, Sapienza University of Rome and the IETR, University of Rennes 1 (France), sponsored by European Space Agency ESA-ESRIN (Frascati, Rome)
   http://w3.uniroma1.it/geodgeom/corsi-convegni-educazione/2012-Corso%20Ghent/Home.htm

3. Collaboration to the *II Advanced course on radar polarimetry*, ESA-ESRIN, Frascati (RM), 21/01/2013 – 25/01/2013

4. Organization and frontal lectures for the "*II ESA RS: Remote Sensing for Archaeology*", 3-5 June 2013 Matera (IT), sponsored by ESA in collaboration with EARSeL, UNESCO, University of Rome "Sapienza" (Italy), University of Rennes1 (France)
   http://www.earsel.org/SIG/NCH/4th-workshop/index.php

5. TV Interview *Archeologia spaziale*, RAINews24, 3rd April 2013 and related article on ESA (European Space Agency) webpage

This page intentionally left blank

References

[1] MicroImages, Inc. Introduction to remote sensing with TNTmips®, 2012. 11

[2] Piccarreta F., Ceraudo G., Manuale di aerotopografia archeologica. Metodologia, tecniche e applicazioni. EDIPUGLIA, Bari, 2000, ISBN–9788872282687

[3] Musson C., Palmer R., Campana S., In volo nel passato aerofotografia e cartografia archeologica, All'Insegna del Giglio S.A.S. 2005, ISBN 88-7814-499-1

[4] Piccarreta F., Manuale di fotografia aerea, "L'ERMA" di Bretschneider, Roma, 1994, ISBN: 88-7062-602-4

[5] Blom R., Crippen R., Elachi C., Detection of subsurface features, in SEASAT SAR images of Means Valley, Mojave Desert, California, Geology 12: 346-349

[6] Masini N., Coluzzi R., Lasaponara R., Investigating lost medieval villages using satellite and airborne laser scanning: The case of Yrsum in Basilicata (Southern Italy), in Archeologia e Calcolatori 21, 2010, 127-144

[7] Parckak S. H., Satellite remote sensing for archaeology, Taylor & Francis e-Library, 2009, ISBN: 0-203-88146-X

[8] Wang H., Allain S., Méric S., Pottier E., Polarimetric multi-angular RADARSAT-2 data sensitivity to surface parameters, IEEE Geoscience and Remote Sensing Symposium (IGARSS), July 2012, 5125-5128

[9] Lasne Y., Imagerie radar basse fréquence pour l'exploration des zones arides terrestres et martiennes : détection de l'humidité du sous-sol et cartographie de la paléohydrologie. http://tel.archives-ouvertes.fr/tel-00180231/en

[10] El-Baz F., Robinson C.A., Al-Saud T.S.M., SAR images in geoarchaeology of Eastern Sahara, in Remote Sensing in Archaeology, Wisemann J, El Baz F (eds). Springer Verlag: Berlin, 2007, 47-70

[11] Xinqiao L., Huadong G., Yun S., Detection of the Great Wall using SIR-C data in north-western China. Geoscience and Remote sensing, IGARSS '97, Remote Sensing – A scientific vision for Sustainable Development IEEE International 1: 50-52

[12] Blom R., Clapp N., Zarins J., Hedges G., Space technology and the discovery of the lost city of Ubar, IEEE Aerospace Conference, Snowmass, Aspen, USA, February 1997

[13] Moore E., Freeman T., Hensley S., Spaceborne and airborne SAR at Angkor. Introducing new technology to the ancient site, in Remote Sensing in Archaeology, Wiseman J, El Baz F (eds). Springer Verlag: Berlin, 2007, 185-216, ISBN 10-0-387-44615-X

[14] Masini N., Lasaponara R., Satellite Synthetic Aperture Radar in Archaeology and Cultural Landscape: An Overview, in Archaeological Prospection, vol. 20, Wiley Online Library, 2013, DOI: 10.1002/arp.1452

[15] Masahiro E., Ryoshi N., Shimoda H., Sakata T., Zaghloul E.A., Shimada M., A study for archaeology exploration using Spaceborne SAR, http://repository.tksc.jaxa.jp/help/pdf/SP-11-007E/pdf/SP-11-007E/pdf/PI308_Masahiro_Etaya.pdf

[16] Cigna F., Tapete D., Lasaponara R., Masini N., Amplitude change detection with ENVISAT ASAR to Image the Cultural Landscape of the Nazca region, Peru, in Archaeological Prospection, Volume 20, May 2013, 117-131 DOI: 10.1002/arp.1451

[17] Tapete D., Cigna F., Masini N, Lasaponara R, Prospection and monitoring of the Archaeological Heritage of Nazca, Peru, with ENVISAT ASAR, in Archaeological Prospection, Volume 20, May 2013, 133-147 DOI: 10.1002/arp.1449

[18] Linck R., Busche T., Buckreuss S., Fassbinder J.W.E., S. Seren, Possibilities of archaeological prospection by high-resolution X-band satellite

radar – A case study from Syria, Volume 20, Issue 2, May 2013, 97-108 DOI: 10.1002/arp.1444

[19] Lee J.S., Pottier E., Polarimetric Radar Imaging. From Basics to Applications. Taylor & Francis Group, Boca Raton 2009, ISBN: 978-1-4200-5497-2

[20] Fundamental of Remote sensing, latest access 02/2014 http://www.nrcan.gc.ca/earth-sciences/geomatics/satellite-imagery-air-photos/satellite-imagery-products/educational-resources/9309

[21] Boerner, W-M, H. Mott, E. Lüneburg, C. Livingston, B. Brisco, R. J. Brown and J. S. Paterson with contributions by S.R. Cloude, E. Krogager, J. S. Lee, D. L. Schuler, J. J. van Zyl, D. Randall P. Budkewitsch and E. Pottier, "Polarimetry in Radar Remote Sensing: Basic and Applied Concepts" in F.M. Henderson, and A.J. Lewis, (eds.), Principles and Applications of Imaging Radar, Vol. 2 of Manual of Remote Sensing, (ed. R.A. Reyerson), 3rd Ed., John Willey & Sons, New York, 1998, ISBN: 0-471-29406-3.

[22] Boerner W.M, Introduction to Radar Polarimetry with assessments of the historical development and of the current state-of-the-art, Proceedings: International Workshop on Radar Polarimetry, JIPR-90, 20-22 March 1990, Nantes, France.

[23] Cloude S. R., Polarisation: Applications in Remote Sensing, Oxford University Press, New York, 2010, ISBN: 978-0-19-956973-1

[24] Mott, H., Antennas for Radar and Communications, A Polarimetric Approach, John Wiley & Sons, New York, 1992, ISBN 0-471-57538-0.

[25] Kostinski A.B. and Boerner W.M., On foundations of radar polarimetry, IEEE Trans. Antennas and Propagation, vol. 34, 1986.

[26] Cloude S.R. and Pottier E., An Entropy Based Classification Scheme for Land Applications of Polarimetric SAR IEEE Trans. Geos. and Rem. Sens., 35, 1, January 1997

[27] Morio J., Refregier P., Goudail F., Dubois-Fernandez P. and Dupuis X., Application of Information Theory Measures to Polarimetric and Interferometric SAR Images, PSIP 2007, Mulhouse, France

[28] Refregier P. and Morio J., Shannon entropy of partially polarized and partially coherent light with Gaussian fluctuations, JOSA A, Vol. 23, Issue 12, pp. 3036-3044, December 2006

[29] Freeman A. and Durden S., A three-component scattering model to describe polarimetric SAR data, in Proc. SPIE Conf. Radar Polarimetry, vol. SPIE-1748, pp. 213-225, San Diego, CA, July 1992.

[30] Freeman A. and Durden S.L., "A Three-Component Scattering Model for Polarimetric SAR Data", IEEE Trans. Geosci. Remote Sens., vol. 36, no. 3, May 1998.

[31] Singh J., Yamaguchi Y , Park S.E., General four-component scattering power decomposition with unitary transformation of coherency matrix, IEEE Transactions on Geoscience and Remote Sensing, vol. 51, no. 5, May 2013

[32] EORC, JAXA, ALOS Research and Application Project, http://www.eorc.jaxa.jp/ALOS/en/about/palsar.htm latest access 02/2014

[33] EO Portal Satellite Mission RADARSAT-2 https://directory.eoportal.org/web/eoportal/satellite-missions/r/radarsat-2 latest access 02/2014

[34] ESA Earth Online RADARSAT-2 https://earth.esa.int/web/guest/missions/3rd-party-missions/current-missions/radarsat-2 latest access 02/2014

[35] DIGITAL GLOBE, QuickBird, http://www.digitalglobe.com/ latest access 02/2014

[36] ESA Earth Online KOMPSAT-2 https://earth.esa.int/web/guest/missions/3rd-party-missions/current-missions/kompsat-2 latest access 02/2014

[37] World Heritage List, 2014, http://whc.unesco.org/en/list/ latest access 02/2014

[38] UNESCO, Djebel Barkal and the Sites of the Napatan Region, Description, http://whc.unesco.org/en/list/1073/ latest access 02/2014

[39] Kendall, T.K., Napatan Temples: a Case Study from Gebel Barkal. The Mythological Nubian Origin of Egyptian Kingship and the Formation of the

Napatan State. In 10th International Conference of Nubian Studies. Rome, September 9–14, 2002

[40] Société des Culture Nubiennes – Archaeological Site – Gebel Barkal http://nubie-international.fr/accueil.php?a=page163010 latest access 02/2014

[41] Jebel Barkal - History and Archaeology of Ancient Napata, Kendall, 2010 http://www.jebelbarkal.org/index.php?option=com_content&view=article&id=66&Itemid=76 latest access 02/2014

[42] Knetsch G., On the geology of Nubia and on geological features and developments in Nubian monuments, Wurtzbourg, 1960 http://unesdoc.unesco.org/images/0015/001548/154886eb.pdf latest access 02/2014

[43] Worrall, G. A., A simple introduction to the geology of the Sudan, in Sudan Notes and Records, Vol. 38, pp. 2-9, University of Khartoum, Khartoum, 1957

[44] UNESCO, Djebel Barkal and the Sites of the Napatan Region, Maps, http://whc.unesco.org/en/list/1073/multiple=1&unique_number=1250 latest access 02/2014

[45] Borgogno Mondino E., Perotti L., Piras M., High resolution satellite images for archeological applications: the Karima case study (Nubia region, Sudan), in European Journal of Remote Sensing, 2012, 45, 243-259 DOI: 10.5721/EuJRS20124522

[46] ESA, EOLi "ESA's Link to Earth Observation" http://earth.esa.int/EOLi/EOLi.html latest access 02/2014

[47] Elachi C., Granger J., Spaceborne imaging radars probe "in depth", IEEE Spectrum, 19, pp. 24-29, 1982

[48] SAR Single Look Complex Image Product http://earth.esa.int/web/guest/-/sar-single-look-complex-image-product-1368

[49] VIGISAT, http://www.vigisat.eu/ latest access 02/2014

[50] GIS Bretel Bretagne Télédétection, http://recherche.telecom-bretagne.eu/bretel latest access 02/2014

[51] Weather Online, Karima, History, http://www.weatheronline.co.uk latest access 02/2014

[52] WunderMap ®, http://www.wunderground.com/wundermap/ latest access 02/2014

[53] PolSARpro software http://earth.eo.esa.int/polsarpro/

[54] NEST software https://earth.esa.int/web/nest/home

[55] Aronoff S., Geographic Information System: a Management Perspective. WDL Publications, Ottawa, Canada, 1989, DOI: 10.1080/10106048909354237

[56] Burrough P.A., Mc Donnell R.A., Principles of Geographical Information Systems (Spatial Information Systems), Oxford University Press, New York, 1998, ISBN: 0-19-823366-3

[57] Galati S., Geographic Information Systems Demystified, ARTECH HOUSE, INC, Norwood, MA, 2006, ISBN-13: 978-1-58053-533-5

[58] Perotti L., Geomatics and geomorphology: new tools and methods for field survey and mapping, Ph.D. course in Earth Sciences, XIX cycle, University of Torino, ITALY, 2007

Resumé

L'analyse de la Polarimétrie SAR pour la détection des structures archéologiques de surface et de subsurface du site de Gebel Barkal (Sudan), inscrit dans la Liste du Patrimoine Mondial depuis 2003, est l'objectif des travaux de recherche effectués dans le cadre de cette thèse de doctorat. En particulier, les capacités de pénétration dans le sol des bandes C et L ont été analysées grâce à l'utilisation des images des capteurs ALOS PALSAR (archivées) et RADARSAT-2 (spécifiquement acquises). En outre, l'activité de recherche illustre les potentialités de l'intégration des données satellitaires polSAR et optiques dans un projet SIG dédié, réalisé grâce à une collaboration avec les Universités de Turin et de Vénice (Italie). La surveillance des sites archéologiques au moyen des images satellitaires polSAR représente un avantage considérable pour la recherche archéologique, alors que les anomalies détectées peuvent concerner les opérations de fouille ou être vérifiées au sol, comme démontré dans ce manuscrit, ou encore elles peuvent contribuer à la réalisation des plans d'intervention pour les sites archéologiques en péril.

Mots clés : Télédétection, SIG, polarimétrie radar, imagerie radar, archéologie

Abstract

Aim of PhD research is to exploit SAR Polarimetry technique for the identification of surface and subsurface archaeological features in the site of Gebel Barkal (Sudan), inscribed in the UNESCO World Heritage List since 2003. Sand penetration capability of both C-band and L-band sensors are discussed analysing archived ALOS PALSAR and RADARSAT-2 specifically acquired (2012-2013) images. Moreover, the research activity illustrates the potential of integrating SAR polarimetric and optical satellite data in a dedicated GIS project, realised in collaboration with the Universities of Turin and Venice (Italy). The monitoring of ancient sites by means of remotely acquired polarimetric SAR data represents a benefit for the archaeological research, where detected anomalies can address archaeological excavations or ground truth verification, as shown in the

PhD dissertation, and where threatening factors affect the integrity of a cultural site.

Key words : Remote Sensing, GIS, radar polarimetry, radar imaging, archaeology